DOKUZ EYLÜL UNIVERSITY

GRADUATE SCHOOL OF NATURAL AND APPLIED SCIENCES

TECTONO-MAGMATIC EVOLUTION OF THE SELENDİ BASIN, WESTERN ANATOLIA

by

E. Yalçın ERSOY

July, 2005

İZMİR

TECTONO-MAGMATIC EVOLUTION OF THE SELENDİ BASIN, WESTERN ANATOLIA

A Thesis Submitted to the
Graduate School of Natural and Applied Sciences of Dokuz Eylül University
In Partial Fulfillment of the Requirements for the Degree of Master of Science
in Geological Engineering, Economic Geology Program

by

E. Yalçın ERSOY

July, 2005

İZMİR

M.Sc. THESIS EXAMINATION RESULT FORM

We have read the thesis entitled **"TECTONOMAGMATIC EVOLUTION OF THE SELENDİ BASIN, WESTERN ANATOLIA"** completed by **E. Yalçın ERSOY** under supervision of **Prof.Dr. Cahit HELVACI** and we certify that in our opinion it is fully adequate, in scope and in quality, as a thesis for the degree of Master of Science.

.....

Prof.Dr. Cahit HELVACI
Supervisor

.....

Prof. Dr.Erdin BOZKURT
(Jury Member)

.....

Assoc.Prof.Dr. Hasan SÖZBİLİR
(Jury Member)

Prof.Dr. Cahit HELVACI
Director
Graduate School of Natural and Applied Sciences

ACKNOWLEDGMENTS

This study was supported by two research projects; TÜBİTAK (ÇAYDAG/103Y124) and Dokuz Eylül University Scientific Research Projects (BAP, 03.KB.FEN.058). My sincere thanks are expressed to Cahit Helvacı, Hasan Sözbilir, Erdin Bozkurt and Fuat Erkül for their invaluable help with fieldwork and discussion. Bora Uzel and M. Sezgül Kayseri are also thanked for his field assistance and Ökmen Sümer for his fruitful discussion. I also extend my special thanks to Cüneyt Akal, Ufuk Elmas, Gökhan Kellecioğlu, Murat Göksal, Çilem Karagöz, Alev Ergene and Orçun Leblebicioğlu for their help during field and office work.

TECTONO-MAGMATIC EVOLUTION OF THE SELENDİ BASIN, WESTERN ANATOLIA

ABSTRACT

Selendi Basin, which is one of the NE-trending Neogene depocenter in western Anatolia, is characterized by mainly two volcano-sedimentary successions separated by angular unconformity. These are Hacıbekir and İnay groups. The field data show the Hacıbekir Group was deposited in the hangingwall of a presently low-angle top-to-the NE normal fault (Kula detachment) that juxtaposed the ductilely-deformed Menderes metamorphics from the brittely-deformed ophiolitic rocks of the İzmir-Ankara zone, during latest Oligocene (?) - Early Miocene. This crustal-scale movement was also associated with the intrusion of syn-extensional crust-derived granite (Rahmanlar granite) in the footwall. Deposition of the Hacıbekir Group was also accompanied by calc-alkaline felsic (Eğreltidağ volcanic unit) to mafic ultrapotassic volcanism (Kuzayır basalt). The geochemical data revealed that the Eğreltidağ volcanic unit was produced from the same source with the Rahmanlar granite, with addition minor mantle component. Geochemical characteristics of the Kuzayır basalt are similar to those of the lamproites. These tectonic and stratigraphic associations indicate that the deposition of the Hacıbekir Group was occurred on a detachment fault that controlled core-complex formation, probably associated with a subduction zone. The deposition of the İnay Group during early Middle Miocene postdated the activity of the detachment faulting. İnay Group also interfingers with the calc-alkaline intermediate-felsic volcanic rocks (Yağcıdağ volcanics). This study also revealed that the olivine-bearing basaltic rocks in the basin do not belong to the Kula volcanic unit, is named on the basis of geochemical data as Kabaklar volcanics.

Keywords: western Anatolia, Selendi Basin, Kula detachment, syn-extensional granite, Neogene volcanism, geochemistry

SELENDİ HAVZASININ TEKTO-NOMAGMATİK EVRİMİ, BATI ANADOLU

ÖZ

Batı Anadolu'da KD uzanımlı havzardan birisi olan Selendi Havzası, birbirlerinden açılı uyumsuzlukla ayrılan iki volkano-sedimanter istif ile kartakterize olur. Bu istifler Hacıbekir ve İnay gruplarıdır. Bu çalışma sonucunda ortaya konulan arazi verileri, Hacıbekir grubunun, sünümlü deformasyona uğrayan Menderes Masifi'ne ait metamorfik kayaçlar ile kırılgan deformasyona uğrayan İzmir-Ankara zonuna ait ofiyolit kayaçlarını bir araya getiren düşük açılı KD'ya eğimli bir normal fay üzerinde en geç Oligosen (?) – Erken Miyosen' de çökeldiğini ortay koyar. Bu kabuksal ölçekli faylanma ayrıca genişleme ile eş yaşlı olarak kabuk ergimesi ile oluşan granit üretmiştir (Rahmanlar graniti). Hacıbekir Grubu' nun çökelimine ayrıca kalk-alkali felsik bileşimli Eğreltidağ volkanik biriminin ve mafik ultrapotasik bileşimli Kuzayır bazaltının yerleşimi eşlik etmiştir. Jeokimyasal veriler, Eğreltidağ volkanik biriminin Rahmanlar graniti ile benzer bir kaynak kayacından, düşük miktarlarda manto bileşenlerinin de katılımı ile oluştuğunu gösterir. Kuzayır bazaltının jeokimyasal özellikleri lamproitlere benzerlik sunar. Bu tektonik ve stratigrafik birliktelikler, Hacıbekir Grubu'nun muhtemelen bir yitim zonu ile aynı zamanlı kor kompleks oluşumu ile sıyrılma fayı üzerinde geliştiğini ifade eder. Erken Orta Miyosen' de çökelen İnay Grubu bu aktivitenin (sıyrılma fayı) bittiğini gösterir. İnay Grubu felsik-asidik, kalk-alkali bileşimli volkanik kayaçlar ile giriklilik sunar (Yağcıdağ volkanik birimi). Selendi havzasında görülen ve daha önce Kula bazaltlarına dahil edilen olivin içerikli bazı bazalt oluşukları, bu çalışma sonucunda ortaya konulan jeokimyasal veriler ile Kula bazaltlarından ayrılmış ve Kabaklar bazaltı olarak isimlendirilmiştir.

Anahtar Kelimeler: Batı Anadolu, Selendi Havzası, Kula sıyrılma fayı, genişleme ile yaşıt granit, Neojen volkanizması, jeokimya.

CONTENTS

Page

ACKNOWLEDGMENTS iii
ABSTRACT iv
ÖZ v
CONTENTS vi
CHAPTER ONE INTRODUCTION 1
1.1. Location of the Selendi Basin 1
1.2. The purpose and methods of study 1
1.3. Previous studies 1
1.4. Established knowledge on the tectono-magmatic evolution and basin formation of Aegean region 4
1.4.1. Tectono-stratigraphic units of the Aegean region 5
1.4.2. Models for the formation of the Neogene depressions in western Anatolia 11
1.4.3. The general characteristics of the western Anatolian Cenozoic magmatism 14
1.4.4. Models for the Late Cenozoic magmatism in western Anatolia 15
CHAPTER TWO GEOLOGY OF THE SELENDI BASIN 26
2.1. Introduction 26
2.2. Menderes Massif metamorphics 27
2.3. Rahmanlar granite 30
2.3.1. Deformation 31
2.4. Ophiolitic rocks 34
2.4.1. Contact relationships between ophiolites and the Menderes Metamorphics 34
2.5. Hacıbekir Group 37
2.5.1. Hacıbekir Group exposed within the Uşak-Güre basin 38
2.5.2. Hacıbekir Group exposed in Selendi Basin 43
2.5.3. Kuzayır basalt 48
2.5.4. Eğreltidağ volcanic unit 49

2.6. İnay group 52
2.6.1. Ahmetler and Ulubey formations 52
2.6.2. Yağcıdağ volcanic unit 53
2.7. Asartepe formation 56
2.8. Kabaklar basalt 56
2.9. Kula volcanic unit 56
CHAPTER THREE PETROGRAPHY AND GEOCHEMISTRY 57
3.1. Petrography 57
3.1.1. Rahmanlar granite 57
3.1.2. Eğreltidağ volcanic unit 57
3.1.3. Kuzayır basalt 58
3.1.4. Yağcıdağ volcanic unit 59
3.1.5. Kabaklar basalt 61
3.2. Classification and trace element characteristics 62
3.2.1. Rahmanlar Granite 63
3.2.2. Kuzayır basalt 72
3.2.3. Eğreltidağ volcanic unit 73
3.2.4. Yağcıdağ Volcanic unit 74
3.2.5. Kabaklar Basalt 76
CHAPTER FOUR PETROGENESIS OF THE MAGMATIC ROCKS 79
4.1. Eğreltidağ volcanic unit and Rahmanlar granite: an anatexitic origin? 79
4.2. Kuzayır basalt: mantle-derived lamproitic melts 84
4.3. Yağcıdağ volcanic unit: subduction zone melts? 87
4.4. Kabaklar basalt: melting of the subduction-modified sub-continental lithosphere 88
CHAPTER FIVE DISCUSSION AND CONCLUSION 91
5.1. Introduction 91
5.2. Revised stratigraphy of the Selendi Basin 91
5.3. Magmatic activity within the Selendi Basin 93
REFERENCES 99

CHAPTER ONE

INTRODUCTION

1.1. Location of the Selendi Basin

The study area is located within the Selendi Basin, one of the main NE-trending basins of western Anatolia. Selendi Basin is bounded by Demirci basin to the west, Uşak-Güre basins to the west, Simav Graben to the north and Gediz Graben to the south (Figures 1.2 & 2.2). The Selendi is the main settlement in the area. The study area lies in the 1/25.000 scale Turkish topographic maps of K21-b1, b2, b3, b4, K22-a1, a4, K21-c1, c2, c4 and K21-d2 (Figure 2.3).

1.2. The purpose and methods of study

The present Master of Science project aims to study of the Miocene volcanic rocks exposing within the Selendi Basin. To do this; field and laboratory studies were carred out during the last two years. The field studies include: (i) geological mapping at a scale of 1/25.000, (ii) preparation of field cross-sections and measured stratigraphic sections, (iii) measurement of structural elements, (iv) collection of rocks samples for petrographic, microstructural and geochemistry. Laboratory studies include preparation of samples for geochemical analysis.

1.3. Previous studies

This section aims to present a brief overview of the tectonic units of the Aegean region and to summarize the models proposed for tectonic and magmatic evolution of the region in previous studies.

First detailed study in the Selendi Basin was documented by Ercan *et al.* (1983). This study revealed that the stratigraphy of the basin is very similar to that of the Uşak-Güre Basin so that the nomenclature of the Uşak-Güre basin is adopted to the Selendi Basin (Ercan *et al.* 1978; Figure 1.1). According to these authors, the

basement of the basins (e.g., Selendi and Uşak-Güre basins) is represented by metamorphic and ophiolitic rocks that are amalgamated along a thrust fault. Metamorphic rocks of the Menderes Massif comprise augen gneisses, schists and marbles. Ophiolites (namely Vezirler mélange; Ercan *et al.* 1983) consist of serpentinites, ultrabasic rocks, radiolarites, cherty limestones and cherts. Ercan *et al.* (1978, 1983) accepted that the basin fill, overlying the basement with an angular unconformity, consists mainly of two distinct volcano-sedimentary successions, namely Hacıbekir and İnay groups. Hacıbekir Group consists, from bottom to top, of Kürtköyü formation, Yeniköy formation, Dikendere volcanic unit and Karaboldere volcanic unit. Kürtköyü formation comprises medium sorted conglomerates that are made up of well-rounded ultrabasic rock fragments. According to their geological map, in some locations the formation consists mainly of metamorphic rocks derived from Menderes Massif (e.g., Pabuçlu area in Selendi Basin). The conformably overlying Yeniköy formation consists of conglomerates, sandstones and limestones. Dikendere volcanic unit is made mainly up of acidic lavas and tuffs, which interfingers with Yeniköy formation. Karaboldere volcanic unit is composed of trachytic and trachyandesitic lavas with pyroclastic rocks. Hacıbekir Group is of Middle-Late Miocene age, and is overlain by İnay Group (Ercan *et al.*, 1978, 1983). İnay group is divided into four units; Ahmetler formation, Ulubey formation, Beydağ volcanic unit and Payamtepe volcanic unit. Ahmetler formation is divided into three members, Merdivenlikuyu member; these are from bottom to top, are Balçıkdere member and Gedikler member, from bottom to top. Merdivenlikuyu member consists of conglomerates. Balçıkdere member comprises intercalation of conglomerate, sandstone, claystone, tuff, marl, limestone. Gedikler member is represented by alternation of claystone and tuff. Ulubey formation comprises lacustrine limestones interfingering with marls and claystones. Beydağ volcanic unit consists of andesitic-dacitic lavas and pyroclastic rocks. The age of the İnay Group is assigned as Pliocene according to paleontological data and is overlain by Asartepe formation and Quaternary Kula volcanic unit (Ercan *et al.*, 1983; Figure 1.1).

Seyitoğlu (1997) revised stratigraphy of the Selendi Basin, using the formation and group names of the Ercan *et al.* (1978, 1983) and suggested that the Hacıbekir

Group is Early Miocene in age. Palynology-based ages from Pabuçlu area range from 20 to 14 Ma (Eskihisar sporomorph assemblage; Benda & Maulenkamp. 1979). The Dikendere volcanic unit in the Eskin area cuts the Hacıbekir Group and yields K-Ar age of 18.9±0.6 Ma. Seyitoğlu (1997) also suggested that the İnay Group is Middle Miocene (18-14 Ma) according to palinologic data from the lignite horizons and K-Ar age of 14.9 ± 0.6 Ma from the volcanic rocks that interfinger with sedimentary successions (Figure 1.1). The Hacıbekir Group was interpretted to have been deposited in a NE-trending basin that was bounded by N-S trending normal faults; the faults are under the İnay Group. This model also argues that the İnay Group was deposited in this basin and overlaps these basin-bounding faults (Seyitoğlu. 1997).

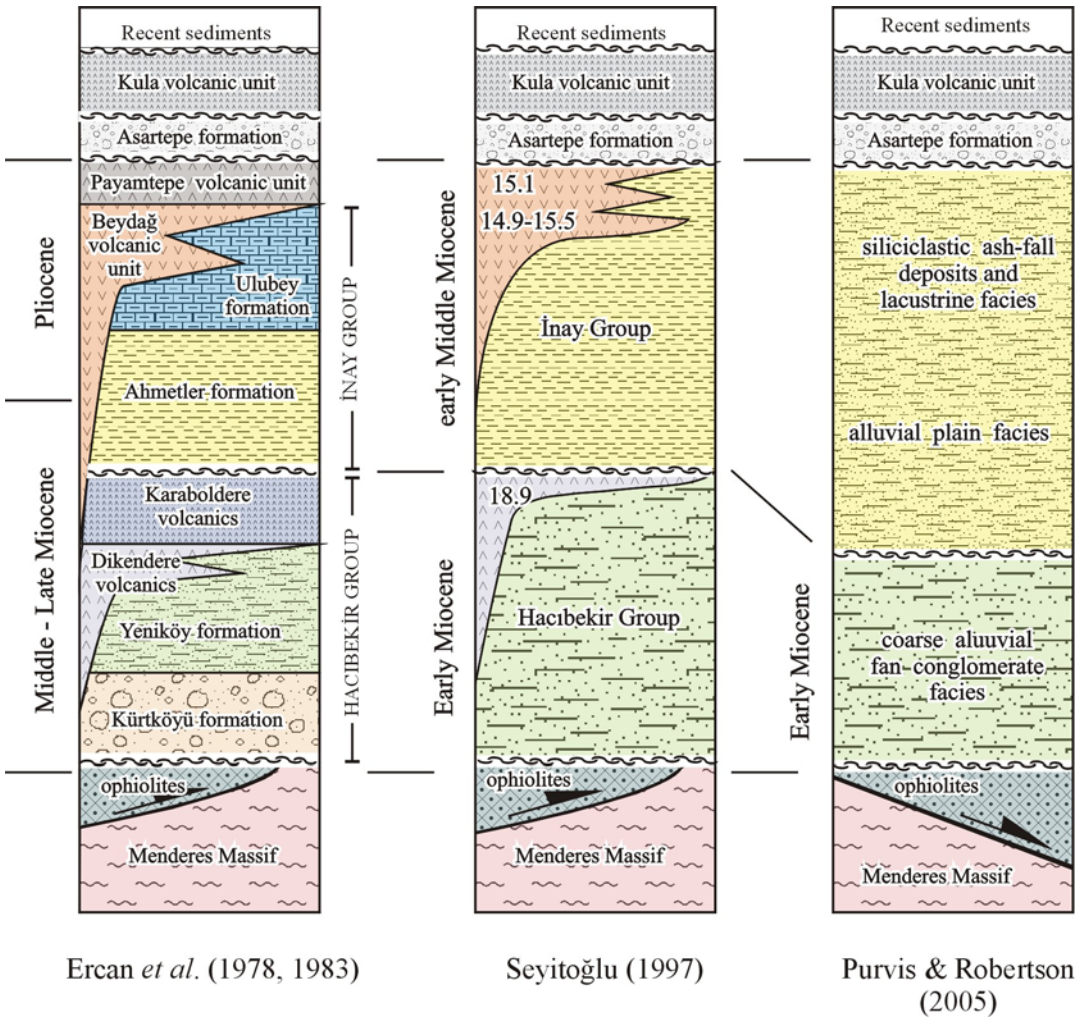


Figure 1.1. Correlation of stratigraphic columnar sections from previous studies in the Selendi Basin.

The stratigraphy of the Selendi Basin has recently been studied by Purvis & Robertson (2004) and Westaway *et al.* (2004). Purvis & Robertson (2004) described the entire basin-fill based on their facies characteristics and suggested that the basin was began to develop in the earliest Miocene as a depocenter on a main breakaway fault juxtaposing the metamorphic rocks of the Menderes Massif and the ophiolitic rocks of the İzmir-Ankara suture zone. The main breakaway fault is represented by a north-facing ductile to brittle low-angle normal fault. The authors also obtained Early Miocene Ar/Ar ages from the tuffs (Yağcıdağ volcanic unit) that interfinger with the İnay Group. The Ar/Ar age data is controversial with K-Ar age measured by Seyitoğlu (1997). Purvis & Robertson (2004, 2005a, b) correlated the stratigraphy of the Selendi Basin with that of the Gördes basin and pointed out that the stratigraphy of the Demirci Basin is different from these basins. On the other hand, Westaway *et al.* (2004) suggested that the basin-fill in the Uşak-Güre and the Selendi Basins are different and can not be correlated.

Another controversy on the tectonostratigraphic evolution of the basin lies in the age of the İnay Group. Bozkurt (2003) suggested that the deposition of the İnay Group might have occurred during Pliocene because the Quaternary basalts from Kula concordantly overlie the sediments of the Ahmetler formation (e.g., İnay Group). Similarly, Westaway *et al.* (2004) argued that the İnay Group can be younger than Early or Middle Miocene, contrary to Purvis & Robertson (2004, 2005a, b) and Seyitoğlu (1997).

1.4. Established knowledge on the tectono-magmatic evolution and basin formation of Aegean region

Western Anatolia has a complex history of Late Cenozoic tectonic and magmatic activity. The region has experienced several tectonic events including subduction, obduction, continental collision and consequent crustal thickening, extension and crustal thinning, and hence, the Late Cenozoic magmatic activity should be thought to be related to all these events. Taking into account the collisional events between Eurasia and Anatolia blocks, and between microplates, it can not easily be concluded that only one subduction event controlled the whole geological evolution of the

region. In order to understand the magmatic evolution of the region it must be taken into account that the core complex formation and the affects the ceased- or continuing- subductions. Because many parameters might be played role in tectono-magmatic evolution, using the only one or sometime two tectonic events and refusing the others also may lead to unrealistic conclusions.

For that reason, in this section, the general features of pre-Miocene basement of western Tukey and Aegean region will be given below.

1.4.1. Tectono-stratigraphic units of the Aegean region

Aegean orogenic belt, including several continental blocks and suture zones (Figure 1.2) was shaped by Alpine orogeny related Neo-Tethyan events (e.g., Carey 1958; Şengör & Yılmaz 1981; Okay *et al.* 1996; Okay & Tüysüz, 1999). Present day configuration of the Aegean region is characterized by several continental fragments with distinctive stratigraphic, structural and metamorphic features (Figure 1.2). Main characteristics of these fragments are summarized below.

1.4.1.1. Rhodope-Pontide fragment

The Rhodope-Pontide fragment comprises the Rhodope-Strandja Massif, Thrace Basin, İstanbul Zone and Sakarya Zone (Figure 1.2). The Rhodope-Strandja Massif (Okay *et al.* 2001) composed of crystalline basement of granite and gneisses and is tectonically overlain by allochthonous Triassic units. Okay *et al.* (1996) regarded that the Stradja Zone is part of the Mesozoic Laurasian active continental margin. The Thrace Basin is a Tertiary sedimentary basin developed during Middle Eocene (Doust & Arıkan 1974; Görür *et al.* 1984). The İstanbul Zone is characterized by non-metamorphic Palaeozoic sedimentary sequence, corresponding with a typical Atlantic-type continental margin (Okay *et al.* 1994; Görür & Okay 1996). The Sakarya Zone is separated from the İstanbul and the Strandja zones by Intra-Pontide Suture (Figure 1.2). At regional scale, it consists of the Sakarya Continent (Şengör & Yılmaz 1981) and the central-eastern Pontides. The Sakarya Continent of Şengör & Yılmaz (1981) was located between the Palaeo – Tethyan and the northern branch of

the Neo-Tethys (Figure 1.2). The Sakarya Zone comprises Palaeozoic granitic and metamorphic rocks of Carboniferous metamorphic ages at the base (Okay *et al.*, 1996). These crystalline rocks are tectonically overlain by a Late Palaeozoic to Triassic accretionary complex with intra-oceanic fore-arc deposits. All these rocks are unconformably overlain by Liassic detritals and Middle Jurassic – Lower Cretaceous limestones and Upper Cretaceous flysch (Okay *et al.* 1996).

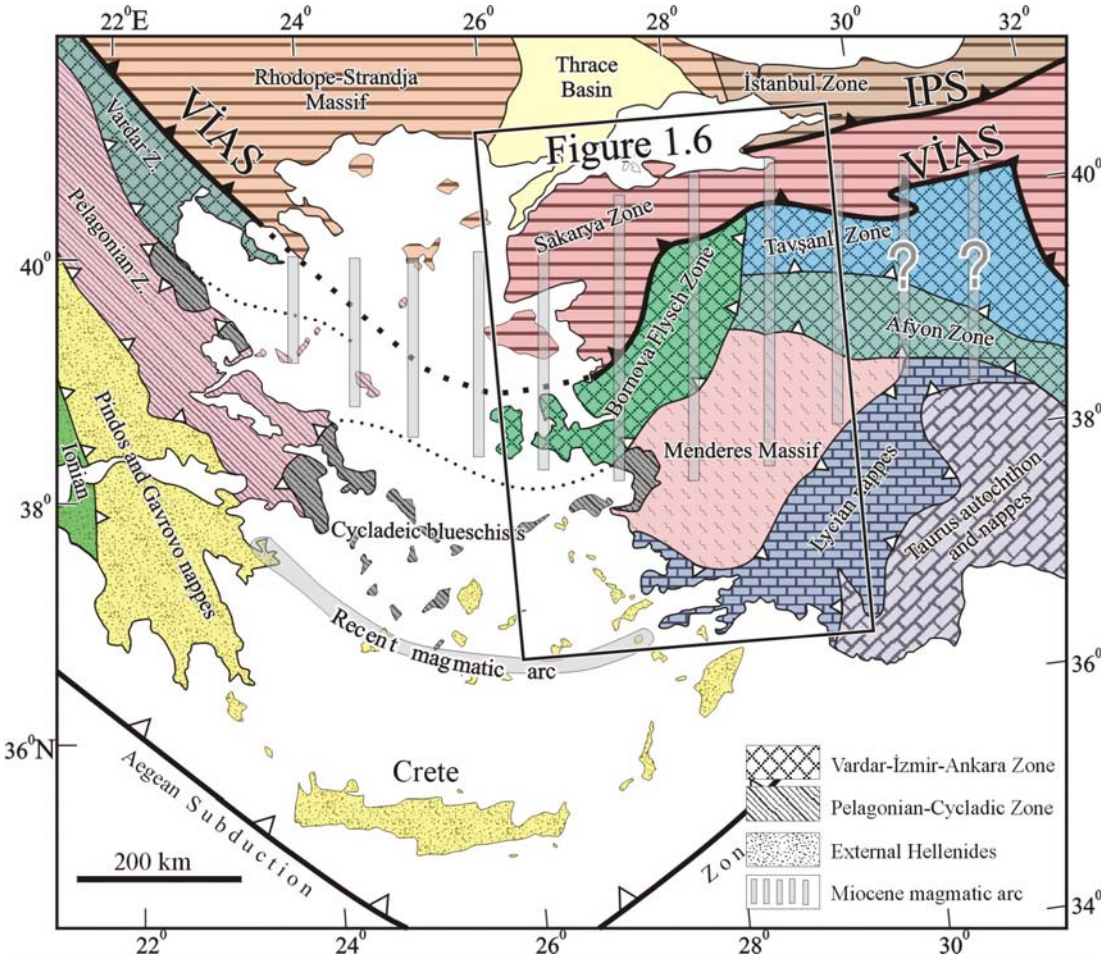


Figure 1.2. Tectonostratigraphic units of the Aegean region (after Lips 1998; Okay & Tüysüz 1999; Jolivet & Patriat 1999; Ring *et al.* 1999, 2001; Okay *et al.* 2001; Parra *et al.* 2002; Jolivet *et al.* 2004). IPS: Intra-Pontide Suture; VIAS: Vardar-İzmir-Ankara Suture zone.

1.4.1.2. Anatolide-Tauride Block

The Anatolide-Tauride block extends from eastern Anatolia in the east to the Pelagonian zone in the west (Figure 1.2). The Anatolide-Tauride block comprises of several tectonostratigraphic units which amalgamated during Middle Eocene (Şengör & Yılmaz 1981; Okay *et al.* 1996). These are, from north to south, Vardar-İzmir-

Ankara zone, Menderes Massif and Lycian Nappes. The Vardar-İzmir-Ankara zone comprises Vardar zone, Bornova Flysch zone, Afyon zone and Tavşanlı Zone (Figure 1.2).

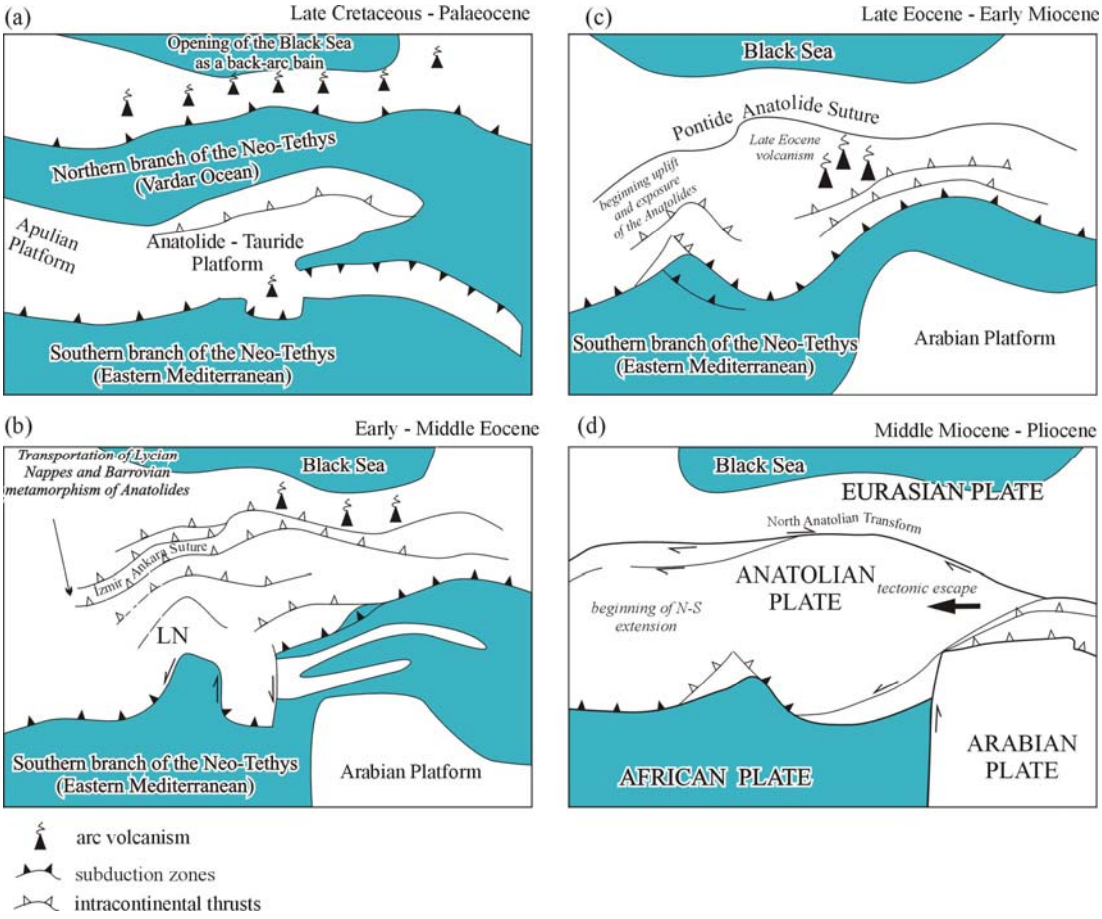


Figure 1.3 Palaeotectonic map showing Neo-Tethyan evolution from late Cretaceous to Pliocene (after Şengör & Yılmaz 1981). **(a)** Northward subduction of the northern branch of the Neo-Tethys (Vardar Ocean) beneath Eurasia in the Late Cretaceous – Palaeocene interval, leading to the Pontide volcanic arc and the opening of the Black Sea as a back-arc basin; **(b)** Closure of the northern branch of the Neo-Tethys along the Vardar-İzmir Ankara suture zone in early – middle Eocene, and southwestward tectonic transportation of Lycian and Tauride nappes leading to Barrovian metamorphism of the Anatolides beneath the nappes; **(c)** North – south shortening continued after the closuring and Anatolides were uplifted and unroofed (Menderes Massif in Oligocene and Kırşehir Massif in Late Eocene); **(d)** The collision of the Anatolian and the Arabian Plates along Bitlis-Zagros Suture zone in Burdigalian, and consequently westward tectonic escape of the Anatolian Plate along North Anatolian and East Anatolian transfer faults. The tectonic escape led to N-S extensional regime in western Anatolia (Şengör & Yılmaz 1981).

The Vardar zone, which is correlated with the İzmir-Ankara-Zone, separates the Rhodope continental block from the Pelagonian zone further to the southwest. It is represented by ophiolitic occurrences tectonically overlying the Pelagonian zone (Walcott & White 1998).

In the Aegean region, Vardar-İzmir-Ankara suture zone separates the Rhodope-Pontide Fragment from Anatolides and represents the closure of the northern branch of the Neo-Tethys (Figures 1.2 and 3). The closure of the ocean was diachronous; it started in Late Cretaceous in the west and proceeded until the Early Eocene in the east (Görür *et al.*, 1983; Tüysüz, 1993).

The Bornova Flysch Zone comprises chaotically deformed Upper Maastrichtian – Palaeocene greywacke and shale with Mesozoic neritic limestone blocks of several kilometers large (Erdoğan 1990; Erdoğan *et al.* 1990; Okay & Siyako 1993; Okay *et al.* 1996). Okay (1996) postulated that it was formed in a transfer zone during Late Cretaceous owing mainly to its non-metamorphic character (Figure 1.4).

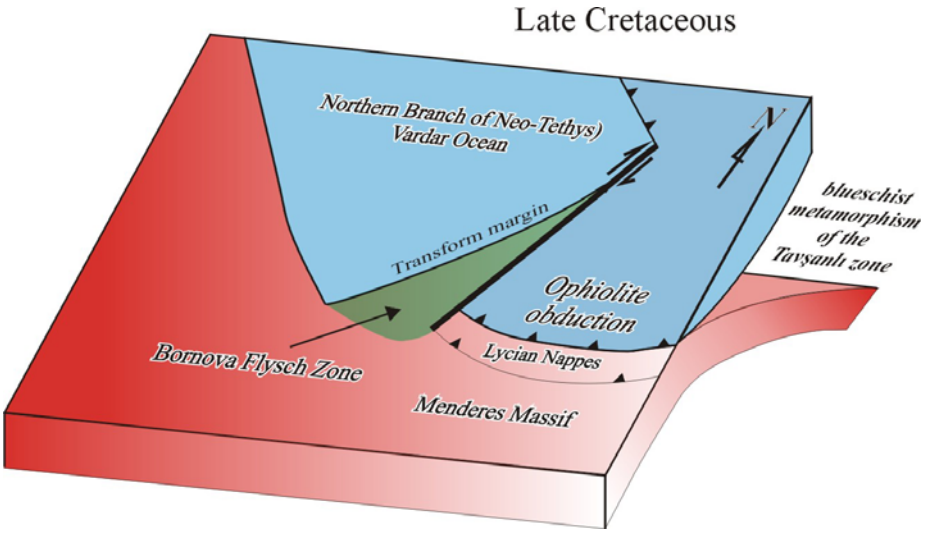


Figure 1.4. Late Cretaceous evolution of the Anatolide-Tauride block according to Okay *et al.* (1996). Ophiolite obduction led to blueschist metamorphism of its northern part. The triangular area (green area) illusturates the depocenter of the Bornova Flysch zone, which is free from the ophiolite obduction.

The Tavşanlı Zone forms a blueschist belt, representing the northward subducted passive continental margin of the Anatolide-Tauride platform (Figure 1.4, Okay 1986; Okay *et al.* 1996, 1998). The blueschists metamorphism occurred in Turonian-Coniacian (Late Cretaceous; Okay & Kelley 1994). The Afyon zone comprises shelf-type Devonian to Palaeocene sedimentary sequence metamorphosed in greenschist facies (Göncüoğlu *et al.* 1992; Okay *et al.* 1996).

1.4.1.3. Menderes Massif

The Menderes Massif forms the westernmost part of the Anatolides. It consists of augen gneisses, metagranites, low- and high-grade schists, paragneisses and metagabros with eclogite relics, marbles (Şengör *et al.* 1984; Candan, 1995; 1996; Oberhänsli *et al.* 1997, 1998; Candan *et al.* 1998, 2001; Bozkurt & Oberhänsli 2001). It has been concluded that the augen gneisses, intruded into schists, have a granitic protolith of Tertiary (Oligocene) in age (*for detailed description see* Bozkurt & Oberhänsli 2001). Based on Bryzoan assemblages and zircon radiometric analyses the cover schists have been dated as Ordovician – Devonian (Konak *et al.* 1987; Loos & Reischmann 1999). Just above the schists, the fosiliferous grey marbles dated as Permian (Özer 1998). Marbles starts with basal meta-conglomerate (Dürr 1975), and consists of Upper Triassic – Liassic marbles intercalated with schists and metavolcanics. The succession continues upward with Jurassic – Lower Cretaceous massive marbles and Upper Cretaceous rudist-bearing marbles (for details, see Bozkurt & Oberhänsli 2001 and Özer *et al.* 2001 and references therein).

Menderes Massif shows a polyphase metamorphism (e.g., Bozkurt & Oberhänsli 2001 and references therein). These are: (1) pre-Alpine metamorphism which affected the high-grade rocks occurred under granulite, eclogite, amphibolite (M1; pre 550-Ma; Candan *et al.* 2001) and greenschist (M2; pre-230 Ma; Akkök 1983) facies conditions; (2) middle-Alpine metamorphism occurred under blueschist facies condition (M3; 40 Ma; Oberhänsli *et al.* 1998); main Menderes metamorphism (MMM) occurred under amphibolite-greenschist facies condition (M4; 35-36 Ma; Lips *et al.* 2001); late Alpine metamorphism occurred under greenschist condition (M5; 12,2 – 19,5 Ma; Hetzel *et al.* 1995a). It is widely accepted that the pre-Alpine deformational history of the Menderes Massif includes the Pan-African orogeny and the Permo-Triassic Cimmerian event (for detail see Bozkurt & Oberhänsli 2001 and references therein). Alpine deformational history of the Menderes Massif includes contractional (Eocene; Bozkurt 1995; Hetzel *et al.* 1998) and extensional events (Bozkurt & Park 1994; Hetzel *et al.* 1995a-b; Koçyiğit *et al.* 1999a, b; Bozkurt 2000, 2001b; Sözbilir & Emre 1996; Lips *et al.* 2001).

The Menderes Massif has been given its massif character by contractional Alpine deformation which also contemporaneous with MMM. This deformation is characterized by regional foliation defining a dome shape in a regional scale (Bozkurt & Oberhänsli 2001 and references therein). It is widely accepted that the continental collision between the Sakarya Continent and the Anatolide-Tauride Platform along the Vardar-İzmir-Ankara Suture Zone resulted in the southward migration of the Lycian Nappes above the Menderes Massif during the late Palaeogene. The migration has buried and deformed the Menderes Massif (Figure 1.3; Şengör & Yılmaz 1981; Şengör *et al.* 1984).

The following late Alpine extensional deformation exhumed the Menderes Massif along crustal-scale low-angle detachment faults, accompanied by core complex formation (Bozkurt & Park 1994, 1997a, b; Hetzel *et al.* 1995a, b, 1998; Emre 1996; Emre & Sözbilir 1997; Koçyiğit *et al.* 1999a, b; Bozkurt 2000, 2001a, b; Gessner *et al.* 2001a-b; Işık & Tekeli 2001; Lips *et al.* 2001; Sözbilir 2002; Özer & Sözbilir 2003; *Ring et al.* 2003, Işık *et al.* 2003, 2004; Bozkurt & Sözbilir, 2004; Seyitoğlu *et al.* 2000, 2002, 2004; Jolivet et al. 2004, Rimmelé et al. 2003a, b; Catlos & Çemen 2005; Ring & Collins 2005). It is widely accepted that the styles of detachment faulting, which controlled the exhumation of the Menderes Massif and basin formation at the surface, was bivergent (Hetzel *et al.* 1995a; Gessner *et al.* 2001b). Based on sedimentological and radiometric data, recent studies showed that this deformation commenced ca. 20 Ma and continued by ca. 12 Ma (Seyitoğlu & Scott 1996a; Hetzel *et al.* 1995a; Catlos & Çemen 2005). According to the available literature, the extensional tectonics in western Anatolia started in the late Oligocene, although some workers accept that as middle Miocene or younger (e.g., Şengör 1979, 1987; Şengör *et al.* 1985; Görür *et al.* 1995).

1.4.1.4. Tectonostratigraphic units in Greece

The Pelagonian Zone comprises Mesozoic platform sequence, resting on detrital Permian and Jurassic chaotic sequence. It tectonically overlies the Pindos (Aubouin 1959; Stampfli *et al.* 2003) and the Gavrovo (Aubouin 1959) nappes, and the Cycladic Blueschists (Godfriaux 1965) (Figure 1.2). The Cycladic Blueschists

consists of two main tectonic units. The upper unit contains various intercalated fragments of ophiolites, Permian sedimentary rocks and high temperature metamorphic rocks. The lower unit shows a polyphase metamorphism history, including (1) Eocene (~ 42 Ma) high-pressure, blueschist facies metamorphism; (2) Oligocene/Miocene (20–25 Ma), regional metamorphism; and (3) Miocene (14–20 Ma) contact metamorphism associated with the intrusion of I-type granitic rocks (Schliestedt *et al.* 1987; Jolivet *et al.* 2004). The Cycladic Blueschists tectonically overlies the Menderes Massif in western Anatolia (Ring *et al.* 1999). The Pindos, Gavrovo and Ionian zones form the external Hellenides. The Pindos nappes are made of pelagic and siliceous deposits from the late Triassic to the Eocene. The Gavrovo nappe is consist of platform sequence of Triassic-Eocene in age (Aubouin 1959).

1.4.2. Models for the formation of the Neogene depressions in western Anatolia

There are two different trending Neogene depressions in western Anatolia: (a) N-NNE trending basins and (b) E-W trending grabens. Several models proposed concerning the cause, age and development of these basins tectonics in western Anatolia. These are *cross-graben model* (Şengör, 1987), *orogenic collapse model* (Seyitoğlu & Scott, 1996b), two-stage *episodic extension model* (for Gediz Graben, Koçyiğit *et al.*, 1999a), and *pulsed extension model* (including Gediz Graben and NE-trending basins, Purvis & Robertson, 2004).

The ***cross-graben*** model of Şengör (1987) predicts the NE-trending Early Miocene basins began to develop as "palaeotectonic Tibet-type cross-grabens" under N-S Palaeogene compression and shortening, and then, they were replaced by neotectonic Aegean-type cross-grabens (*replacement structures*) under the following N-S extensional regime commencing in the Tortonian (Figure 1.5, Dewey & Şengör 1979; Şengör 1979, 1987; Şengör *et al.* 1985; Görür *et al.* 1995; Çemen *et al.* 1999; Bozkurt 2003). Tortonian and younger basins belong to the N-S extensional regime related to the tectonic escape of Anatolian block along the North Anatolian Fault (NAF) zone (Figure 1.3d) since the late Serravallian (ca. 12 Ma). According to this view, the basin-bounding oblique-slip faults (accommodation faults) never cut the main breakaway fault (low-angle detachment fault) which exhumed the Menderes

Massif, and hence, the NE-trending basins have developed on hanging-wall of the detachment (Figure 1.5).

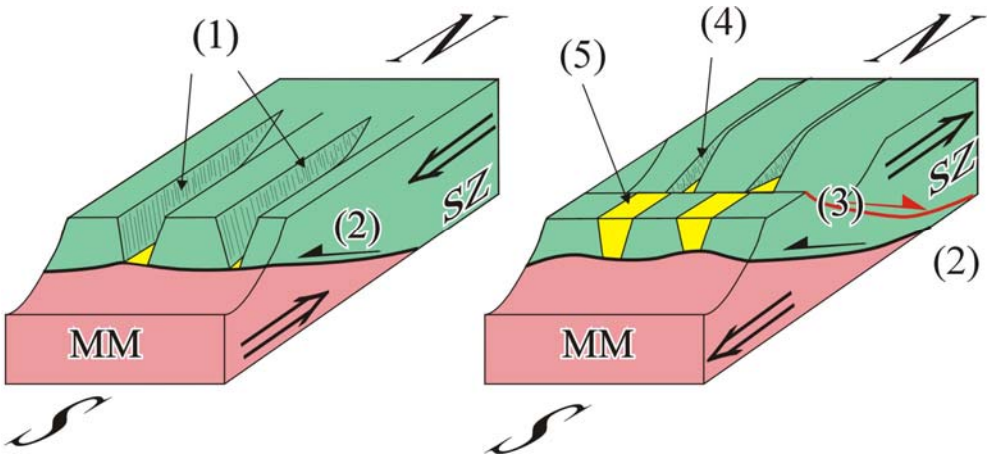


Figure 1.5. The block diagrams showing the development of the Aegean cross grabens (after Şengör, 1987). Palaeotectonic Tibet-type cross grabens (1) were formed by N-S convergence between the Anatolide block and the Sakarya Zone along the İzmir-Ankara suture zone (2). Since Tortonian, N-S extension resulted in a low-angle main breakaway fault (3) which exhumed the Menderes Massif. Differential stretching in the hanging-wall forms the Neotectonic Aegean-type cross grabens (4) which is bounded by oblique-slip faults. Former graben-fills remained in the footwall of the main fault as "hanging" grabens (5).

The ***orogenic collapse*** model of Dewey (1988) considers that the both NE- and E-W-trending depressions began to develop coevally during latest Oligocene – Early Miocene times, in a neotectonic N-S extensional regime that was resulted from the orogenic collapse of the over-thickened crust (Dewey 1988; Seytioğlu & Scott 1991; 1992a, b, 1994, 1996a, b; Collins & Robertson 1998).

According to the ***back-arc spreading model***, (McKenzie 1978a, b; Le Pichon & Angelier 1979, 1981; Jackson & McKenzie 1988; Kissel & Laj 1988; Meulenkamp *et al.* 1988; Avigad & Garfunkel 1991; Jolivet *et al.* 1994; Robertson & Grasso, 1995; Hetzel *et al.* 1995b; Le Pichon *et al.* 1995; Meijer 1995; Meijer & Wortel 1997; Avigad *et al.* 1997; Jolivet *et al.* 1998; Okay & Satır 2000; Avigad *et al.* 2001; Rosenbaum *et al.* 2002) the post-Oligocene extension in the Aegean region was governed by subduction zones triggered by gravitational instability of old, dense oceanic lithosphere (the model is schematized in Figure 1.7). This caused an extension in the overriding plates as a result of slow convergence rates combined with rapid subduction rates (Royden, 1993; Rosenbaum *et al.*, 2002). On the other

hand, there is no agreement on when the northward subduction along the Aegean trench and roll-back began. There are several views in the initiation of the subduction and roll-back processes: (a) Early Tertiary (Spakman *et al.* 1988; Taymaz *et al.* 1990; 1991), (b) Late Eocene – Early Oligocene (Thomson *et al.* 1998); (c) Late Oligocene (~ 33 Ma; Kastens 1991); (d) Early Miocene (~ 26 Ma; Meulenkamp *et al.* 1988); late Miocene (~ 13 Ma; Le Pichon & Angeliar 1979) or late Miocene – Pliocene (~ 13 Ma; Jackson & McKenzie 1984; ~ 5-10 Ma; Mc Kenzie 1978b; Mercier 1981).

The ***two-stage, episodic*** extensional model proposed for the extensional tectonics in western Anatolia, which accepted that two or more of the above mechanism played role in the Late Tertiary extensional tectonics in the region. According to this view, Late Cenozoic basins and grabens in western Anatolia have developed as a result of two-stage (episodic) extensional tectonics; the fist one is related to the orogenic collapse (Dewey 1988), and second one is related to the present neo-tectonic extensional phase commenced during the Pliocene (Koçyiğit *et al.* 1999a, b; Bozkurt 2000, 2001a, 2003; Yılmaz *et al.* 2000; Bozkurt & Sözbilir 2004). In this view there is a compressive phase in the Late Miocene – Early Pliocene interval, separating the two periods of extension, and hence, extensional tectonics in this region is episodic rather than continuous style. The closuring of the Bitlis-Zagros suture zone (late Serravalian, ~12Ma; Dewey *et al.*, 1986) was followed by late Serravalian – Early Pliocene compressive phase. In the late Early Pliocene the Anatolian plate started to escape westward. This view presumes that the westward escape of the Anatolian is not commenced in the Middle Miocene as regarded previously (e.g., Dewey *et al.*, 1986) but commenced in Early Pliocene (~ 5Ma; Barka & Kadinisky-Cade 1988; Westeway 1994).

Recently the ***pulsed extension*** model have been proposed for the Late Tertiary extensional tectonics of the western Anatolia, which presumes that neither continuous-style nor two-stage, but has a rather complex history showing at least three different phase of extension (Purvis & Robertson 1997, 2004, 2005a, b). This model predicts that the first "pulse" of the N-S extension took place in late Oligocene giving rise to low-angle normal faulting that created N-S trending "scoop-shaped"

depressions in which sediments accumulated during Early-Middle Miocene (e.g., Gördes and Selendi Basins). This phase of extension was droved by roll-back processes of Aegean subduction system. The second "pulse" of extension occurred in Early Miocene – Late Miocene which gave rise to E-W trending basin formation related to the exhumation of the Menderes Massif, similarly was droved by roll-back processes. The last "pulse" of the extension responsible to again the E-W- trending grabens, which controlled by tectonic escape of Anatolian plate (Purvis & Robertson 1997, 2004, 2005a, b).

1.4.3. The general characteristics of the western Anatolian Cenozoic magmatism

The origin and evolution of the widespread calc-alkaline and following alkaline volcanism in western Anatolia (Figure 1.6) although has been well-studied, there is no consensus among the workers in this controversial subject. From north to south, gradual decreasing in age of the volcanic rocks and their compositional variation with time has been differently interpreted by workers taking into account the tectonic evolution of the region. This implies that there is a close harmony between the tectonic regime and the composition of the volcanic rocks. Indeed, it is well-known that the volcanic and magmatic rocks, formed in various tectonic setting exhibit different chemical characteristics, particularly in trace and rare earth element contents and isotopic composition. Thus using these features would give some information about the ancient tectonic regime and the origin and evolution of the volcanic rocks.

In western Anatolia, volcanic rocks from latest Oligocene to Quaternary can be divided into two groups based on their chemical composition with temporal and spatial distribution (Yılmaz 1989, 1990; Savaşçın & Güleç 1990; Güleç 1991; Seyitoğlu & Scott 1992b; Ercan *et. al*. 1997; Seyitoğlu *et al.* 1997; Savaşçın & Oyman 1998; Yılmaz *et al.* 2000, 2001; Aldanmaz *et al.* 2000, 2002). The magmatic rocks of the Late Oligocene - Early Miocene time are mainly from rhyolite to basaltic andesite in composition and exhibit calc-alkaline and shoshonitic affinity. These rocks enriched in HREE with respect to LILE and LREE, and have higher $^{87}Sr/^{86}Sr$ while lower $^{143}Nd/^{144}Nd$ isotopic composition (e.g., Güleç 1991; Aldanmaz

et al. 2000). These geochemical features are roughly similar to those of the arc volcanics. There is a time break in volcanic activity from end of the Middle Miocene to beginning of the Late Miocene in western Anatolia (e.g., Yılmaz 1989; Yılmaz *et al.* 2001). The volcanic rocks of mainly Late Miocene – Early Pliocene are more basic in composition and exhibit alkaline character. These rocks depleted in HREE and enriched in LILE, HFSE, MREE and LREE. In addition to these geochemical characteristics, the volcanic rocks of the Late Miocene – Early Pliocene exhibit lower $^{87}Sr/^{86}Sr$ and higher $^{143}Nd/^{144}Nd$ isotopic contents (e.g., Güleç 1991; Aldanmaz *et al.* 2000). These geochemical characteristics are roughly similar to those of the OIB magmas (e.g., Sun & McDonough 1989; McKenzie & O'Nions 1995; Wedepohl & Baumann 1999). On the other hand, the alkaline basaltic volcanism in the Miocene-Pliocene was changed from potassic to sodic character (e.g., Kula volcanics: Ercan & Öztunalı 1982; Ercan *et al.* 1992; Güleç 1991; Alıcı *et al.* 2002).

1.4.3.1. The concept of "central volcanics"

One of the important features of the NE-trending basins is that the volcanic centers in the basin, that interfingering with the basin fill. They are clearly seen in the Gördes, Demirci, Selendi and Uşak-Güre basins. This was explained by Seyitoğlu & Scott (1994) and Bozkurt (2003) as pointed out that the "central volcanics" in these basins recalls the pull-apart model. According to Bozkurt (2003) "central volcanics" emplaced response to the basin evolution that stretches the basement. According to Bozkurt (2003), this model fits with the cross-graben model of the Şengör (1987).

1.4.4. Models for the Late Cenozoic magmatism in western Anatolia

The magma generation is caused by three fundamental ways including: (1) bringing the material to the less depths (*depressurization*); (2) changing the composition of the material, hence reducing its melting point; and (3) raising its temperature (e.g., Abbott & Van Ness 1972; McKenzie & Bickle 1988; Wilson, 1989; Iwamori *et al.* 1995). The first process expresses the melting through adiabatic decompression (e.g., Lewis & Randall 1961; McKenzie & Bickle 1988). This type of

magma generation is generally seen at mid oceanic ridges (e.g., Presnall *et al.* 2002), where there are upwelling mantle zones in which melting begins at ca. 50 km depth.

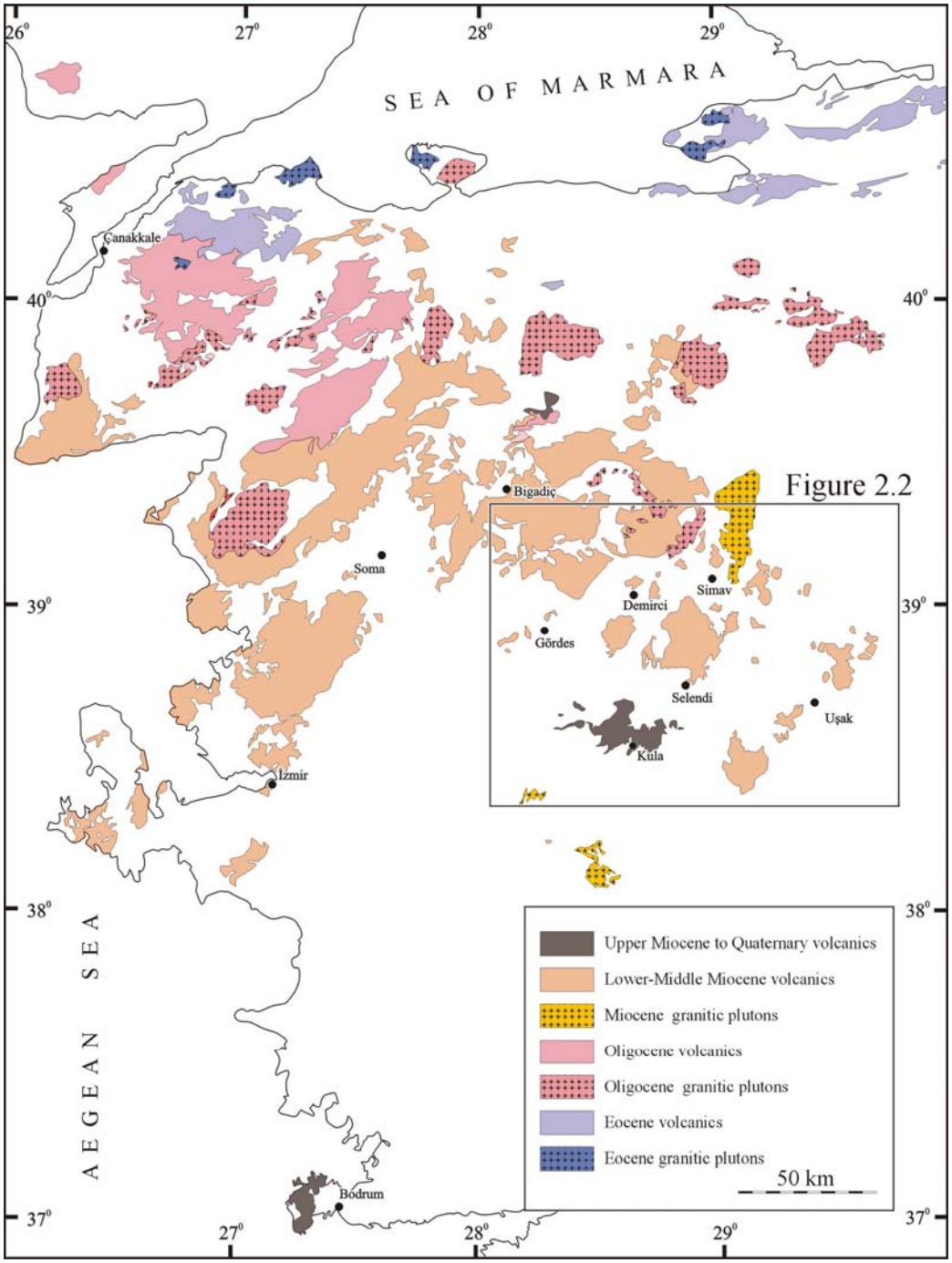


Figure 1.6. The distribution of the magmatic and volcanic rocks in western Anatolia.

The second way operates the most important role in subduction zones where two plates converges. In subduction zones, the material in the mantle wedge is subjected

to higher pressures. The predominant process that melts the material in subduction zones is addition of incompatible chemical species to the overriding mantle lithosphere from the sinking oceanic slab. These are mainly water, potassium, sodium and other incompatible elements (Pearce 1982, 1983; Pearce & Parkinson 1993; Pearce & Peate 1995; Pearce *et al.* 1995). This is subduction zone metasomatism, that causing to decrease in the melting point of the mantle (Hirschmann *et al.* 1999). It also affects the geochemical features of the magmas, e.g., giving rise to depletion of Ta and Nb with respect to the LILE. This geochemical feature is called as "subduction component" (Pearce 1983). The third process includes that very hot material is brought into contact with colder one, therefore warming up the colder material conductively. This process is used for the lithospheric delamination that brings up the hotter mantle into the contact with directly colder crust (e.g., von Blanckenburg & Davies 1995; Şengör *et al.* 2003; Keskin 2003).

The subduction systems, and subsequently collisional settings, especially in where compressional and extensional tectonics is followed by each other throughout the collision of microplates (e.g., Aegean region in Alpine-Himalayan belt), explaining the generation and evolution of volcanism gets a more complexity due to involving different stages of collisional and extensional tectonics and related magma production. In these regions, (e.g., western Mediterranean, western Anatolian) subduction events have been accomplished by the core complex formation (e.g., Lister *et al.* 1984). This section firstly presents the general characteristics of the region, and then, summarizes models proposed for the origin of the western Anatolia Late Cenozoic volcanism in the light of the tectonic models.

The distribution of the volcanic and magmatic rocks in western Anatolia is shown in Figure 1.6. One can conclude that the magmatic activity in the region has migrated from north to south throughout the Middle-Late Cenozoic.

1.4.4.1. Two-stage episodic volcanism

It has been widely accepted that the magmatic activity of western Anatolia from late Oligocene to Quaternary can be thought as a consequence of compressional and

following extensional tectonic regimes (Yılmaz 1989, 1990; Savaşçın & Güleç 1990; Güleç 1991; Ercan *et al.* 1997; Aldanmaz *et al.* 2000, 2005; Yılmaz *et al.* 2000, 2001) and thus, this view can be mentioned as "*two-stage episodic magmatism*". According to this view, after the collision between Sakarya Continent and Anatolide-Toride platform along the northern branch of the Neotethys (Şengör 1979; Şengör & Yılmaz 1981; Yılmaz 1990), ongoing N-S convergence is caused to forming of the Late Oligocene - Early Miocene calc-alkaline volcanic rocks (Figure 1.7a). The post-collisional volcanic rocks of this stage have been accepted as product of "Tibet-type magmatism". The mechanism which started the volcanism is thought to be lithospheric delamination or slab detachment (e.g., Aldanmaz *et al.* 2000; also see sections of "delamination" and "slab-detachment"). It is suggested that these magmas were formed as a consequence of the contamination of the mantle-derived magmas with crustal material, and thus, that these rocks have a hybrid source (Yılmaz *et al.* 2001). The geochemical similarities between arc volcanics and the Late Oligocene - Early Miocene calc-alkaline volcanic was interpreted by the workers as the magma source (lithospheric mantle) of the calc-alkaline volcanic rocks enriched by a subduction component, which was probably inherited from the pre-collision subduction event (Yılmaz 1989, 1990; Savaşçın & Güleç 1990; Güleç 1991, Aldanmaz *et al.* 2000; Yılmaz *et al.* 2000, 2001).

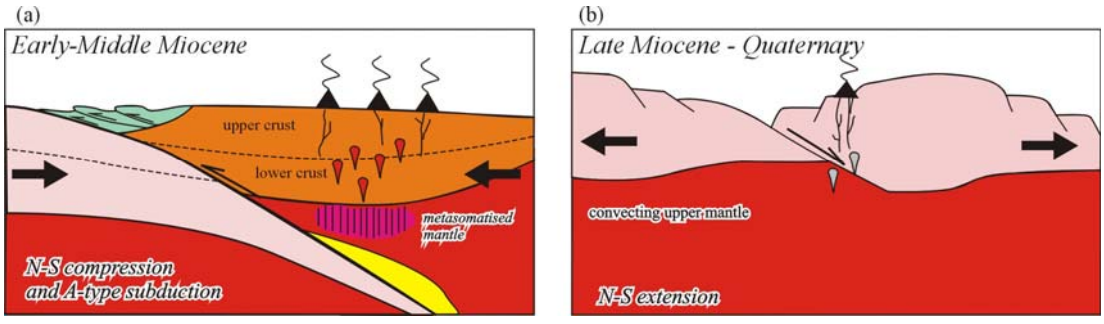


Figure 1.7. Models for two-stage episodic volcanism: **(a)** The Early-Middle Miocene magmatism under the compressional regime (after Yılmaz 1989). The intermediate volcanic rocks of hybrid nature were formed as a consequence of the N-S compression, from mixing of mantle and lower crustal melts. **(b)** Late Miocene – Quaternary extensional tectonics resulted in alkali basaltic volcanism (e.g., Kula volcanism) (after Aldanmaz *et al.* 2000).

This view also predicts that the magmatic activity ceased in late Middle Miocene (~14 Ma) – early Late Miocene (~10 Ma) interval and recommenced after Late

Miocene with changing in its composition (Yılmaz 1989, 1990; Yılmaz *et al.* 2000, 2001). In Late Miocene - Early Pliocene, second magmatic activity was developed, related to the N-S extensional tectonics (Figure 1.7b). The volcanic rocks, formed in this stage are alkaline basic in composition and similar to the rift magmas (e.g., Yılmaz 2001). The starting mechanism of this stage of new magmatic activity was thought to be decompressional melting (e.g., Aldanmaz 2000), response to lithospheric thinning.

1.4.4.2. The roll of the roll-back on the subduction system

It has been proposed that the middle-late Cenozoic Aegean volcanic evolution was caused by the rollback of the African plate, based on geochemical, radiometric age, isotopic and tectonic data (McKenzie 1978b; Le Pichon & Angelier 1979; Kissel & Laj 1988; Meulenkamp *et al.* 1988; Meijer 1995; Avigad *et al.* 1997; Okay & Satır 2000; Rosenbaum *et al.* 2002). The roll-back process results from the negative buoyancy of aging oceanic lithosphere relative to the asthenosphere (Elsasser 1971; Molnar & Atwater 1978; Uyeda & Kanamori 1979; Dewey 1980; Royden 1993; Gvirtzman & Nur 1999; Herzer *et al.* 2003; Figure 1.8). Cooling and thickening oceanic lithosphere causes a horizontally density contrasts which produce the "ridge push" force, and hence subduction to become more rapid than accommodated by large scale plate convergence (McKenzie 1969; Smith & Toksöz 1972; Lister 1975; Spence 1987). The "slab pull" force is the negative buoyancy of subducted oceanic lithosphere. In the case of slab roll-back, with an increase of subduction dip angle, from a compressional to an extensional tectonics develops at the front of the overriding plate, either within the fore-arc or in the back-arc to maintain crustal continuity (Kanamori 1977; Uyeda & Kanamori 1979). In this model, sinking of the subducted lithosphere leads to regressive motion of the subduction hinge towards the oceanic side (Figure 1.8b) and to back-arc spreading.

The forces acting on subduction system is summarized in Fig 1.8a (after Spence 1987). Subduction is occur when Fsp + Frp exceeds the sum of resisting forces. "Slab pull" force (Fsp) and "ridge push" (Frp) act together to subduct oceanic lithosphere. The corner flow (Fcf) resists the plate falling to the vertical. In case of

Fn > Fcf the seaward propagation of the hinge take place (hinge roll-back, Figure 1.8b) implying the entire subduction system slowly propagates seaward (Spence 1987).

The relationship between the migration of a subduction zone toward ocean and back-arc magmatism and volcanism has been well-studied (e.g., Uyeda & Kanamori 1979; Rosenbaum *et al.* 2002; Yamaji 2003) and was also proposed for western Anatolia. According to this model, all volcanic rocks in western Anatolia formed in a continental arc setting. The changing in composition and decrease in age of volcanics, from north to south, was related to southward retreatment of the Aegean trench during the Late Oligocene and Early Miocene (Borsi *et al.* 1972; Fytikas *et al.* 1976, 1980, 1984, 1985; Pe-Piper & Piper 1989; Zeilinga de Boer 1989; Okay & Satır 2000). The mechanism causing to melting involves the decompression in the mantle wedge. This model also well-explain the ocean-ward migration of an arc-related magmatism.

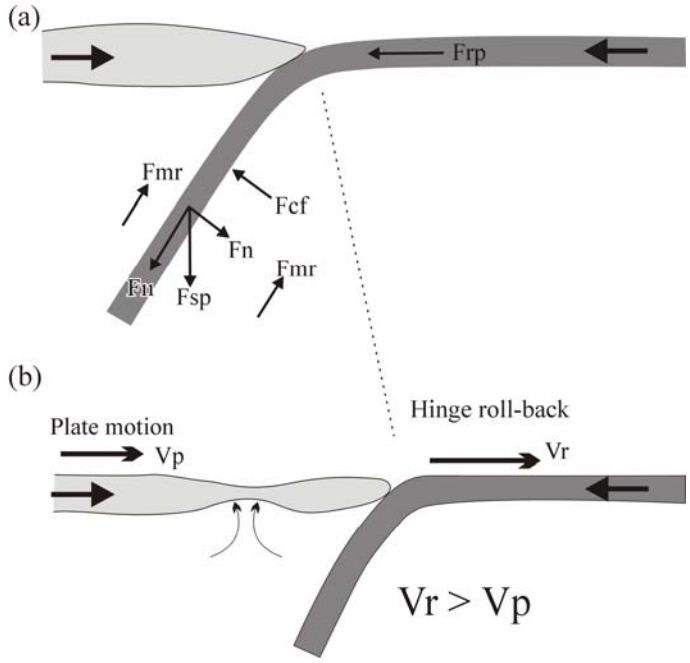


Figure 1.8. The evolution of subduction rollback process with hinge migration. **(a)** Frp: ridge push; Fsp: slab pull; Fcf: corner flow; Fsp is broken into two components, one is Fn and the other Fn; Fmr: viscous resistance of the mantle; see text for detailed description. Vp and Vr vectors are the two components of the vertical negative buoyancy (F) of the subducting slab. If the slab is cold and dense, the component R cannot be supported by the mantle asthenosphere, and the subduction zone is pulled backward; **(b)** back-arc extension forms when the rate of subduction rollback (Vr) exceeds the rate of convergence (Vp) (a) from Spence (1987), and (b) from Lonergan & White (1997).

1.4.4.3. Main causes of the back-arc extension

The development of the extensional tectonics in back-arc settings can be explained in several ways. These models include active diapirism, gradual migration, convection-driven extension, harzburgite diapirism. According to the *active diapirism*, uprising diapir resulted from frictional heating at subduction zone or fluids released from dehydration of downgoing slab causes to split the arc (Karig 1974). Two parts of the splitting arc are progressively separated by seafloor spreading (Figure 1.9a). In the *gradual migration*, it is assumed that subducting slab is snapped off near the hinge and presumably the subducting slab is too light to go down and so a new subduction is initiated at oceanwards. The arc stays near the hinge and the asthenosphere wells up behind it (Figure 1.9b). The model of the *convection-driven back-arc extension* was proposed by Toksöz & Bird (1977). This model requires subsidiary convection cells which are driven by the downward drag of the subducting slab (Figure 1.9c). According to this model spreading would occur 10 My after the start of the subduction. The model of the *harzburgite diapirism* (Oxburgh & Parmentier 1978) depends on the fact that refractory lithosphere is less dense and more buoyant that normal fertile lithospheric mantle, because it has lost its basalts component at mid oceanic ridges. In this case, it would rise when it is heated to same temperature as surrounding mantle material (Figure 1.9d).

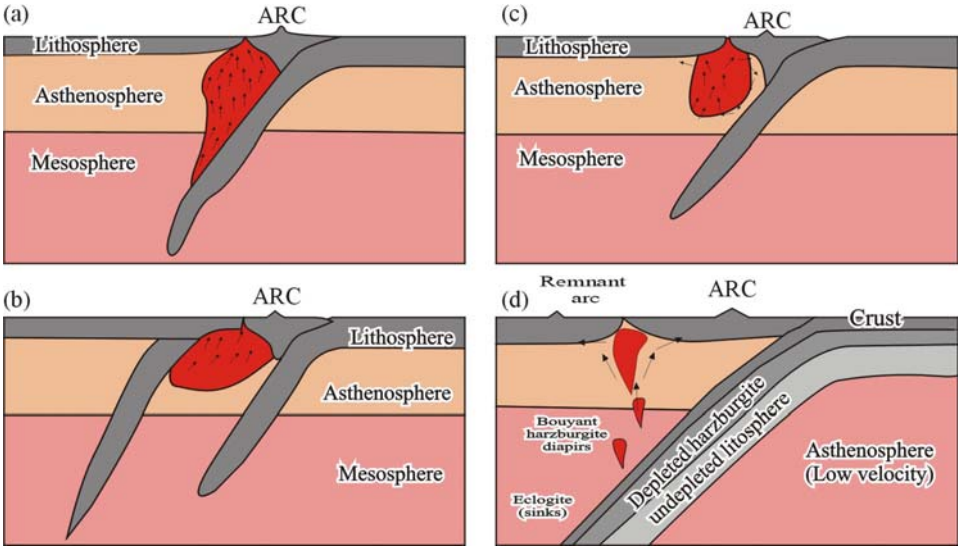


Figure 1.9. Models for back-arc extension: **(a)** active diapirism; **(b)** gradual migration; **(c)** convective-driven extension; **(d)** harzburgite diapirism (from http://www.le.ac.uk /geology/art /gl209/lecture5/lecture5.html).

1.4.4.4. Gravitational collapse and continental magmatism

It was proposed a gravity-driven flow of an orogenic crust under its own weight (von Bemmelen 1954; Bucher 1956; Ramberg 1980; England 1982; Molnar & Chen 1982, 1983; Coney & Harms 1984; McClay *et al.* 1986; Dewey 1988; Ménard & Molnar 1988; Molnar & Lyon-Caen 1988; England & Houseman 1989; Platt *et al.* 1998; Collins & Robertson 1998; Rey *et al.* 2001). This model assumes that gravitational potential energy stored in thickened crust during convergence can be released by way of lateral spreading, thus triggering extension and thinning of the thickened crust (Figure 1.10; e.g., Dewey 1988). When forces that support the lateral contrast in gravitational potential energy that builds up during lithospheric deformation decrease, the gravitational anomaly may relax. Rey *et al.* (2001) reclassified this processes as "divergent" and "convergent" collapse both of which subdivided into fixed- and free-boundary collapse. In Figure 1.10 only divergent modes of collapse has shown with mechanisms of fixed- and free- boundary collapse. In this model the free-boundary represents the subduction zone (Figure 1.10c), as for the case of Aegean region.

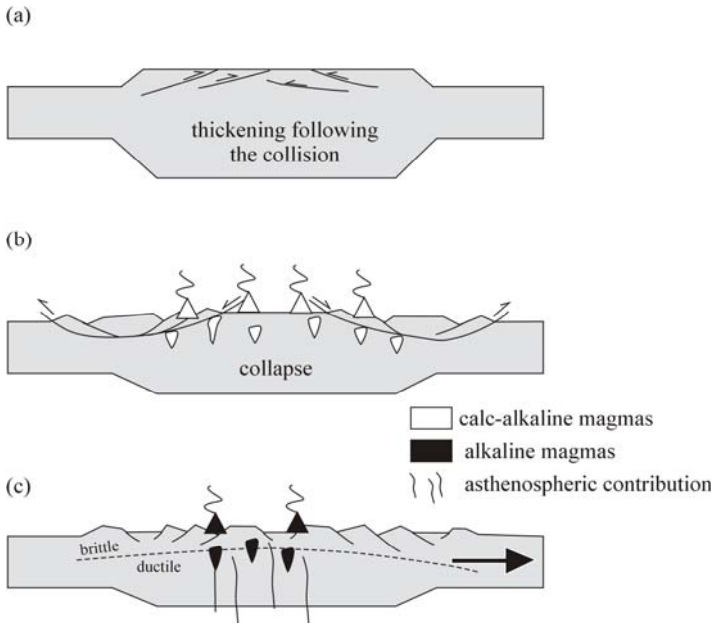


Figure 1.10. Various types of gravitational collapse of an over-thickened crust. **(a)** over-thickened lithosphere prior to collapse; **(b)** fixed-boundary collapse; **(c)** free-boundary collapse (modified from Rey *et al.* 2001). Black arrow in **(c)** shows the movement of the collapsing crust along its free boundary, representing by a subduction zone.

This model was used to explain the basin formation and Late Tertiary volcanic activity in western Anatolia by Seyitoğlu & Scott (1992b), and Seyitoğlu *et al.* (1997). Some workers which accept that the extensional tectonics in western Anatolia began during Late Oligocene and continued until now uninterruptly, suggested that all the magmatic rocks of western Anatolia formed in extensional setting related to orogenic collapse of the over-thickened crust (Seyitoğlu & Scott 1991, 1992b; Hetzel *et al.* 1995b; Seyitoğlu 1997). This model explains the changing in the magma composition in terms of the lithospheric thinning throughout the extension. As the extension goes on, the asthenospheric contribution to the magmas increases, and the composition of the magmas changes from calc-alkali to more alkaline.

1.4.4.5. Lithospheric delamination (removal of thickened lithospheric root)

The delamination and delamination magmatism was discussed widely by Kay & Kay (1993). Lithospheric delamination, which is one of the causes to continental extension and accompanying magmatism after collision, is sinking of dense mantle lithosphere into less dense asthenosphere (Figure 1.11; Bird 1979; Platt & Vissers 1989; Kay & Kay 1991, 1993; Schott & Schmeling, 1998; Platt *et al.* 1998). The delamination of the lithosphere can be thought to be two kinds, one referees to the detachment of an oceanic lithosphere after cessation of a subduction event (slab breakoff), and another describes that the detachment of a continental lithospheric roots of an over-thickened crust after a collisional tectonics. In the both cases, delamination of the lithosphere also causes a regional uplift and orogenic collapse (de Boorder *et al.* 1998).

Lithospheric delamination after continental thickening that follows the collision causes continental magmatism accompanied by lithospheric thinning and exhumation of deep-crustal rocks. This process brings the hot asthenosphere into contact with the Moho (Bird 1979; Aldanmaz *et al.* 2000; Keskin 2003; Elkins-Talton 2005) and promotes massive crustal melting and predicts a progressive migration of the resultant volcanism in the direction of delamination propagation (Turner *et al.* 1999). This model was used by Aldanmaz *et al.* (2000) to explain the Early – Middle

Miocene volcanism in western Anatolia. The melting mechanism of the mantle lithosphere was caused by perturbation of geotherm by heat transfer either a mantle plume or an upwelling asthenospheric mantle. The heat transfer was occurred either by lithospheric delamination of a thickened lithosphere or by detachment of subducted slab (slab breakoff). The slab breakoff model will summarized below.

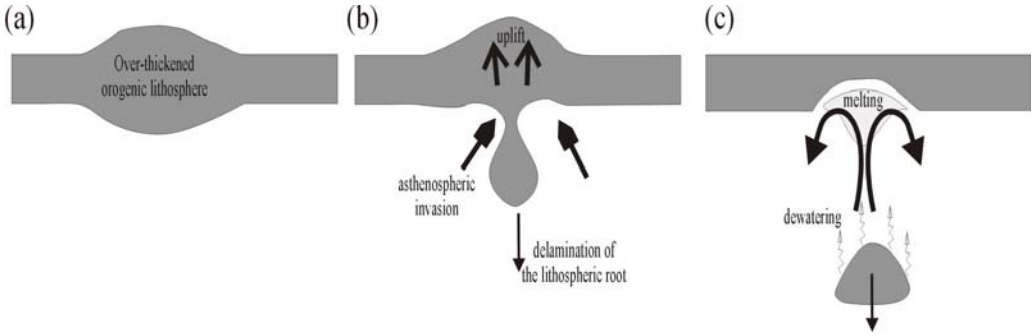


Figure 1.11. Litospheric delamination model. According to delamination model crustal roots beneath the over-thickened crust detaches and regional uplift occurs exhuming the deep-crustal rocks **(a)**. Delamination of the crustal roots leads to asthenospheric invasion **(b).** Heat transfer to the crust and dewatering of the delaminated roots lead to melting overlaying mantle and crust **(c)** (after Elkins-Talton 2005).

1.4.4.6. The model of slab breakoff (slab detachment)

The model of slab breakoff referrers that oceanic lithosphere detaches from continental lithosphere during continental collision just after closuring an ocean (Figure 1.12, von Blanckenburg & Davies 1995; Nemcok *et al.* 1998; Carminati *et al.* 1998a, b; Davies & von Blanckenburg 1999; van der Meulen *et al.* 2000; van de Zedde & Wortel 2001; Atherton & Ghani 2002; Mahéo *et al.* 2002; Coulon *et al.* 2002; John & Parkinson 2002). The subduction of the dense oceanic lithosphere, and buoyant continental lithosphere after the collision, creates opposing buoyancy forces and, this leads to extension in the subducted slab (Davies & von Blanckenburg 1999). The detachment of the slab can occur at depths as shallow as 35 km (van de Zedde & Wortel 2001).

The main effect of the detachment of a lithospheric slab is that the asthenosphere flows up into the gap above the sinking slab and warms up the overlying material can be more than 500^0C. In this case asthenosphere and overriding metasomatised lithosphere begins to partial melting in a few million of years (van de Zedde &

Wortel 2001). These events accompanied by crustal anatexis (Figure 1.12d). In this perspective, the magmas from this lithospheric mantle would carry a subduction component inherited from subduction (metasomatised and enriched mantle), which display a typical subduction-related geochemical imprint (Zeck *et al.* 1992; von Blanckenburg & Davies 1995; Davies & von Blanckenburg 1999; Gvirtzman & Nur 1999; Maury *et al.* 2000). Consequently three-types of melting are expected: (1) asthenospheric melting, (2) partial melting of the lithospheric mantle, and (3) crustal melting (Figure 1.12d). The slab breakoff model has been used to explaining syn-collisional (Atherton & Ghani 2002) and post-collisional (Maury *et al.* 2000; Coulon *et al.* 2002) rifting and magmatism.

It is widely accepted that the slab breakoff process give rise to (1) volcanic rocks with subduction-related geochemistry, and (2) progressive magmatic change from calc-alkaline to alkaline character of magmas (Carminati *et al.* 1998a; Maury *et al.* 2000), which is the predominant features in many subduction-related region (Alboran Region: Carminati *et al.* 1998a; central Mexico: Ferrari 2004; south Tibet: Mahéo 2002; Caledonian: Atherton & Ghani 2002; Taiwan: Teng *et al.* 2000).

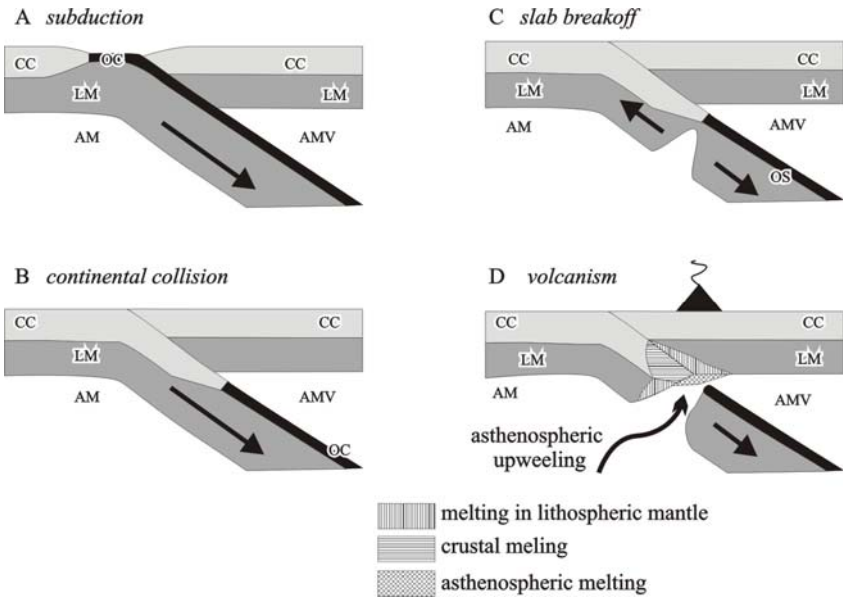


Figure 1.12. The development of slab breakoff [A, B, C: after Davies & von Blanckenburg (1999); D: after Davies & von Blanckenburg (1999) and van de Zedde & Wortel (2001)]. The subduction event **(A)** leads to the continental collision **(B)** between two converging plates. The dense oceanic slab detaches from buoyant continental lithosphere **(C),** and this gives rise to asthenospheric upwelling **(D)**. (*CC*: continental crust; *OC*: oceanic crust; *LM*: lithospheric mantle; *AM*: astenospheric mantle; *AMV*: astenospheric mantle wedge; *OS*: detaching oceanic slab).

CHAPTER TWO

GEOLOGY OF THE SELENDI BASIN

2.1. Introduction

In this chapter, the stratigraphy of the rock units exposed within the Selendi Basin (Figures 2.1 & 2.2) and the contact relationships will be presented.

In this study, mapping was carried out at six localities in the Selendi area in order to: (i) establish the stratigraphy, and (ii) describe tectonic setting and volcanic evolution of the Selendi Basin (Figure 2.3).

The basement rocks – metamorphic rocks (Menderes Massif metamorphics) and granitic rocks (Rahmanlar granite) – are covered by two distinct volcano-sedimentary successions that are separated by a basin-wide angular unconformity: (1) Hacıbekir Group and (2) İnay Group. Ophioilitic rocks of the İzmir Ankara Zone are previously regarded as a part of the basement rocks, but in this study they are included into the Hacıbekir Group. The Hacıbekir Group includes sedimentary rocks (Kürtköyü and Yeniköy formations) and interfingering volcanic rocks (Kuzayır basalt and Eğreltidağ volcanic unit). Kuzayır basalt and Eğreltidağ volcanic unit described for the first time in this study. The outcrops of the Eğreltidağ volcanic unit, around the Eğreltidağ (Figure 2.3), previously mapped as a part of the Beydağ and Karaboldere volcanic units. The İnay Group consists of Ahmetler and Ulubey formations intercalated with Yağcıdağ volcanic unit. İnay group is disconformably overlain by Asartepe formation. The Quaternary Kula basalt forms the products of latest volcanism in the region; it disconformably overlies the older successions.

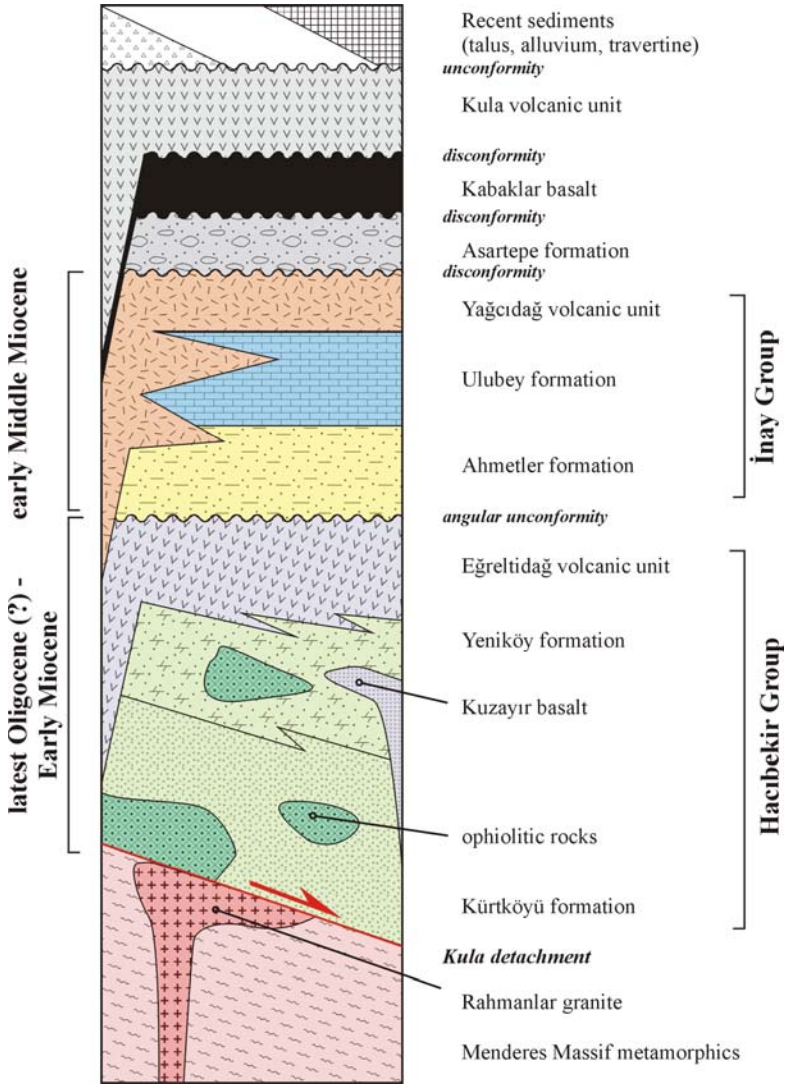


Figure 2.1. Generalized columnar section of the Selendi Basin.

2.2. Menderes Massif metamorphics

Metamorphic rocks of the Menderes Massif comprise augen gneiss, marble and schist. In the Eskin area, metamorphic rocks are represented by augen gneisses. They consist of large K-feldspar and plagioclase porphyroclasts embedded in a fine-grained matrix of feldspar, quartz and mica (both biotite and muscovite). Size of feldspar porphyroclasts may reach up to 4-5 cm. They exhibit well-developed gneissic foliation striking NE and dipping 40-60^{o} NW. In the Kula area, metamorphic rocks are made up mylonitic gneisses, mica schists, garnet-mica schists and locally marbles with northeast-striking foliations varying from 25 to 50^{o}.

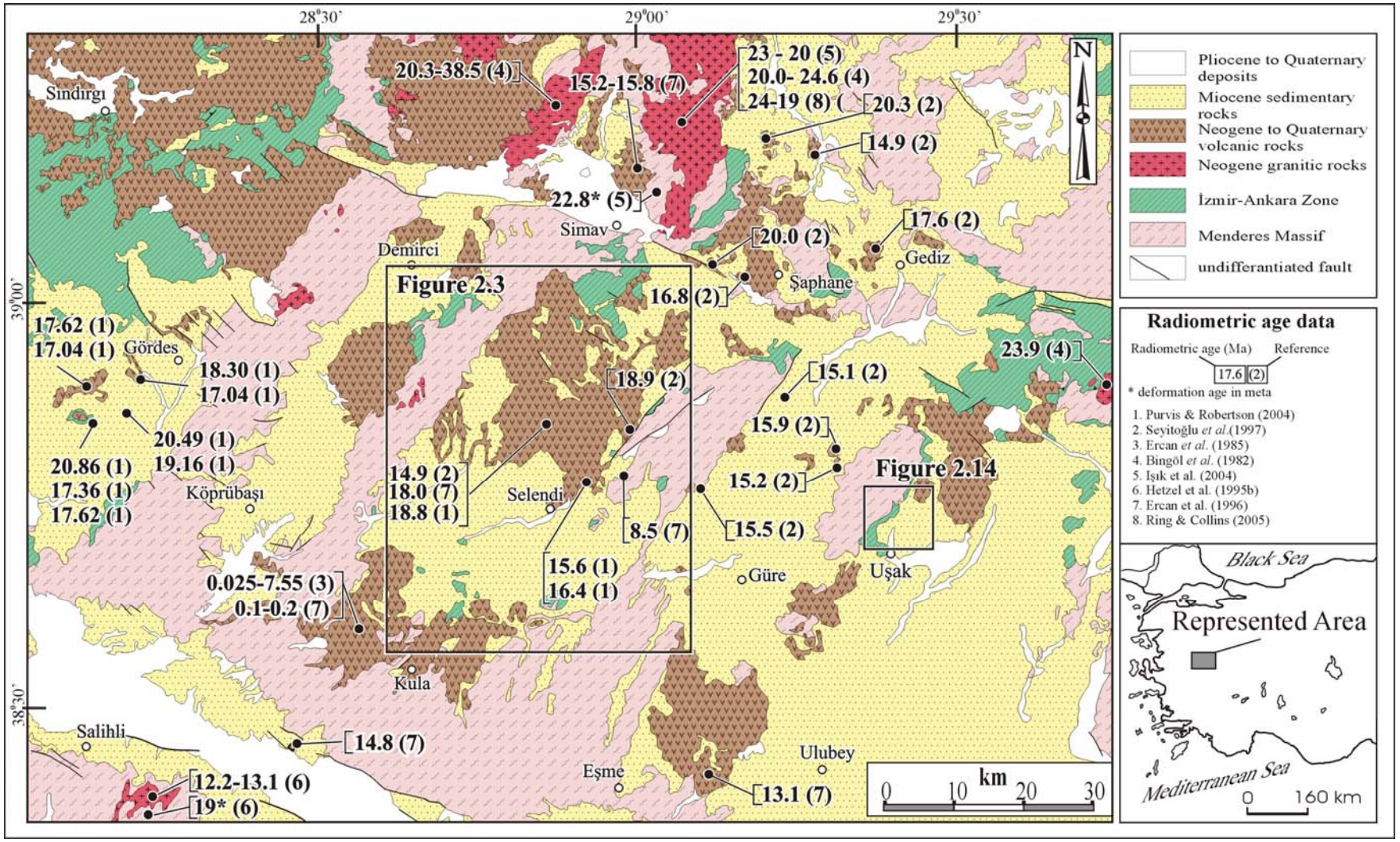


Figure 2.2. Published radiometric age data plotted on the generalized geological map of the Selendi and surrounding region.

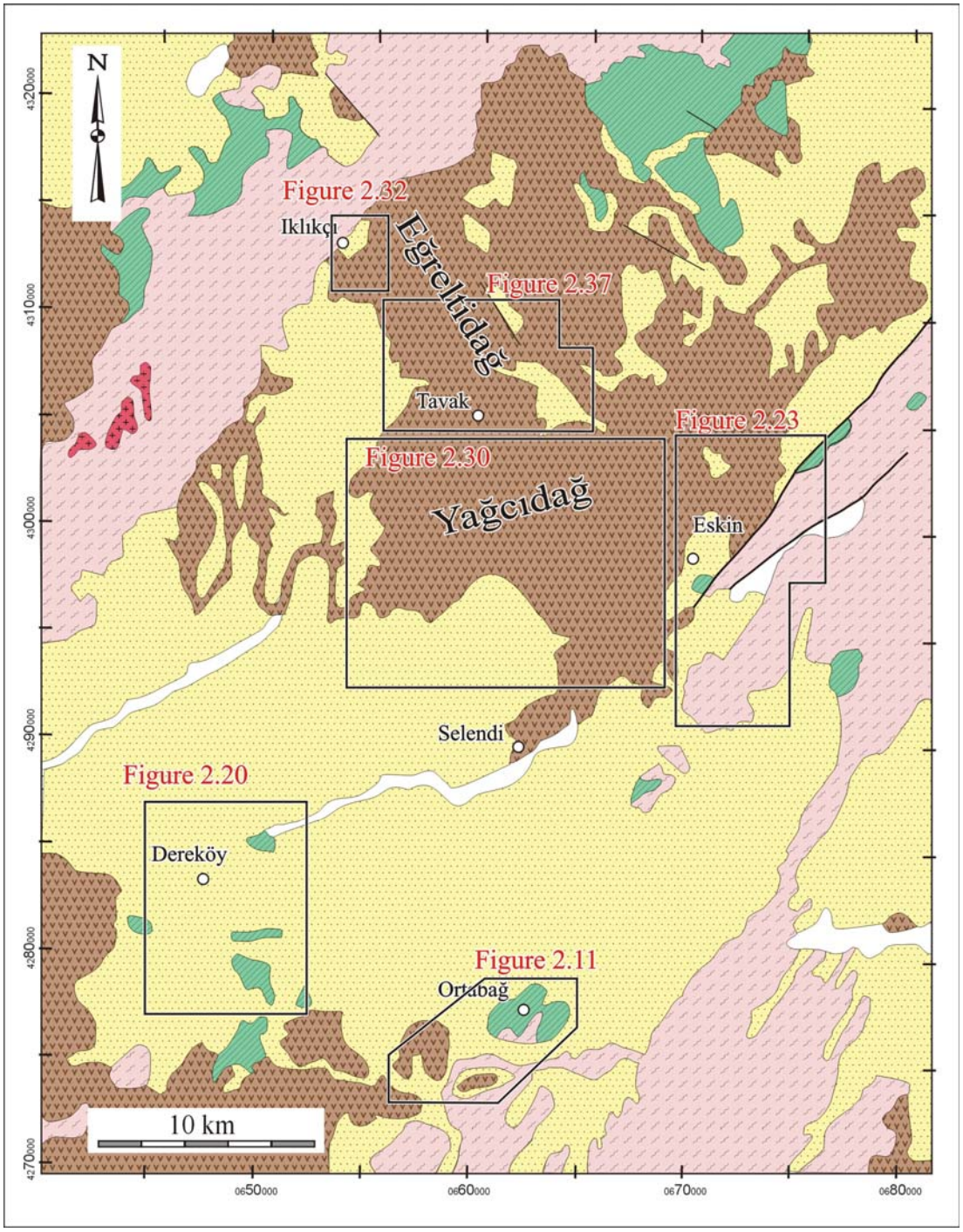


Figure 2.3. Generalized geological map of the Selendi Basin. See Figure 2.2 for location and legend of the rock units.

Mica schists consist of preferably-oriented white mica (muscovite) and fewer biotites. In the garnet-mica schists, garnet porphyroblasts are surrounded by muscovite and biotite. They display typical spiral-shaped inclusion trails and syn-tectonic deformational structures that indicate top-to-the-NE sense of shear (Figures

2.5, 7 and 10). Marbles, which crop out in the north of the Kula area, consist mainly of recrystallized calcite and rare muscovite.

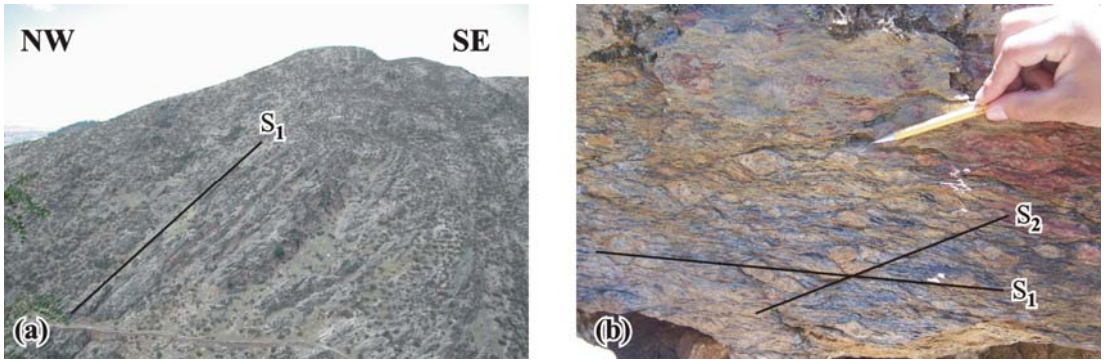


Figure 2.5. Field photos showing well-developed mylonitic gneisses and related structures. **(a)** the gneissic foliation dipping 40-55^{o} NW and **(b)** the rock display two distinct fabrics with former S_1 gneissic foliation and overprinting S_2 shear band foliation. The S_2 indicates a top to NE sense of shear.

2.3. Rahmanlar granite

Two granitic stocks, which crop out in the Eskin area between Rahmanlar and Çakırlar villages, are equigranular garnet-bearing granites and include xenoliths of high-grade metamorphic rocks such as migmatites, gneisses, quartzite and several schists. The stocks intruded into the mylonitic gneisses of the Menderes metamorphics (Figures 2.6 and 2.23). Although the granitic stocks usually appear to be equigranular, they display increasing foliation through the outer contact with host rock. It is important to note that there is no any contact metamorphic aurora and their contact is characterized by a shear zone.

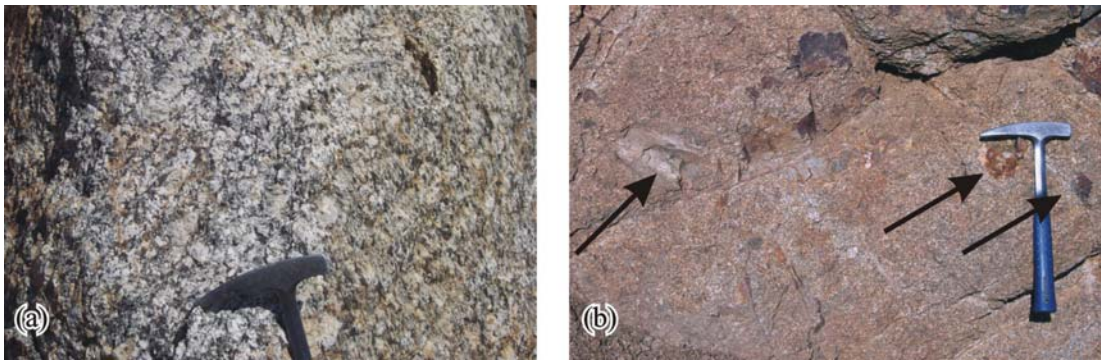


Figure 2.6. Field views of the Rahmanlar granite. **(a)** equigranular texture and **(b)** high-degree metamorphic xenoliths (arrowed) of country rock enclosed within the granite. Hammer is 33-cm long.

2.3.1. Deformation

The metamorphic rocks of the study area display evidence for two distinct phases of deformation, D_1 & D_2. D_1 is observed only in the metamorphics while D_2 was also affected the Rahmanlar granite.

D_1 deformation is characterized by a penetrative S_1 gneissic foliation defined by alternating quartz-feldspar; and mica-rich bands (Figure 2.5). S_1 foliation is restricted to metamorphic rocks and not affected the Rahmanlar granite. S_1 gneissic foliation commonly strikes NE-SW and dips NW (Figures 2.10). D_1 deformation was attributed to the main Menderes metamorphism by many workers (Şengör & Yılmaz 1981; Şengör *et al.* 1984; Bozkurt 1995; Dora *et al.* 1995; Hetzel *et al.* 1995a, b, 1998; Bozkurt & Satır 2000; Okay 2000, 2001).

D_2 deformation affected both of the Menderes metamorphics and Rahmanlar granite, and produced a S_2 mylonitic foliation and L_2 stretching mylonitic lineation. S_2 mylonitic foliation is characterized by aligned micas and recrystallized and elongated quartz (Figures 2.8 and 2.9). S_2 mylonitic foliation commonly strikes NE and dips NW as well as S_1 foliations. L_2 mylonitic stretching lineation plunges towards mainly NE and less SW (Figures 2.10 and 24).

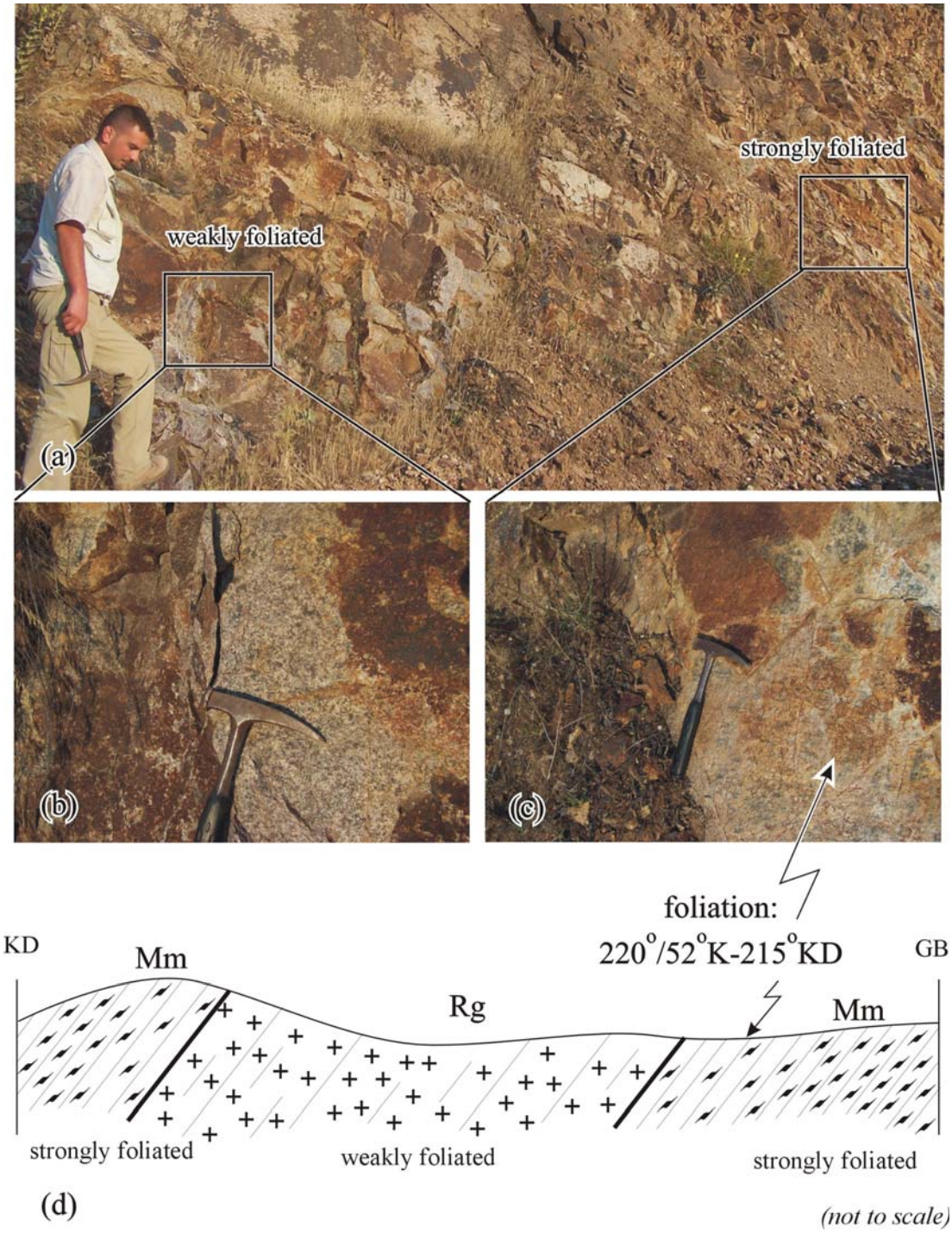


Figure 2.7. Tectonic contact relationship between the Rahmanlar granite and the Menderes metamorphics: **(a)** field view of the contact showing contrast in the degree of the foliation in granite to the hosting metamorphics, **(b)** close-up of the weakly foliated granite, **(c)** close-up of strongly foliated granite, **(d)** schematic cross-section showing the contact relationship between Rahmanlar granite (Rg) and Menderes metamorphics (Mm). Hammer is 33-cm long.

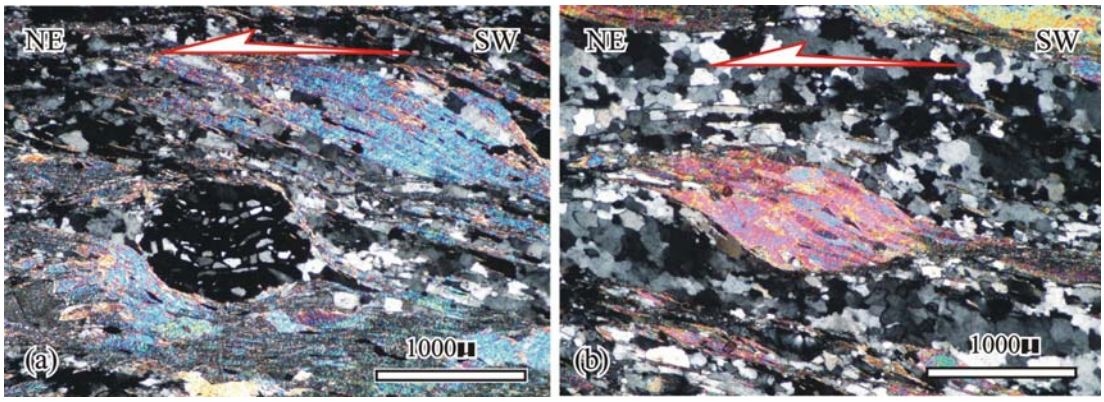


Figure 2.8. Thin section views showing asymmetrical microstructures in the mica schists and garnet-mica schists; **(a)** mica "fish" structure (+N); **(b)** syn-tectonic garnet porphyroclast with quartz inclusions and non-fibrous strain shadows (+N). Samples are cut perpendicular to the foliation and parallel to the stretching lineation. Both microphotographs are crossed Nichols. Both kinematic indicators indicate top-to-the-NE (dextral) sense of shear.

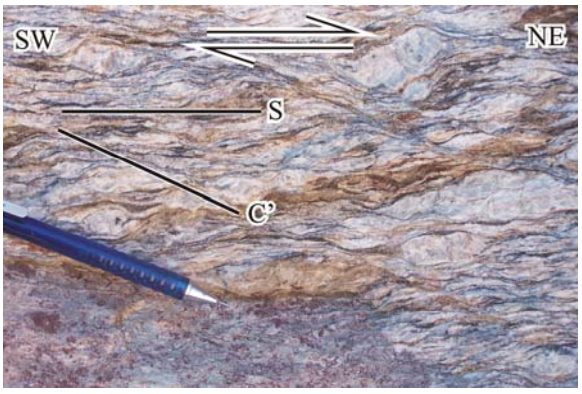


Figure 2.9. Field photograph of mylonitic gneisses displaying S-C' fabrics from eastern border of Selendi Basin. S and C' planes are defined by feldspar porphyroclasts and aligned micas respectively. S= S-plane, C'= C'-plane, C' refers the S_2 foliation. Photograph parallel to the stretching lineation and normal to the foliation. The fabrics are consistent with op-to-the-NE (dextral) shearing. Pencil is 13-cm long.

Asymmetrical porphyroclasts, mostly common in mylonites, are predominantly composed of K-feldspar, plagioclase, garnets and polymineralic aggregates of feldspar, quartz and micas (both of muscovite and biotite). Feldspar porphyroclasts are similar to the σ-type porphyroclasts described by Passchier & Simpson (1986) and Passchier & Trouw (1996). They have narrow mantles and elongated tails of variably sized dynamically recrystallized quartz, feldspar and mica indicating top to NE sense of shear (Figure 2.8). In some samples garnet porphyroclasts includes quartz inclusions and show non-fibrous strain shadows (Figure 2.8b). Mica fishes are inclined with a narrow angle to the mylonitic foliation indicating top to NE sense of shear (Figure 2.8a). Well-developed C'-type shear band cleavages in mylonitic

gneisses (Figure 2.9) also indicate top to NE sense of shear. D_2 deformation has been accepted as extensional structures in this study. The evidence to this are: (1) S-C angular relationship, (2) displaced broken grains of feldspar in a ductile matrix, (3) obliquely elongate recrystallized grains and subgrains of quartz to the main foliation (4) asymmetric mica "fish" structures, (5) ductile to brittle transition in the deformation towards the low-angle fault all together indicate top to NE normal sense of shear. Therefore, D_2 deformation and related textural features is thought to be related to the exhumation of the Menderes Massif, associated NNE-SSW-directed crustal extension in late Tertiary in western Anatolia (cf. Bozkurt & Park 1994, 1997a, b; Hetzel *et al.* 1995a, b; 1998; Emre & Sözbilir 1997; Koçyiğit *et al.* 1999a; Bozkurt 2001a, b; Gessner *et al.* 2001a, b; Lips *et al.* 2001; Işık & Tekeli 2001, Işık *et al.* 2003, 2004).

2.4. Ophiolitic rocks

Ophiolitic rocks, previously named as Vezirler mélange, consist of serpentinite and ultramafic rock slices and recrystallised limestone blocks in a matrix composed of sandstone and mudstone intercalations. In some locations, serpentinites contain magnesite occurrences due to the alteration of these rocks. Silicification of ultramafic rocks and limestones extensively occurs and can be observed directly on the metamorphic rocks along low-angle faults (Figure 2.10).

2.4.1. Contact relationships between ophiolites and the Menderes Metamorphics

Ophiolites overlie the Menderes metamorphics along a tectonic contact. The contact is well exposed in the south of the Ortabağ village (Figures 2.11 and 12). The contact is gently northeastward dipping where dip amount ranges between 10-13^{o} and the slickenlines plunge toward NE (Figure 2.12). This contact is also correlated with the shear zone between the Rahmanlar granite and the Menderes metamorphics, and is interpreted as a detachment fault.

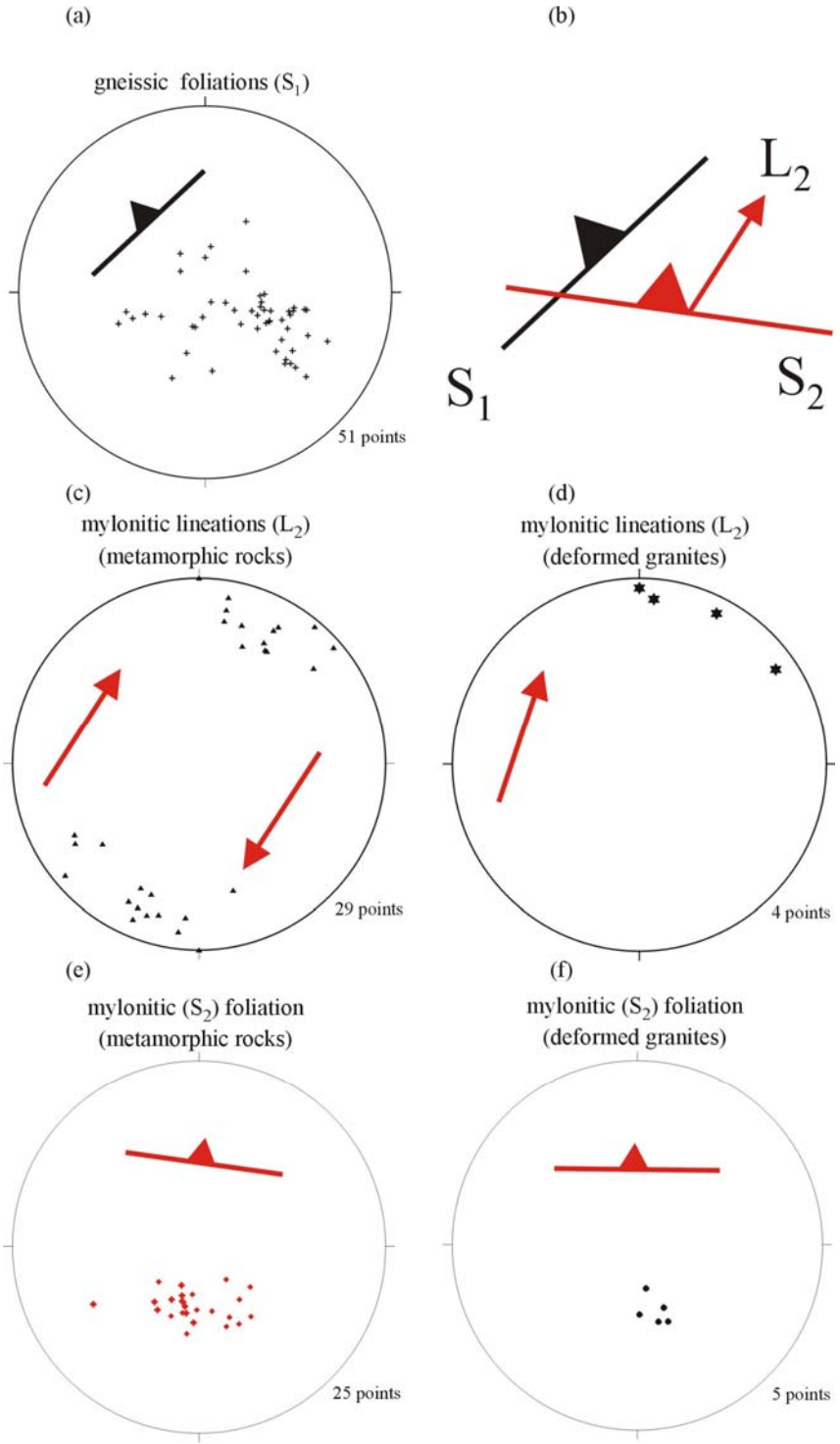


Figure 2.10. Lower hemisphere equal-area stereographic plots of poles to **(a)** gneissic foliation (S_1), **(b)** The cross-cut relation between S_1 and S_2, (c-d) mylonitic lineations (L_2) of metamorphics and the granite, **(e-f)** mylonitic foliation (S_2) and lineation (L_2) of metamorphic and granitic rocks in Selendi Basin.

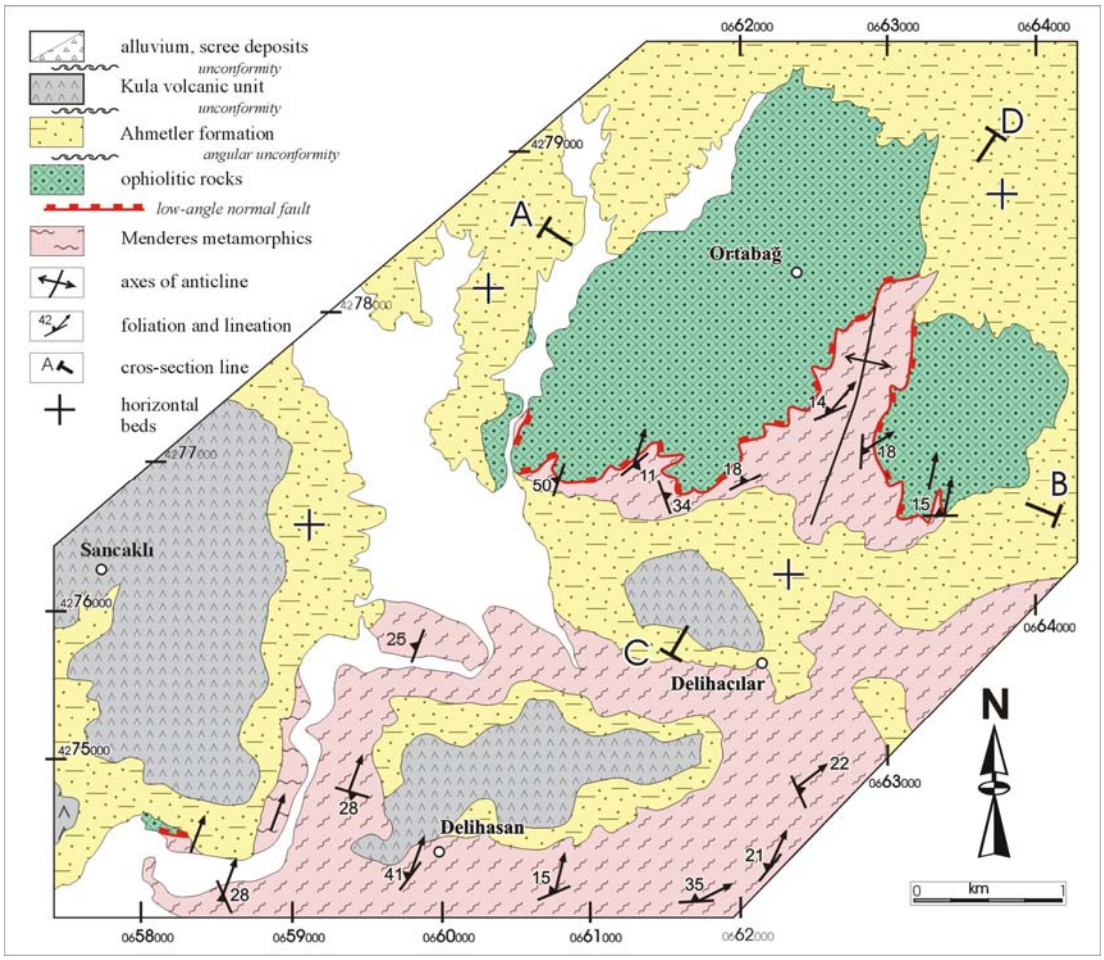


Figure 2.11. Geological map of the Ortabağ area. See Figure 2.3 for location.

The detachment surface from the Ortabağ area is also characterized by NE-trending corrugations. Strikes of the corrugations are parallel to the slickenlines. The anticline axes in this area (Figure 2.11) also parallel to the corrugations, and these may closely be associated.

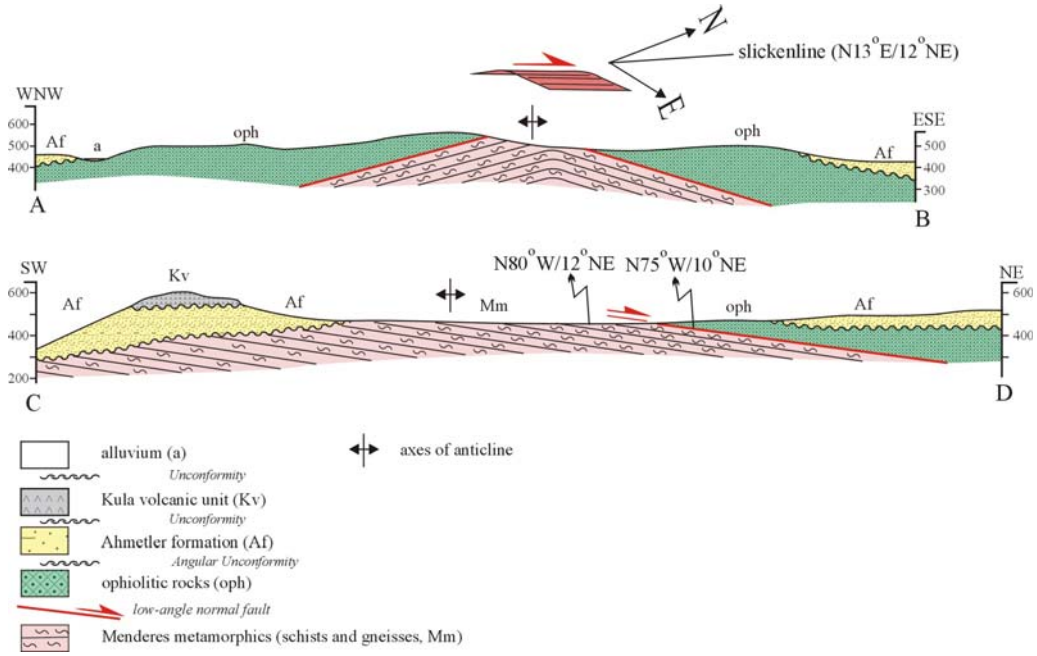


Figure 2.12. Cross-sections showing the contact relationship between ophiolitic rocks and the Menderes metamorphics from the Ortabağ area. See Figure 2.11 for location.

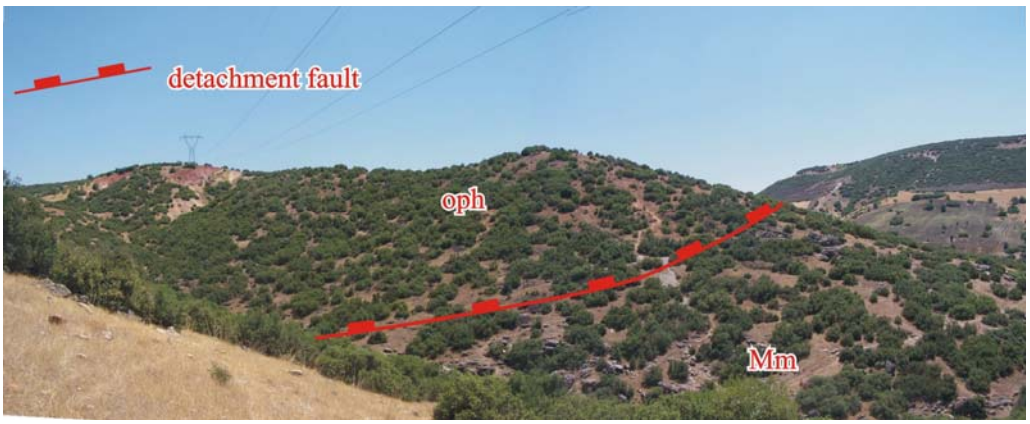


Figure 2.13. Field photo showing the contact relationship between ophiolitic rocks and the Menderes metamorphics.

2.5. Hacıbekir Group

The name Hacıbekir group was first introduced by Ercan *et al.* (1983) in the Uşak basin. This study has shown that the group in the Uşak-Güre and Selendi Basins displays different lithological, sedimentological and tectonic features. Field-based work, including measured stratigraphic sections, geologic mapping and

sedimentological determinations, was carried out in order to demonstrate differences of successions in the each basin.

2.5.1. Hacıbekir Group exposed within the Uşak-Güre basin

In the Uşak Basin, the Hacıbekir group begins with ophiolite-derived conglomerates (Kürtköyü formation) that unconformably overlie the ophiolitic rocks (Figures 2.14 and 15). These conglomerates vertically pass into metamorphic-derived conglomerates (composed of several schists, marble and quartzite) coal-bearing sandstone alternations through the upper parts and then massive limestones appear (Figure 2.17 and 18). Syn-sedimentary faults are common throughout the section. Most important characteristic of the unit in the Uşak Basin is the presence of post-sedimentation shear structures at the base of the unit, which may indicate a NE-directed movement of the Hacıbekir Group (Figure 2.16). Another structural feature is the abundance of southwest-tilted beds within the Hacıbekir Group (Figure 2.14).

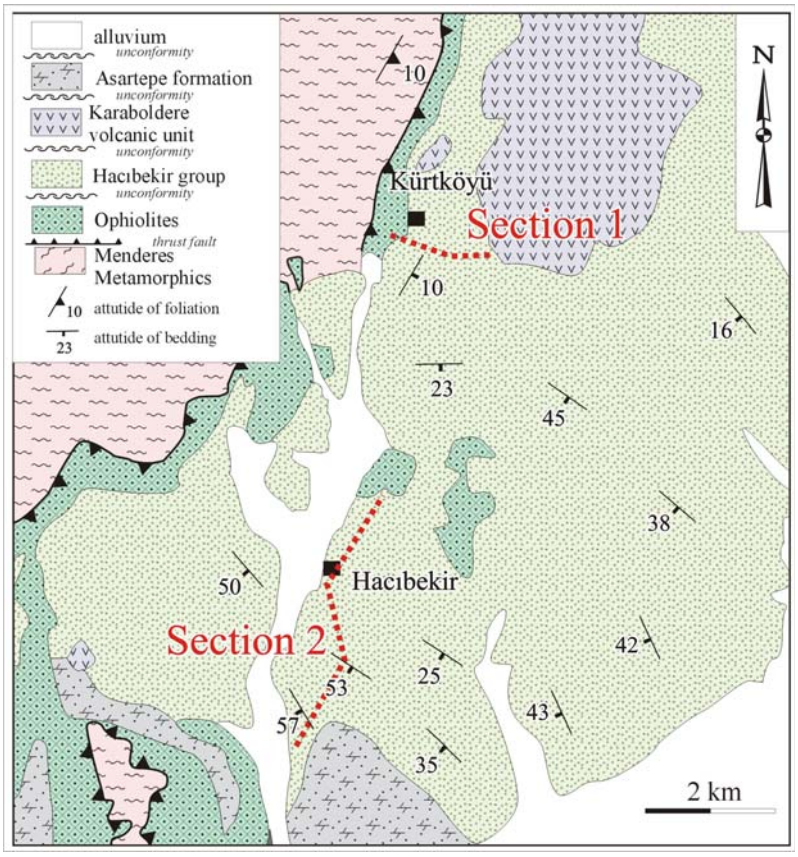


Figure 2.14. Geological map showing distribution of Hacıbekir Group and lines of measured sections. See Figure 2.2 for location.

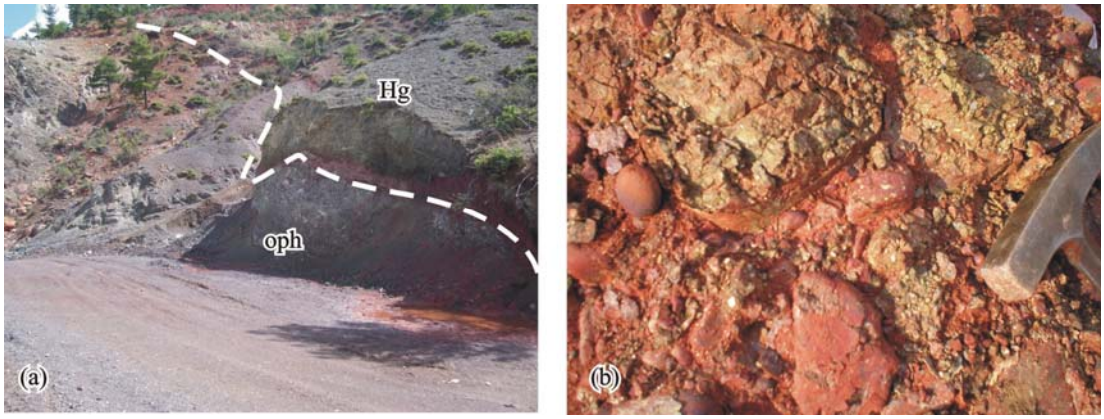


Figure 2.15. Field photos of Hacıbekir Group: **(a)** angular unconformity between ophiolites and Hacıbekir group (Kürtköyü formation), and **(b)** close-up of ophiolite-derived conglomerates from Uşak-Güre basin.

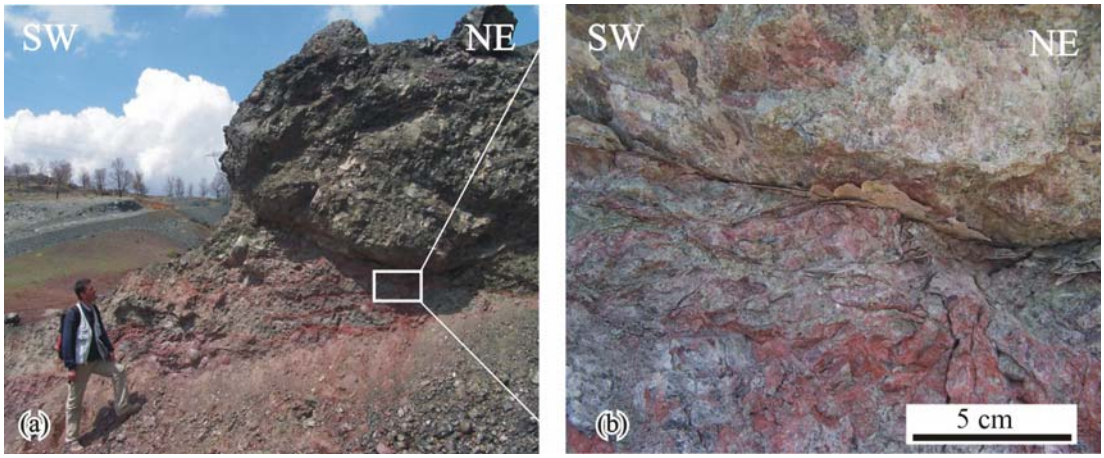


Figure 2.16. Field photos of post-sedimentary deformation structures at the base Kürtköy formation. (**a** and **b**). The shear sense indicates a NE-directed movement of the Hacıbekir Group in the Uşak-Güre basin.

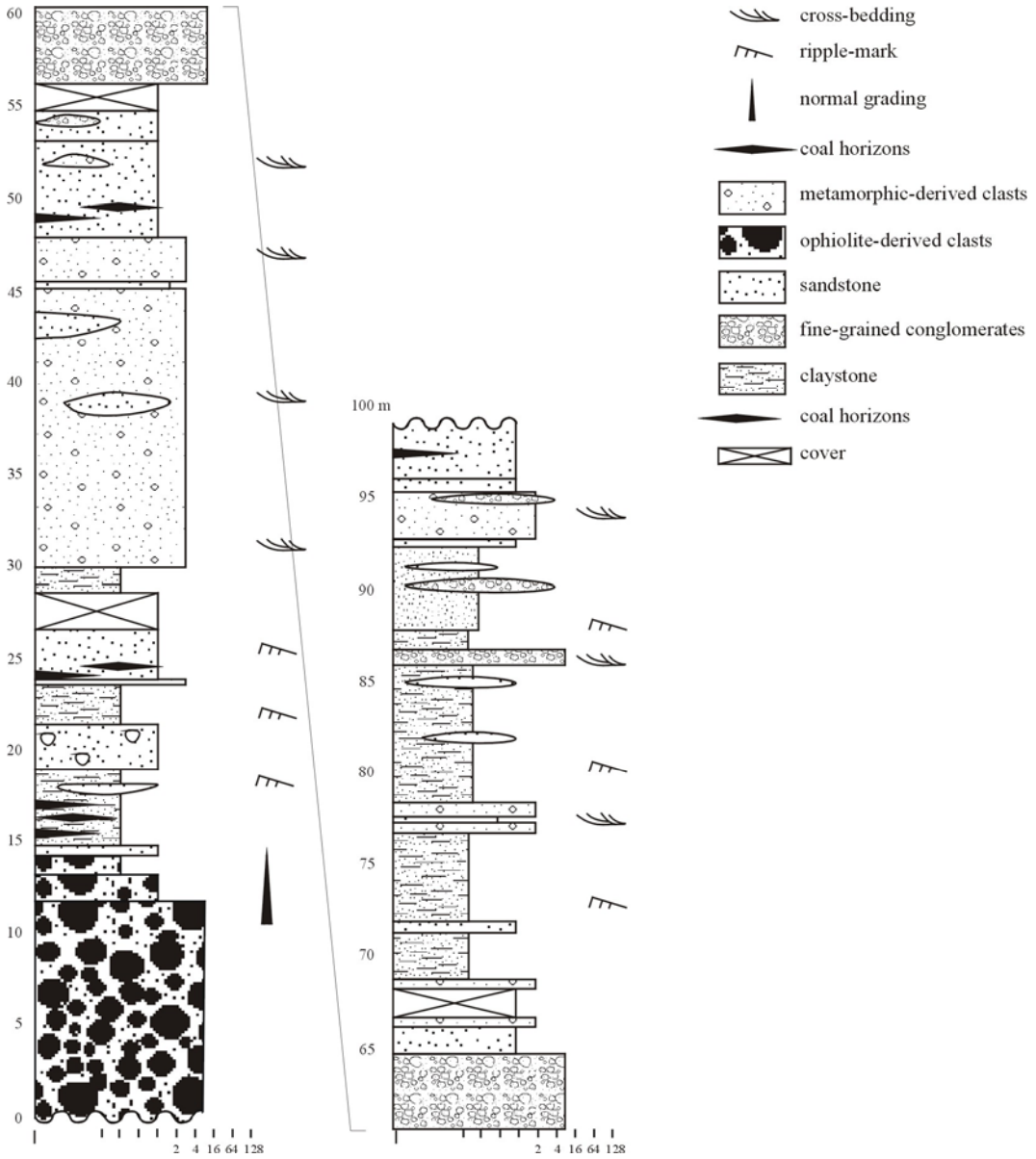


Figure 2.17. A reference section from the Hacıbekir Group (Section I in Figure 2.14).

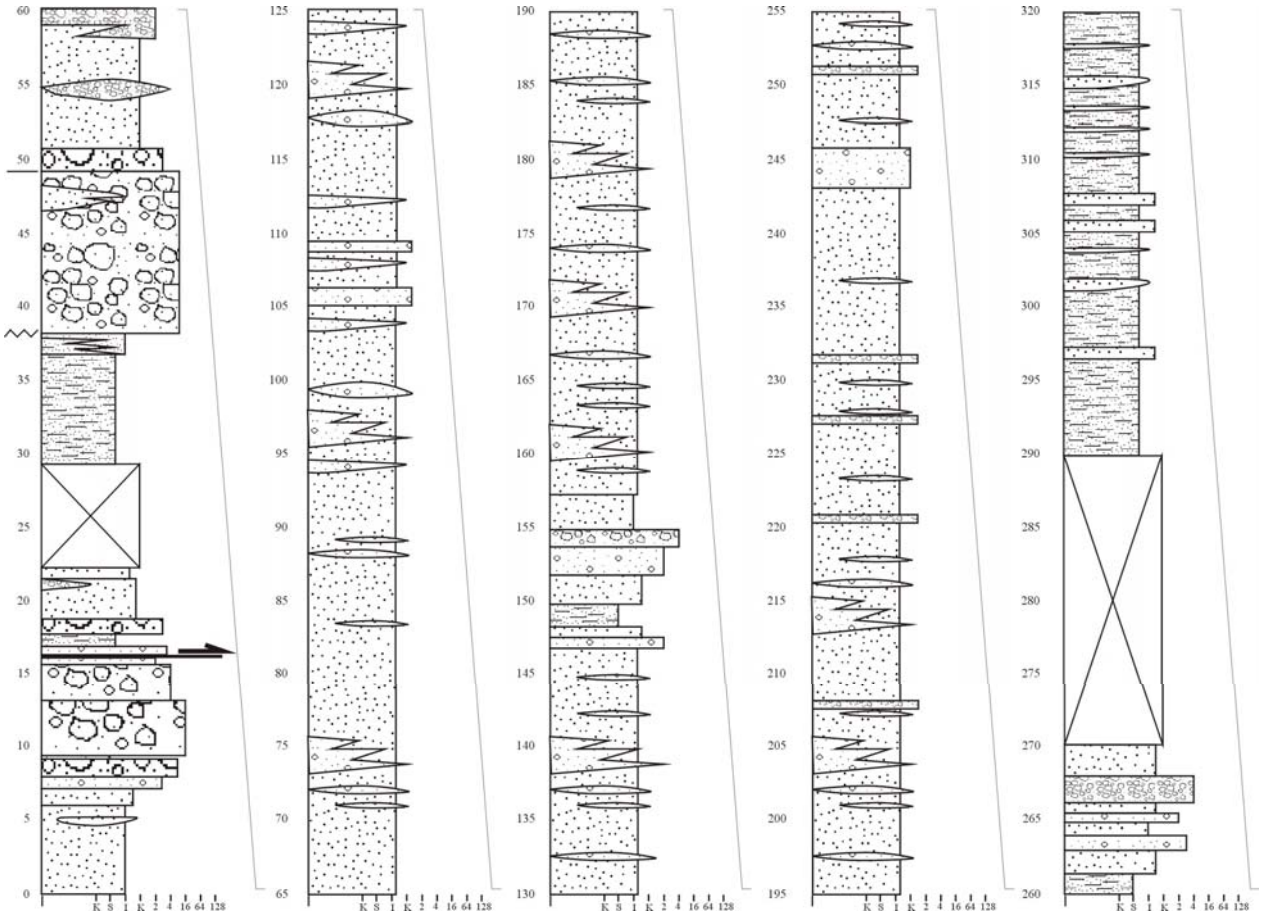


Figure 2.18. Type section from the Hacıbekir group (Section II in Figure 2.14) See Figure 2.17 for legend.

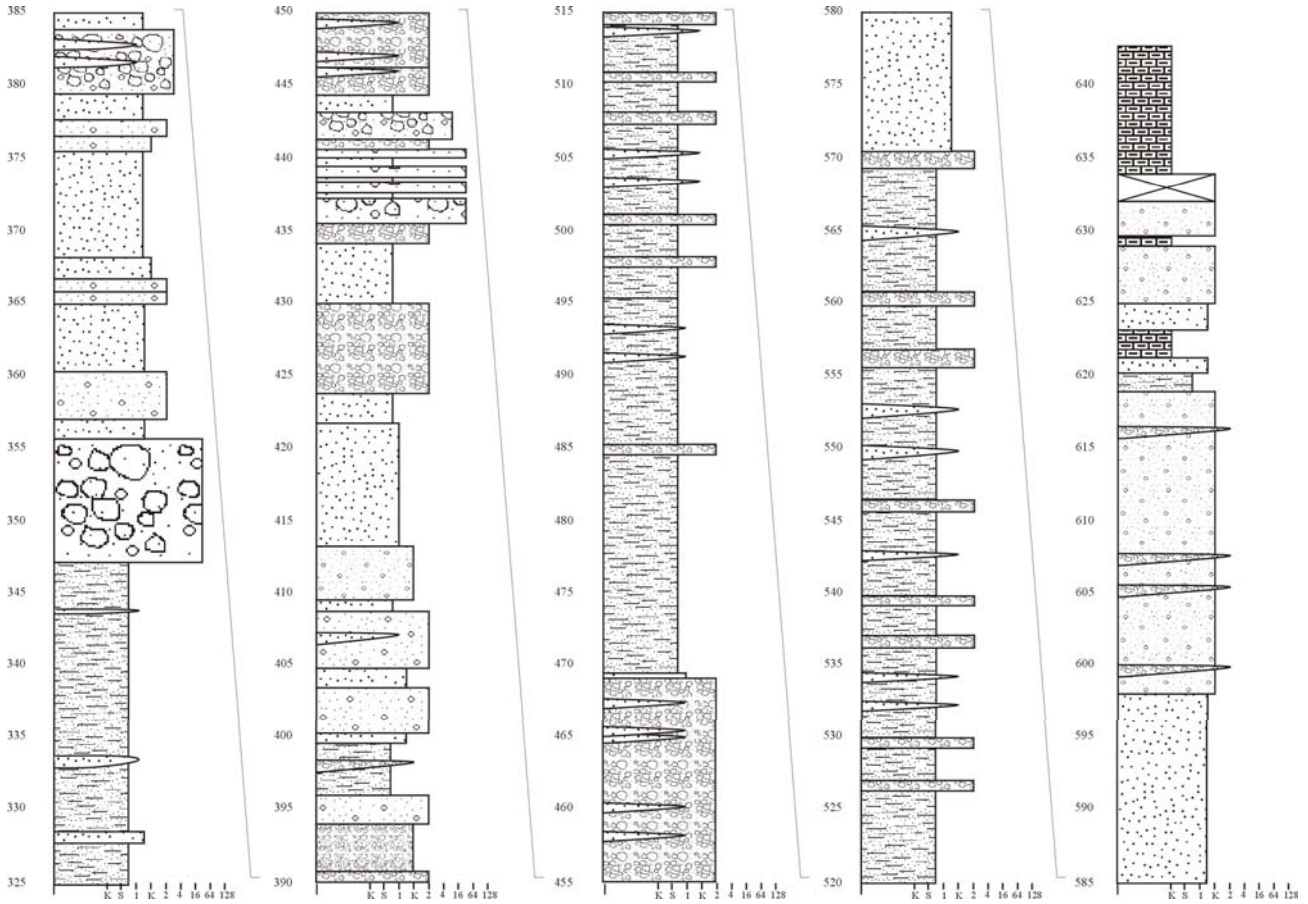


Figure 2.18 continued

2.5.2. Hacıbekir Group exposed in Selendi Basin

In the Selendi Basin, the Kürtköyü formation is characterized by conglomerate, sandstone and minor limestone and claystone intercalations (Figures 2.19 and 20). Kürtköyü formation crops out in a large region in Dereköy area. Conglomerates are massive to thick-bedded (up to 1 m) and are made up of metamorphic clasts derived form Menderes Massif (Figure 2.19). Sandstones are usually interbedded with claystones and limestones. Sandstone and conglomerate intercalations generally include sedimentary structures such as normal and reverse grading, channel-fill structures and cross-bedding.

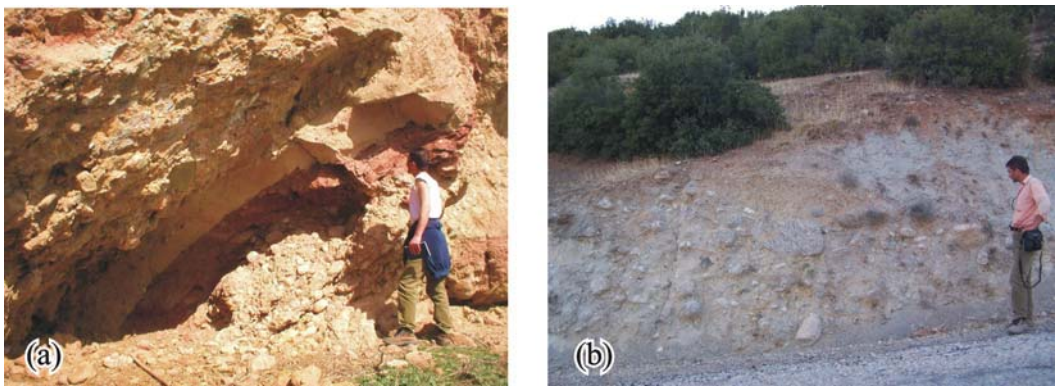


Figure 2.19. Field photos from the Kürtköyü formation: **(a)** conglomerate-sandstone alternation, and **(b)** metamorphic-derived (mainly augen gneisses of the Menderes Massif) conglomerates.

Most important characteristic of the unit is the presence of olistostromal blocks of ophiolitic rocks and recrystallised limestones. The size of the blocks may reach up to 1 km in diameter and are inferred to have been derived from the rocks of the İzmir Ankara Zone (Figure 2.21). The clastic rocks of the Kürtköyü formation show soft-sedimentary deformation structures along the contact. This contact has been previously mapped as a stratigraphic unconformity (Ercan *et al.* 1983; Seyitoğlu 1997; Purvis & Robertson 2004, 2005b).

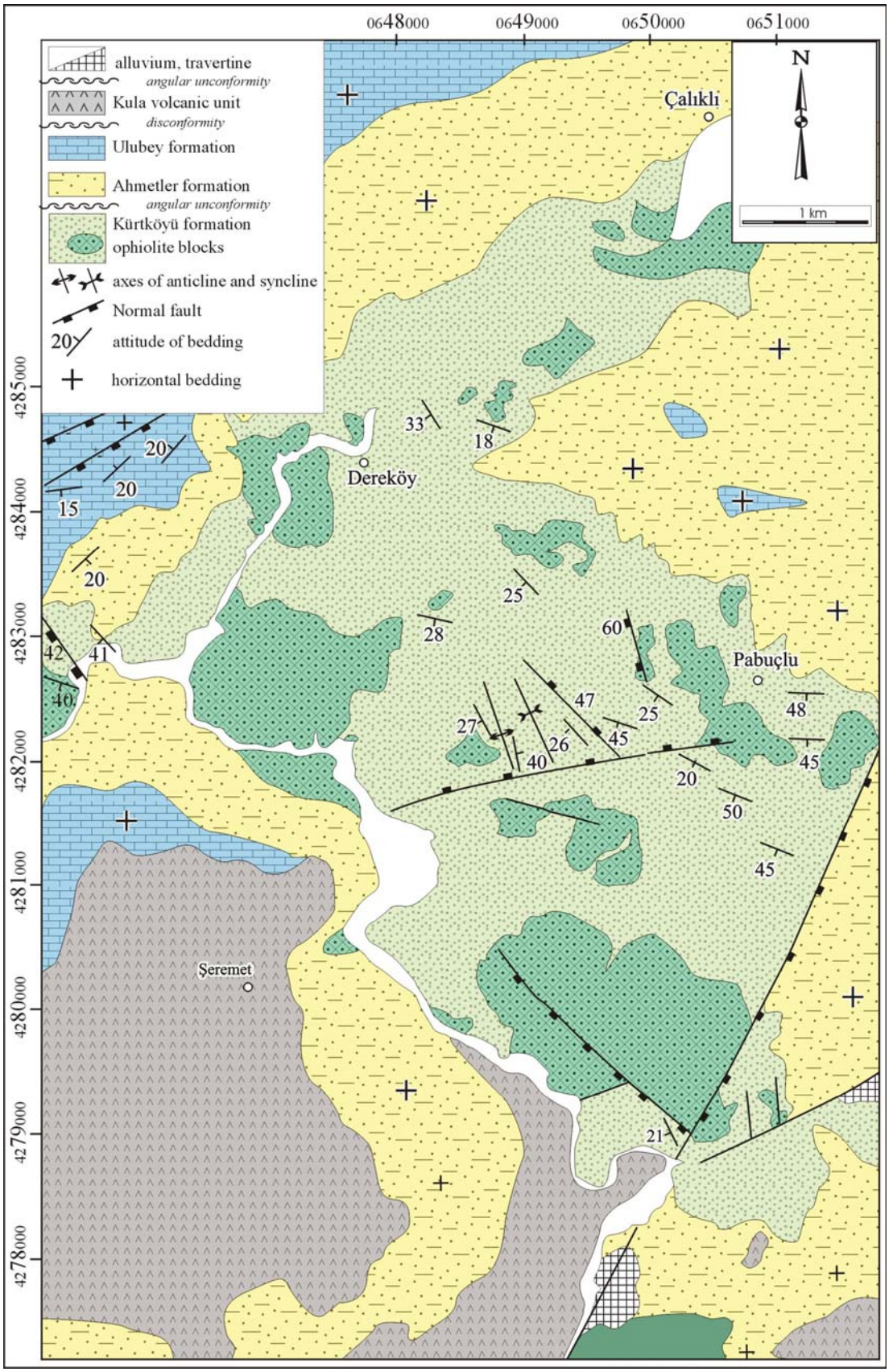


Figure 2.20. Geological map of the Dereköy-Çalıklı area. See Figure 2.3 for location.

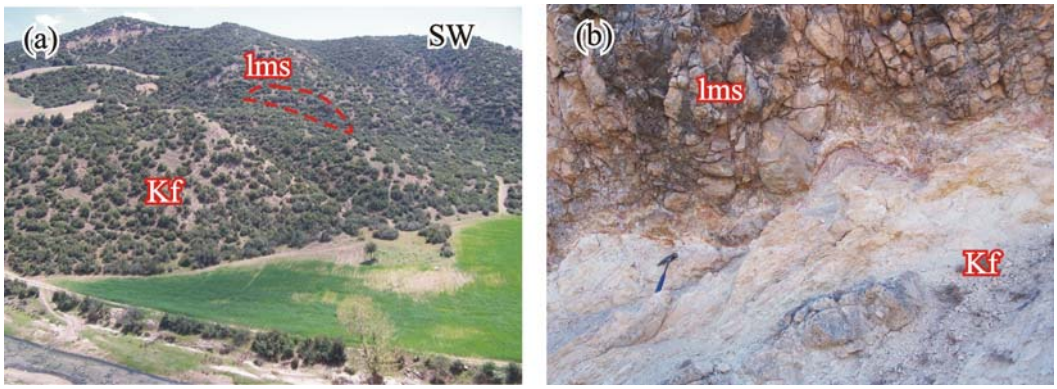


Figure 2.21. Field photos of the limestone blocks: **(a)** limestone blocks (lms) are surrounded by southwestward tilted coarse-grained conglomerates of the Kürtköyü formation (Kf), and **(b)** close-up of this contact. Hammer is 33-cm long.

Yeniköy formation crops out in Tavak, Iklıkçı and Eskin areas and consists of sandstone, claystone and minor conglomerate intercalations (Figures 2.23-26). Sandstones within the unit are represented by turbiditic beds (Figure 2.25). Most of the turbiditic sandstone beds include top-missing bouma sequences (an ungraded coarse - sand at the bottom [Ta], parallel lamination [Tb], and cross – lamination at the top [Tc]; Bouma 1962). The unit contains several olistoliths of ophiolitic rocks in variable clast sizes from metres to kilometers in diameter (Figure 2.26). The Yeniköy formation is also intercalated with Kuzayır basalt and is conformably overlain by Eğreltidağ volcanic unit (Figures 2.4, 2.30 and 2.31).

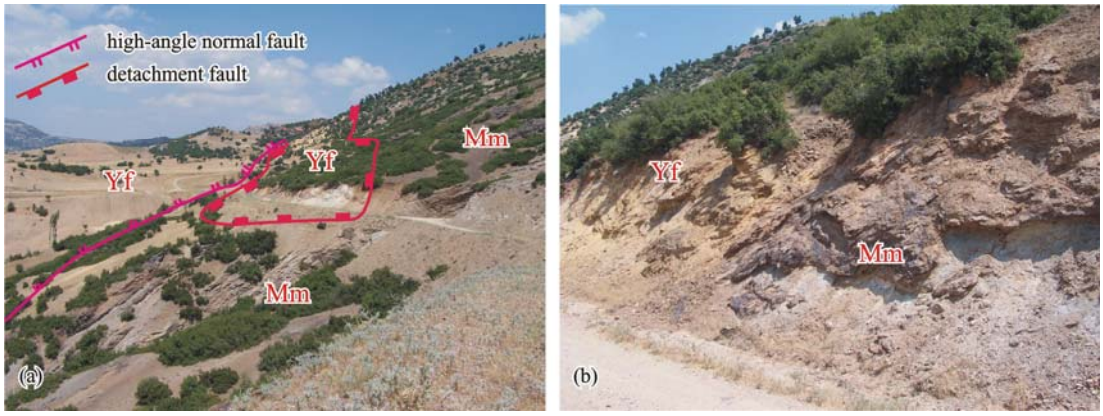


Figure 2.22. Field photos of tectonic contacts between the Yeniköy formation and the Menderes metamorphics. The contact zone is characterized by manganiferous and barite-bearing mineralizations.

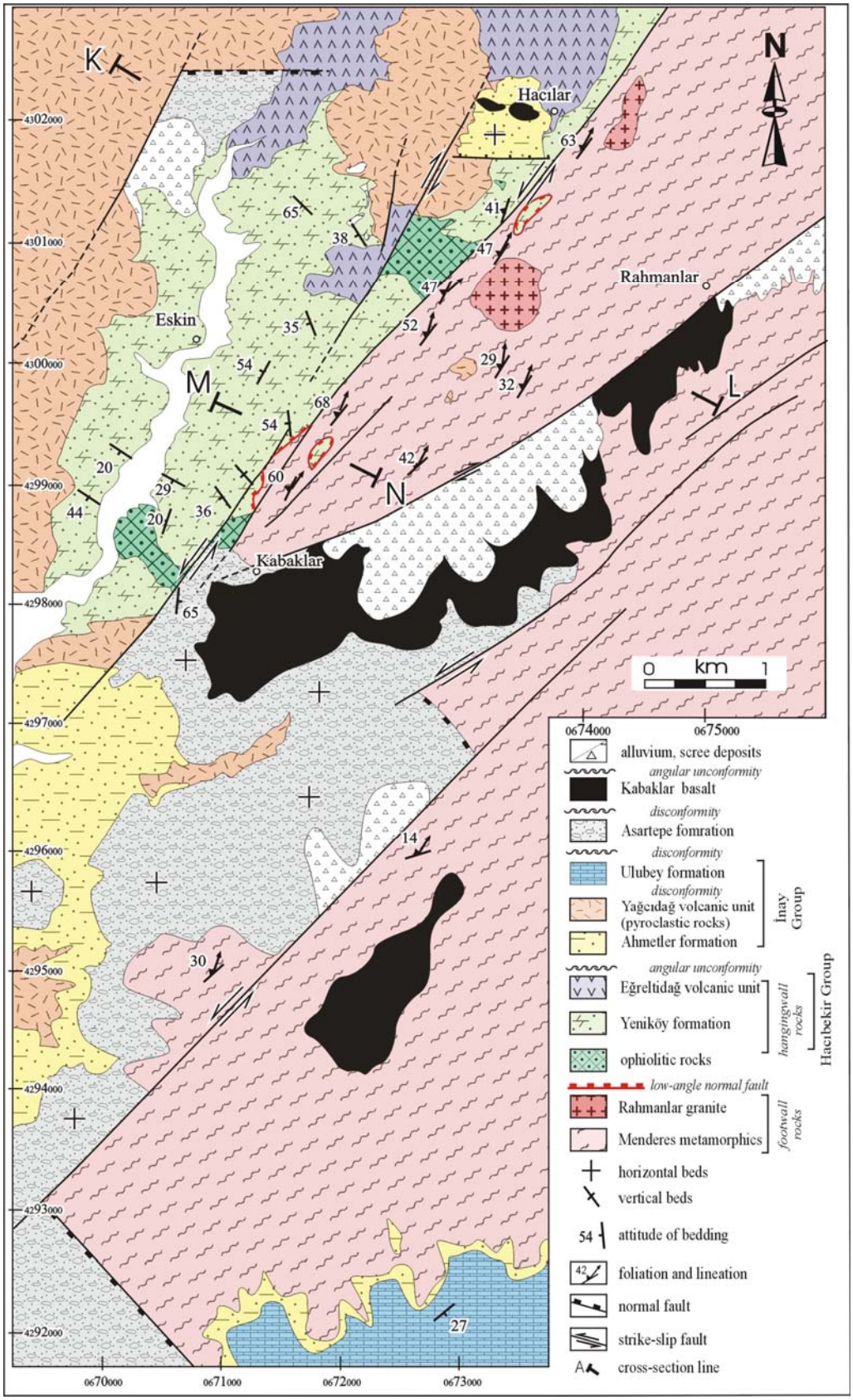


Figure 2.23. Geological map of the Eskin area. See Figure 2.3 for location.

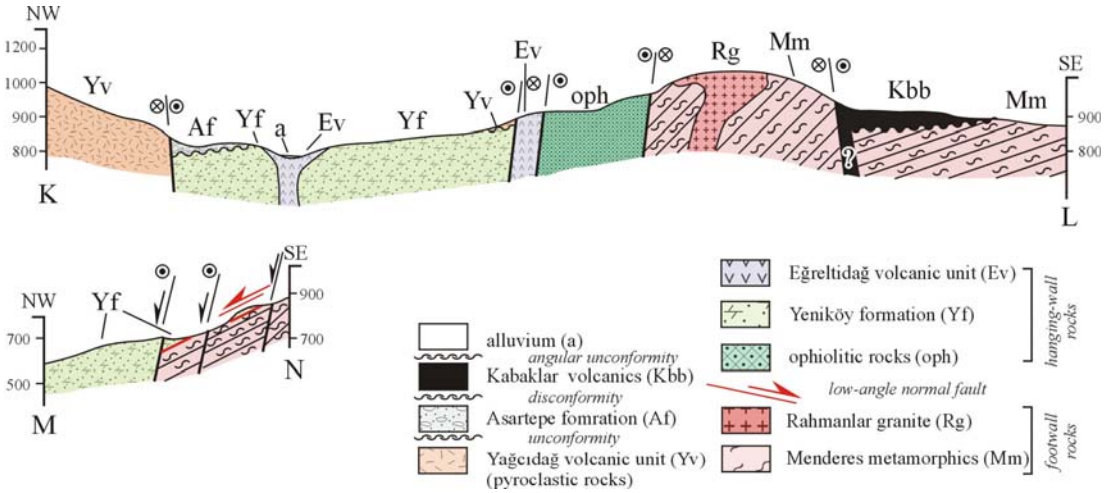


Figure 2.24. Cross sections showing the contact relationship between the rocks units from trhe Eskin area. See Figure 2.23 for location.

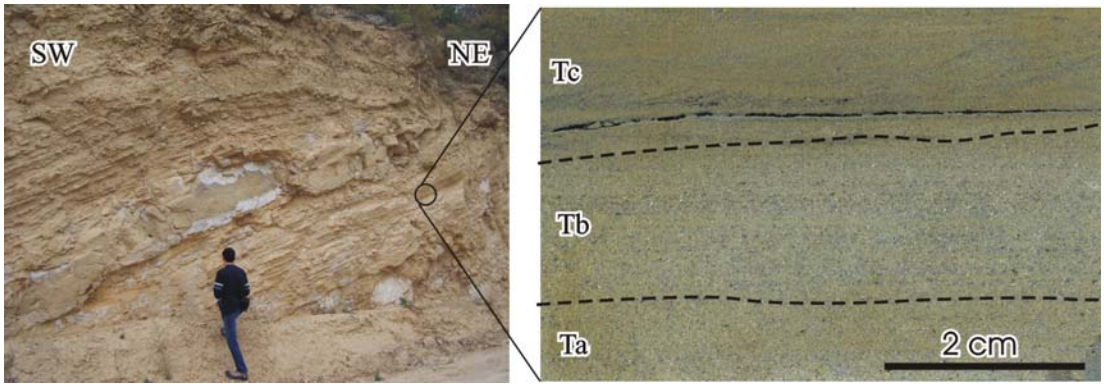


Figure 2.25. (a) Sandstones of the Yeniköy formation in the Eskin area. Note that beds are tilted southwest. **(b)** Turbiditic sandstone layers including bouma sequences (T_a, T_b and T_c).

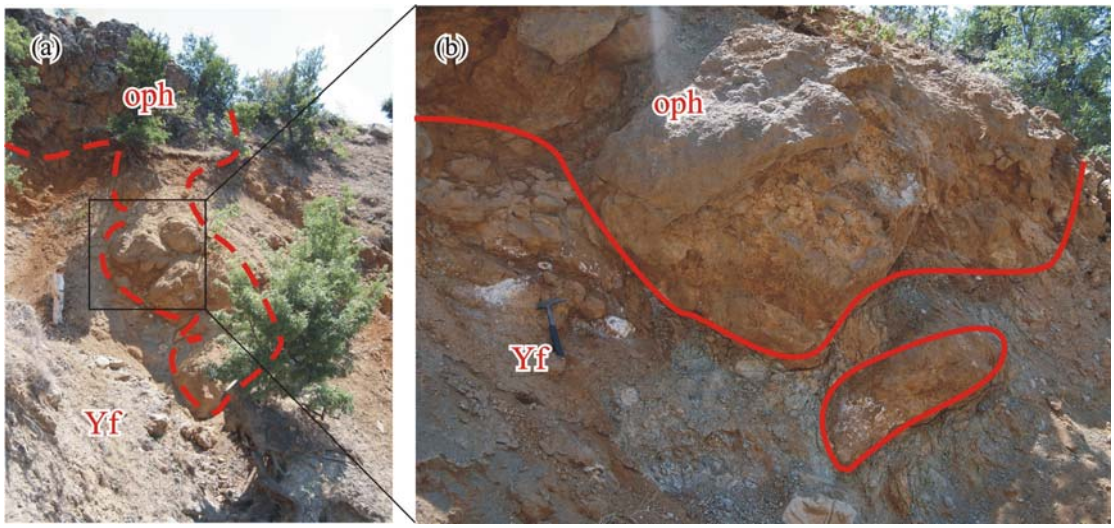


Figure 2.26. (a) Serpentinite blocks embedded within clastic parts of the Yeniköy formation. **(b)** Close-up of the contact between the block and the matrix. (Oph: ophiolites; Yf: Yeniköy formation).

2.5.3. Kuzayır basalt

The Kuzayır basalt crops out around the Kuzayır villages and consists of (syn-sedimentary) basaltic lava flows (Figures 2.27 and 2.28). The lavas flowed onto the clastic sedimentary rocks of the Yeniköy formation. The lava flows are up to 5 m thick and cover an area up to 1 km. In hand specimen, the lavas are characterized by phlogopite minerals within a dark grey to black matrix. The lower contact of the lava flows with the underlying sedimentary rocks display chilled and glassy margins with minor in-situ fragmentation (Figure 2.27), while the upper part of lavas is sharply and conformably overlain by well-bedded sandstones of the Yeniköy formation (Figure 2.28).

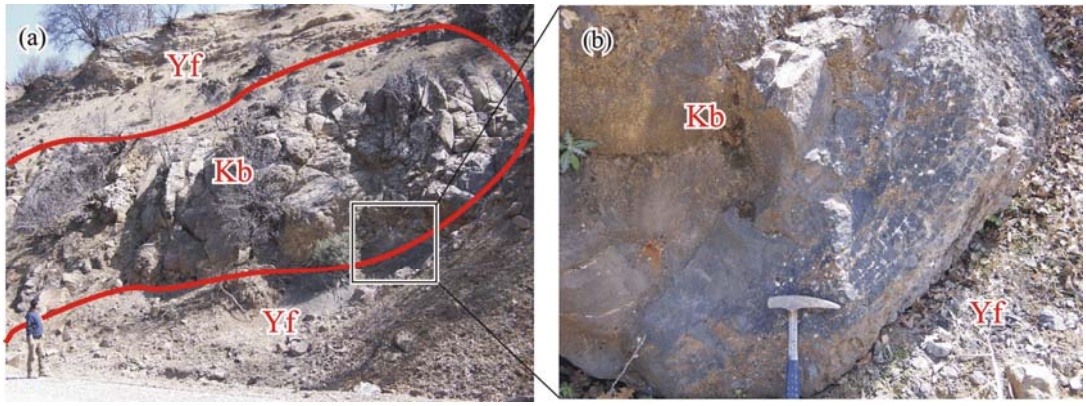


Figure 2.27. Field photos showing the contact relationship between the Kuzayır basalt (Kb) and Yeniköy formation (Yf): **(a)** basaltic lava flow enclosed by sedimentary rocks of the Yeniköy formation. **(b)** Close-up of basal contact of basaltic lava displaying chilled and glassy margins.

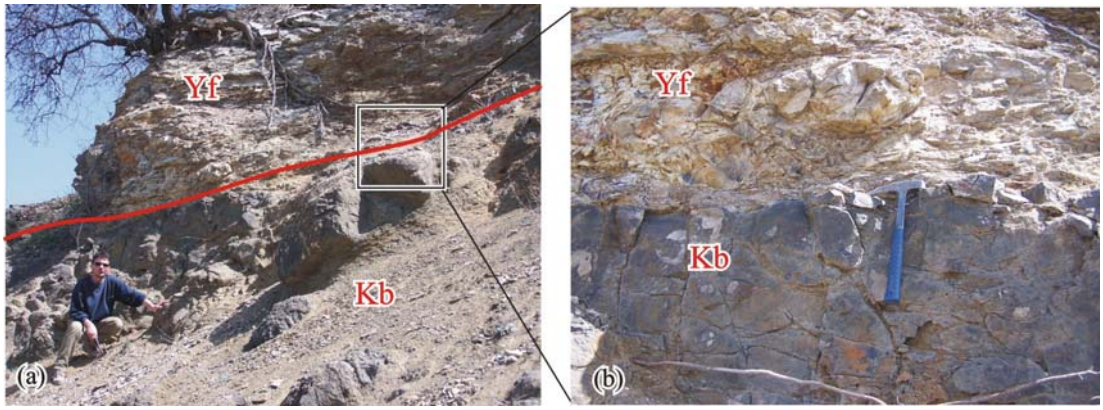


Figure 2.28. Field photos showing the contact relationship between the Kuzayır basalt (Kb) and Yeniköy formation: **(a)** The upper contact between the syn-sedimentary lava flow with Yeniköy formation (Yf). **(b)** Close-up view of the upper contact of the lava flow. Photos are from Tavak region (Kb: Kuzayır basalt; Yf: Yeniköy formation).

2.5.4. Eğreltidağ volcanic unit

Eğreltidağ volcanic unit comprises mainly dacitic-rhyolitic lava flows and pyroclastic rocks. The unit is widely exposed to the north of the Eskin and Tavak areas (Figures 2.23 and 2.30). The volcanic rocks in the north of the Tavak were previously named as Karaboldere or Beydağ volcanic unit (Ercan & Öztunalı 1983). In this study, the unit was described as Eğreltidağ volcanic unit based on field, petrographical and geochemical data.

The unit consists of dacitic-rhyolitic intrusions, lava domes, lava flows, crystal-rich pyroclastic rocks, block- and ash-flow deposits and volcanogenic sedimentary rocks. The dacitic intrusions are distinguished by their typical porphyritic texture with plagioclase, sanidine and quartz in the field. They contain high-grade metamorphic xenoliths of gneisses and migmatites (Figure 2.30). It conformably overlies the Yeniköy formation and is unconformably overlain by the İnay Group (Figures 2.4, 29 and 30-33).

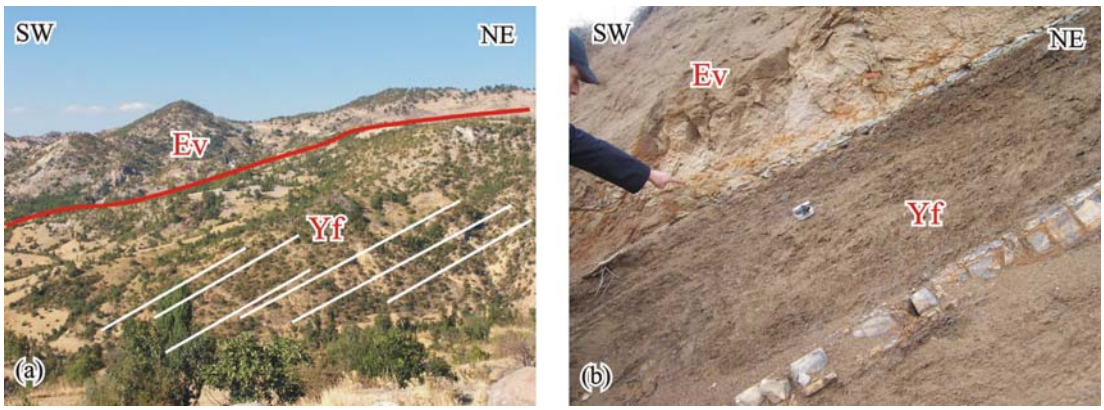


Figure 2.29. (a) Contact relationship between felsic rocks of the Eğreltidağ volcanic unit (Ev) and the Yeniköy formation (Yf). White lines indicate dips of sandstone beds; **(b)** Close-up view of the same contact.

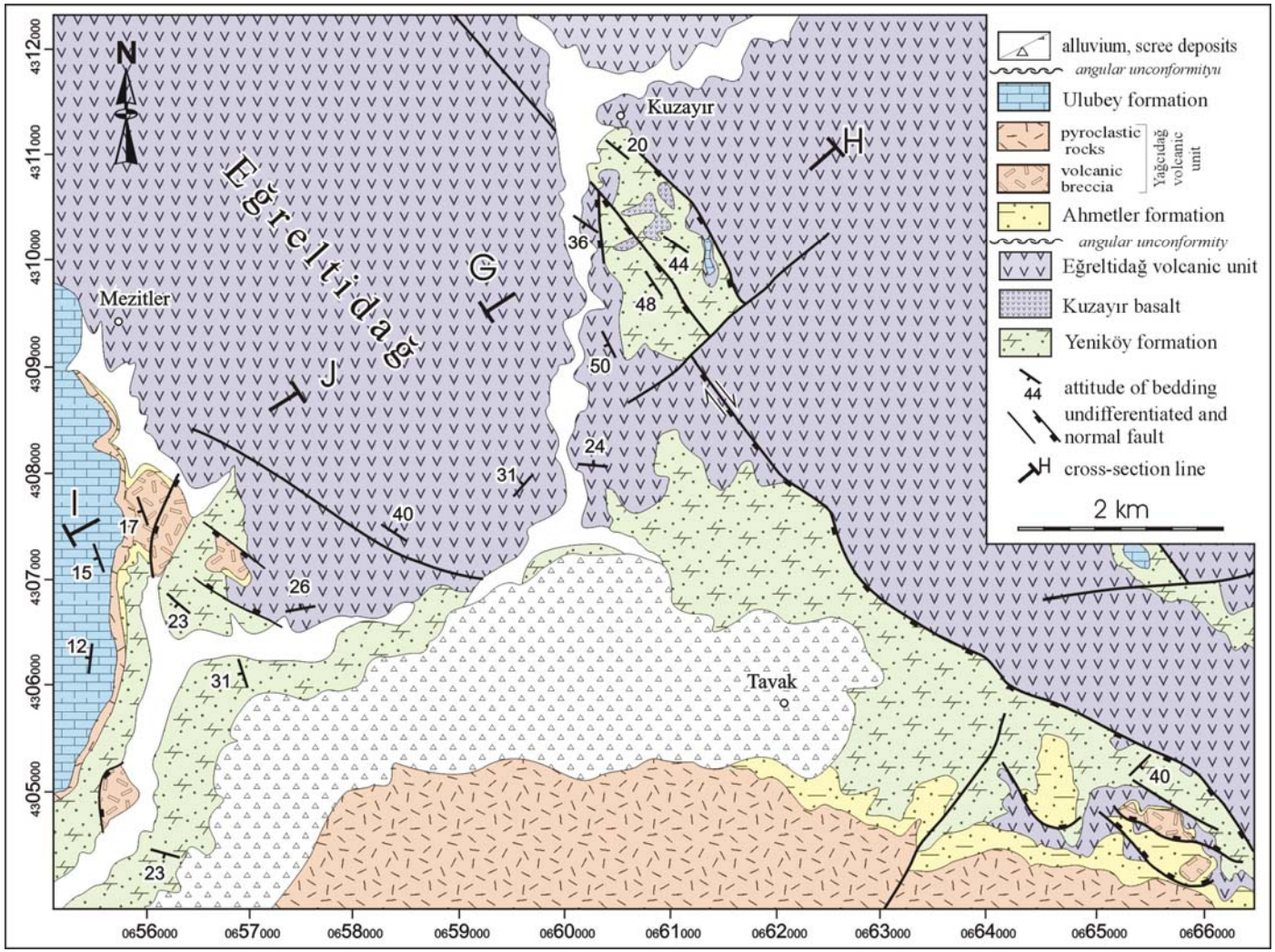


Figure 2.30. Geological map of theTavak area. See Figure 2.3 for location.

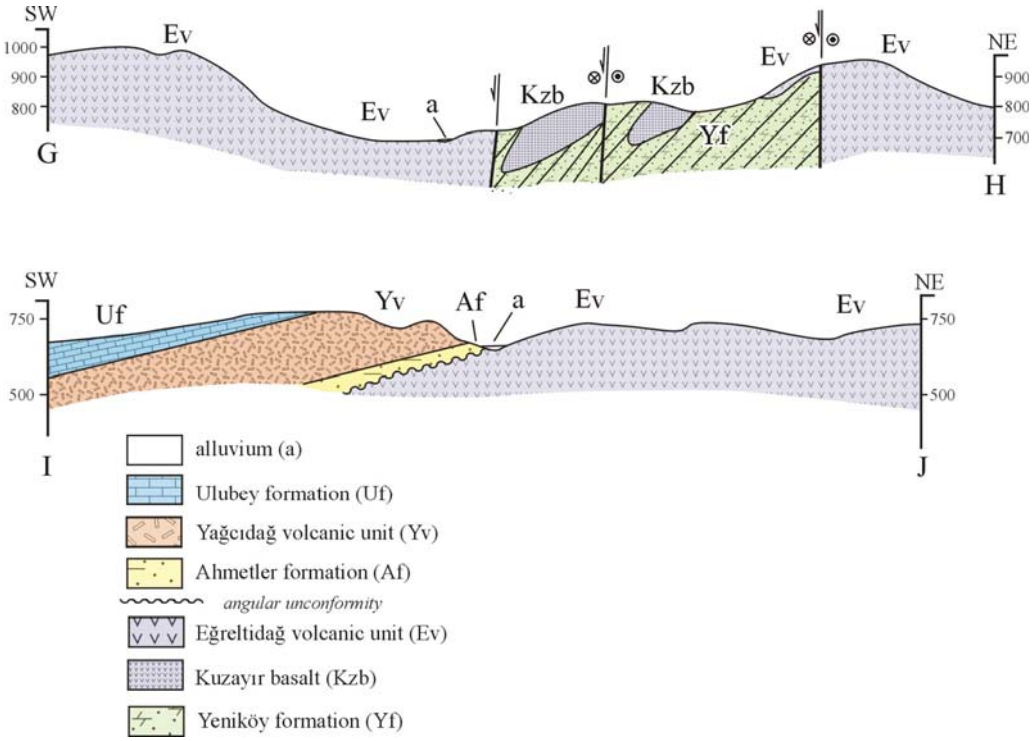


Figure 2.31. Cross-sections showing the contact relationship of the rock units from the Tavak area See Figure 2.30 for location.

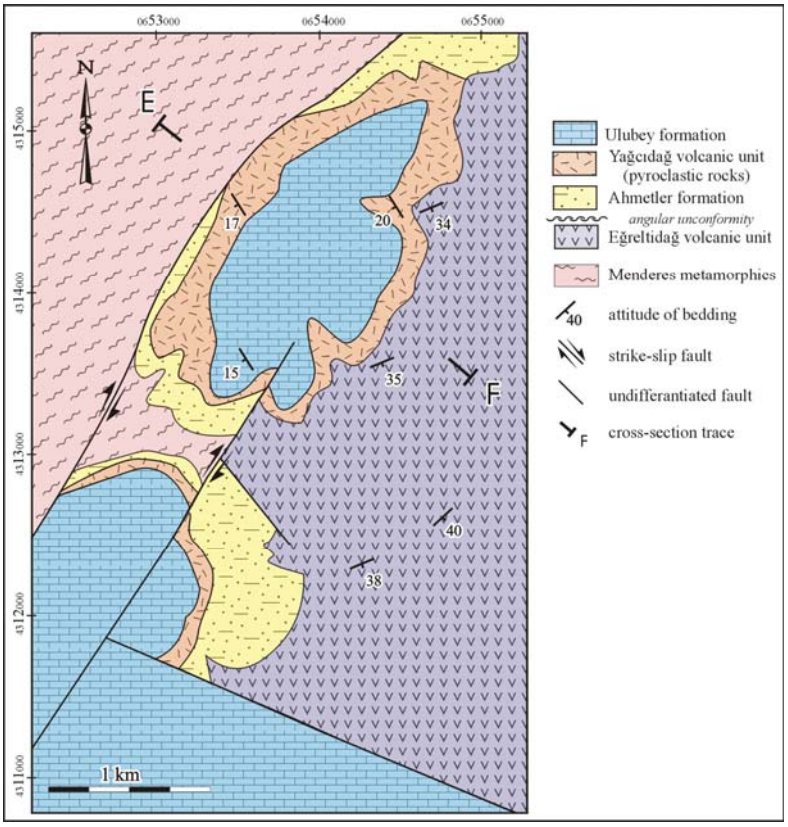


Figure 2.32. Geological map of the Iklıkçı area. See Figure 2.3 for location.

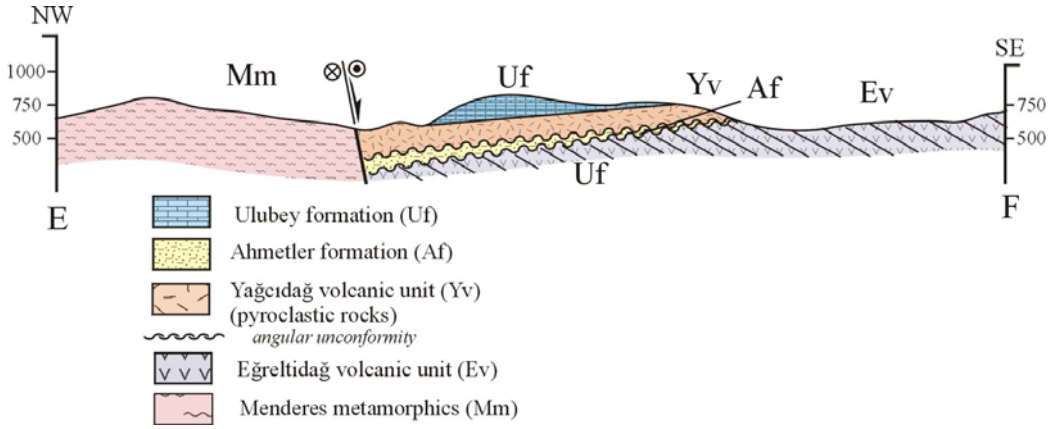


Figure 2.33. Cross-sections showing the contact relationship between the Yağcıdağ volcanic unit and the Eğreltidağ volcanic unit from the Iklıkçı area. See Figure 2.32 for location.

2.6. İnay group

2.6.1. Ahmetler and Ulubey formations

The İnay group, confirming the previous studies, includes two distinct sedimantary units and one volcanic unit, namely Ahmetler formation, Ulubey formation and Yağcıdağ volcanic unit, respectively. The Ahmentler formation crops out in a wide area along the Selendi River and to the south of Selendi. It is composed of conglomerates and tuffaceous detritals at the base. Upward in the section, it consists of wide-spread claystone and minor shales. The semi-lithified claystones are green coloured, and intercalated in some level with ash-fall deposits derived from Yağcıdağ volcanic unit (Figure 2.35). The lower contact of the unit consists of conglomerates and unconformable overlies the older units. In the Kula area (Figure 11), the lower parts of the unit consist of reddish boulder conglomerates derived mainly from the Menderes metamorphics. In the Iklıkçı area (Figure 2.32), between the Eğreltidağ volcanic unit (block- and ash-flows) with the overlying Yağcıdağ volcanics (pyroclastic deposits), the unit is represented by conglomerates derived from the Menderes metamorphics. Ulubey formation consists of limestone and marls. Limestones of the unit include fosiliferous horizons. The top of the Ulubey formation is generally charactrised by silicified limestones.



Figure 2.34. Field views of Ahmetler (Af) and Ulubey (Uf) formations from Dereköy-Çalıklı area **(a)**, and from south of the Selendi **(b)**.

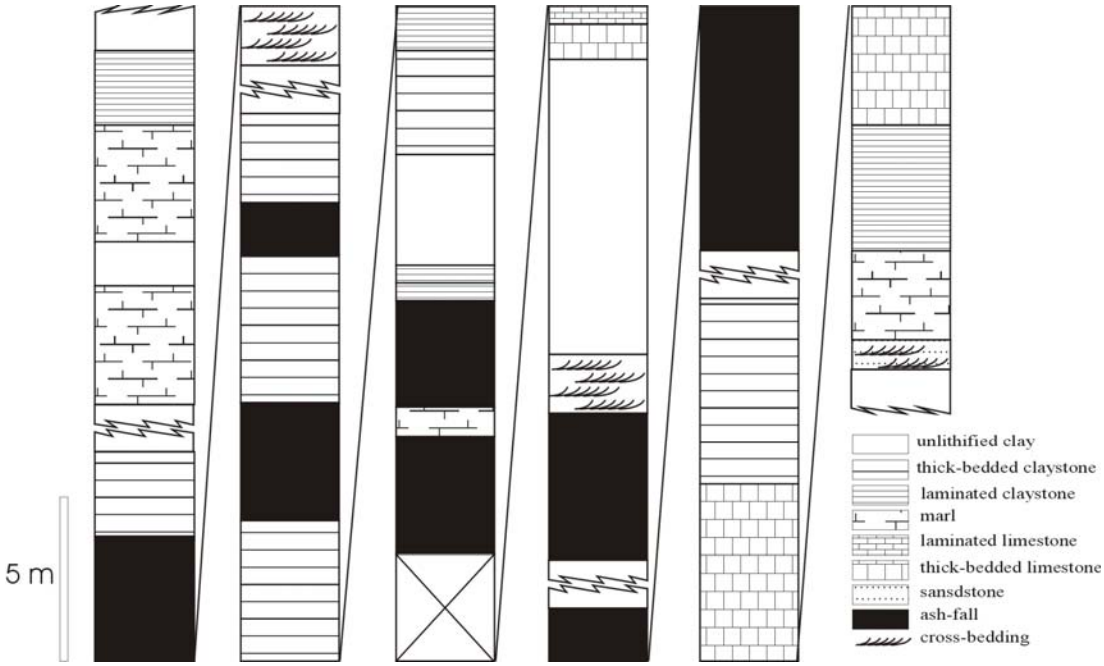


Figure 2.35. Measured reference section from the transitional contact between Ahmetler and Ulubey formations. Note that the syn-sedimentary volcanism.

2.6.2. Yağcıdağ volcanic unit

Yağcıdağ volcanic unit was emplaced through Yağcıdağ volcanic centre (Figure 2.37). The products of the unit include pyroclastic rocks, epiclastic rocks, dacitic lava flow and dykes. Pyroclastic rocks, emplaced in a wide area from Selendi to the Kuşuköy in the north, are composed of ash-fall, ash-flow, block-and ash flow, pyroclastic surge deposits. Wide-spread ash-fall deposits are intercalated with the claystone, marl and limestone of Ahmetler and Ulubey formations. The epiclastic rocks are volcanogenic sandstones and conglomerates, which also interfinger with

the Ahmetler formation. The lava flows are pink or grey colored and plagioclase-phyric. Other phenocrysts are quartz, biotite, and amphibole.

The Yağcıdağ volcanic unit overlies the Eğreltidağ volcanic unit with an angular unconformity. The basal part of the Yağcıdağ volcanic unit is characterized by a well-developed conglomerate layers (Figure 2.36). These conglomerates consist mainly of metamorphic-derived clasts (Ahmetler formation; Figure 2.36).

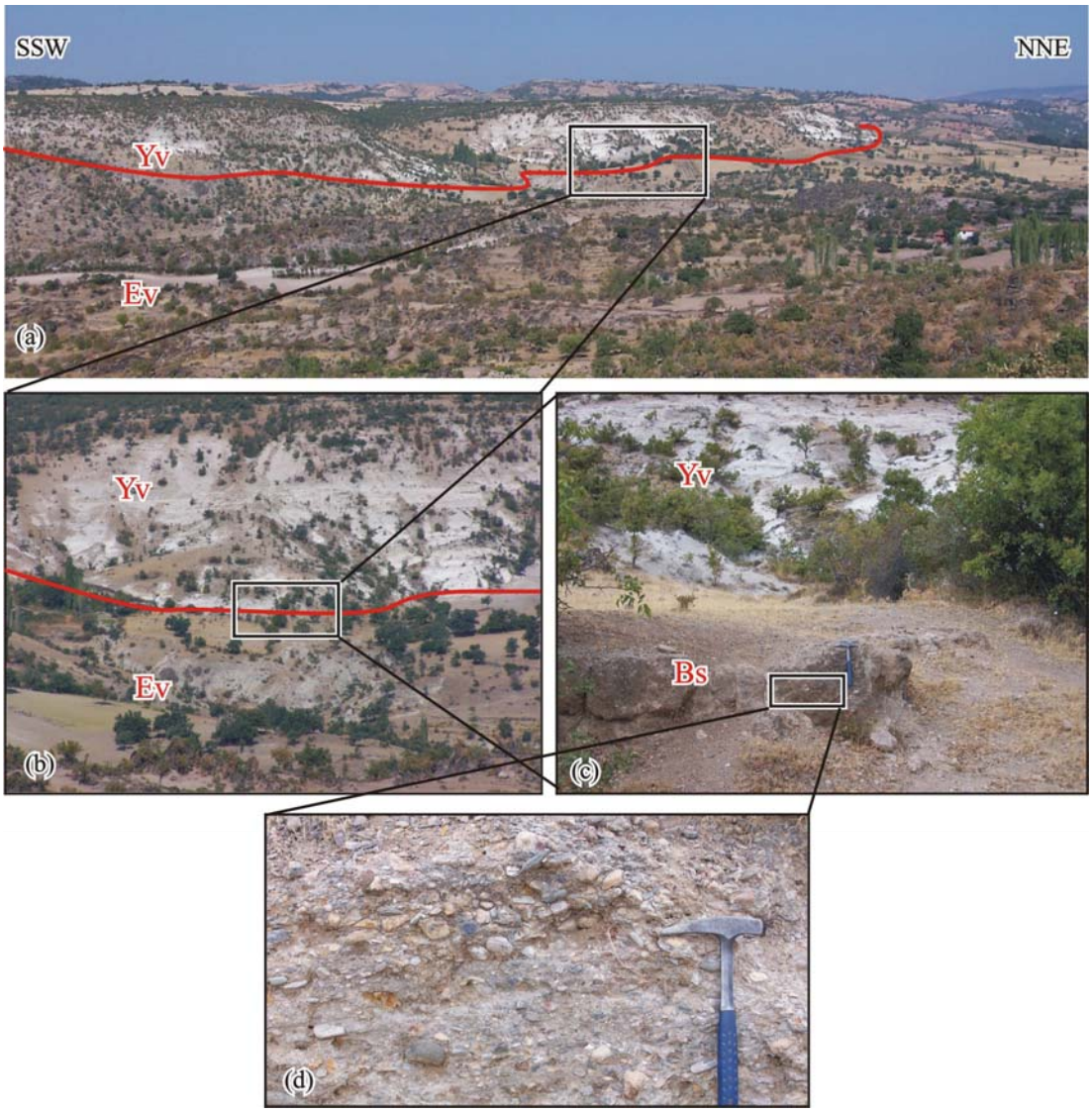


Figure 2.36. (**a, b** and **c**) Contact relationship (angular unconformity) between felsic rocks of the Eğreltidağ volcanic unit (Ev) with the angular unconformably overlying Yağcıdağ volcanic unit (Yv); **(c)** The contact is characterized by well-developed metamorphic-derived basal conglomerate (Bs); **(d)** Close-up view of the basal conglomerate (the red line represents the unconformity). Hammer is 13-cm long.

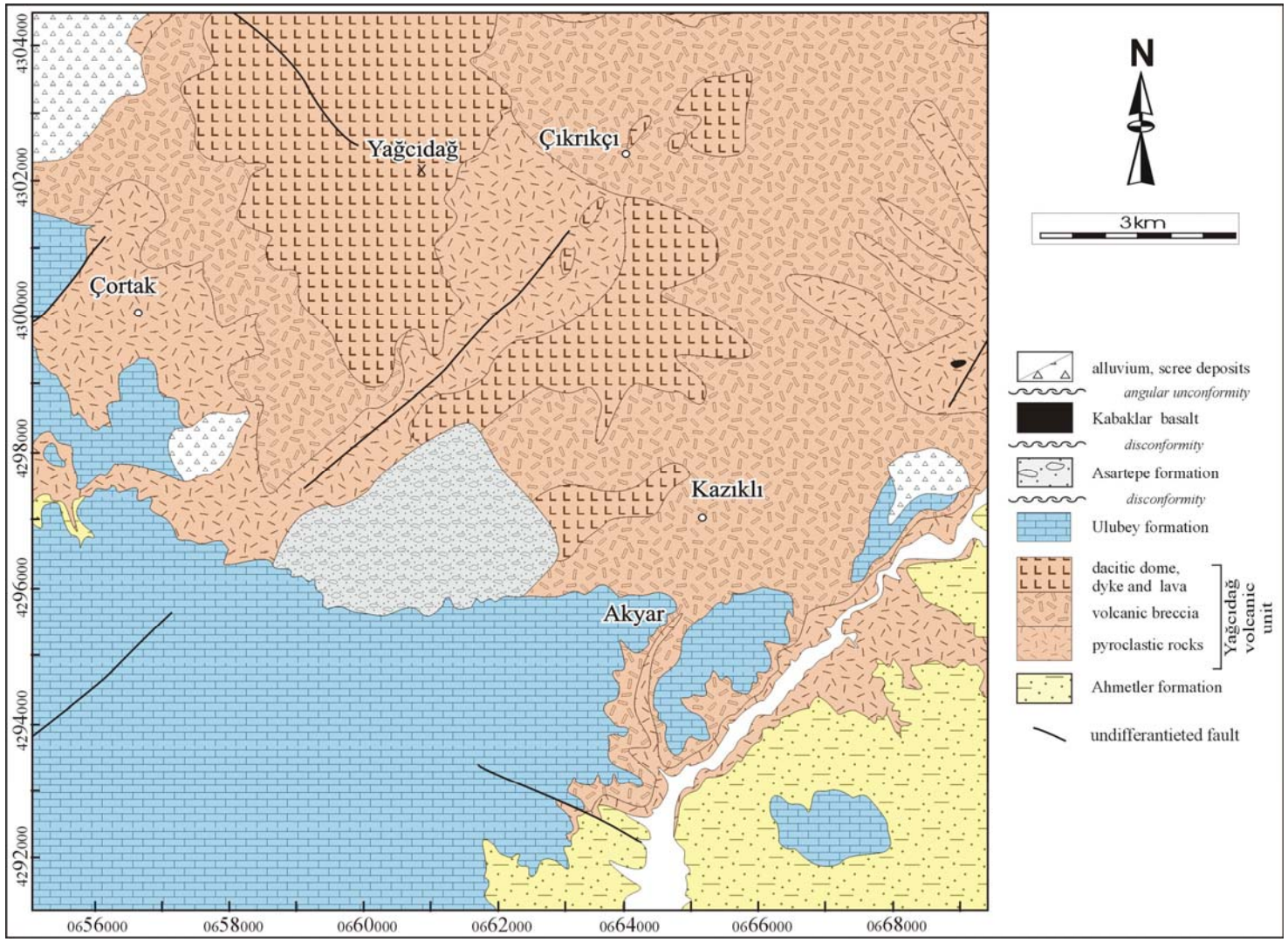


Figure 2.37. Geological map of the Yağcıdağ area. See Figure 2.3 for location.

2.7. Asartepe formation

Asartepe formation composed of reddish conglomerates mainly derived from the Menderes metamorphics, and fewer from other older units. Thick- and medium-thick, semi-lithified conglomerates of the unit crops out mainly near the NE-trending fault zone (Figure 2.23). The unit unconformable overlies the older units and is unconformable overlain by the Kabaklar basalt.

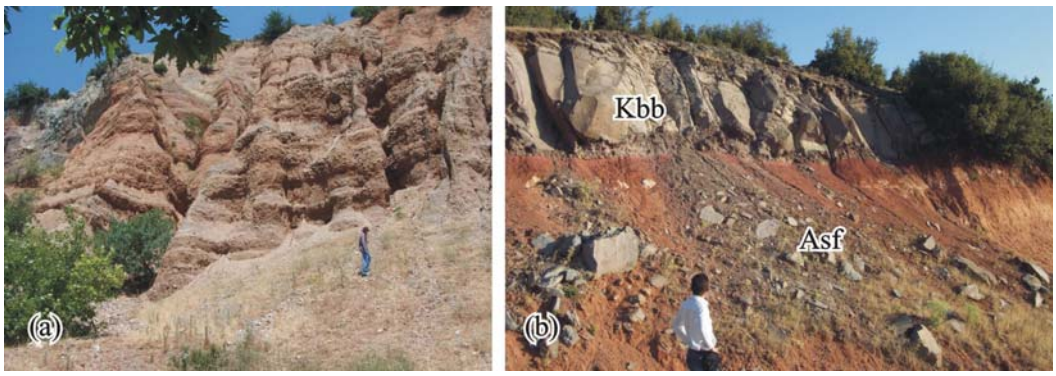


Figure 2.38. (a) The reddish conglomerates of the Asartepe formation, **(b)** the contact between Asartepe formation (Asf) and the Kabaklar basalt (Kbb).

2.8. Kabaklar basalt

The Kabaklar basalt is composed of olivine–phyric basaltic lava flows. It flowed onto the continental sediments of the Asartepe formation. The lava flows are up to 10 m thick and cover an area up to 10 km. It crop outs along the NE-trending faults in the Eskin area. The contact between the Asartepe formation and the Kabaklar basalt is characterized by red coloured baked zone (Figure 2.38b). These rocks were previously named as Kula volcanic unit (Ercan *et al.* 1983), but based on their geochemical features, they are renamed as Kabaklar volcanic unit in this study (see Chapter III).

2.9. Kula volcanic unit

The Kula volcanic unit (Ercan *et al.* 1983) crop outs in the south of the Selendi (Figure 2.19). The reader is referred to Ercan & Öztunalı (1982, 1983), Ercan *et al.* (1983), McKenzie & O'Nions (1995) and Alıcı *et al.* (2002) for detailed description.

CHAPTER THREE

PETROGRAPHY AND GEOCHEMISTRY

3.1. Petrography

3.1.1. Rahmanlar granite

Rahmanlar granite is composed of quartz (35-45%), potassium feldspar (25-35%), plagioclase feldspar (Ab_{80-90}; 25-35%), biotite (5-15%), garnet (3-8%), opaque (ilmenite or magnetite 1-3 %) and accessory minerals (zircon, apatite, 0.5-1%). Quartz minerals are unhedral in shape. Two types quartz can be distinguished in the granites. These are relics of large old quartz grains showing undulose extinction, and recrystallised small subgrains with irregular grain boundaries (Figure 3.1a). K-feldspar minerals are subhedral and altered to mainly serisite. Garnet minerals are replaced by biotite minerals (Figure 3.1b). Biotites generally have oriented giving rise to crude foliation (Figure 3.1b).

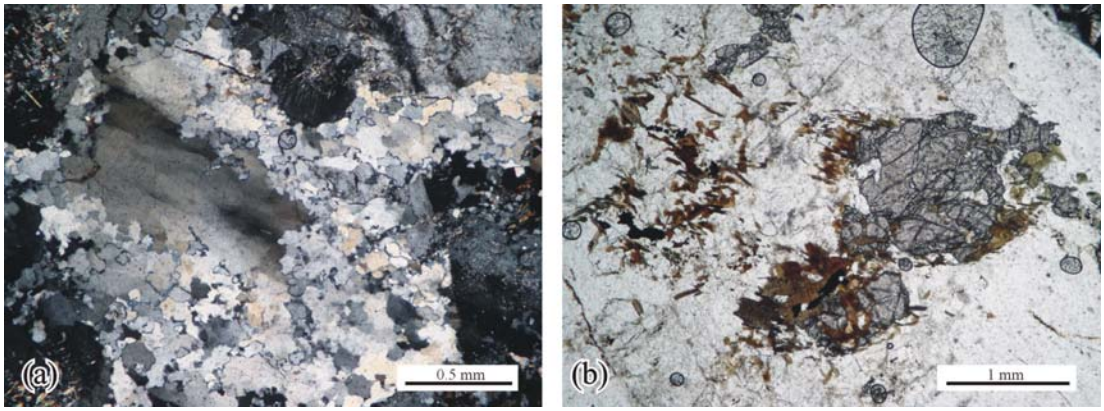


Figure 3.1. Photomicrographs of Rahmanlar granite: **(a)** Dynamically recrystallized quartz and old, large quartz showing undulose extinction (+N); **(b)** garnets was replaced by oriented biotite.

3.1.2. Eğreltidağ volcanic unit

The felsic members of the Eğreltidağ volcanic unit include dacitic and rhyolitic rocks. The modal mineralogy of the lava samples of the unit is characterized by quartz (10-15%) plagioclase (Ab_{55-65} 15-20%), sanidine (5-10%), biotite (3-5%), green amphibole (3-5%) and opaque (1%). Quartz crystals are generally embayed.

Plagioclase crystals are usually resorbed due to magma reaction between early formed minerals indicating that the physicochemical conditions of magma were changed (Figure 3.2a). Similar features can be seen in the biotites in which resorbed parts yielded opaque minerals (Figure 3.2b). The lavas are generally porphyritic with subhedral plagioclase, sanidine and biotite and unhedral quartz phenocrysts. In some samples, amphiboles overprinted the earlier formed and embayed clynopyroxene crystals (Figure 3.2b). Some lavas exhibit vitrophyric texture with small phenocryst. The matrix of these samples is characterized by perlitic texture (Figure 3.2c-d).

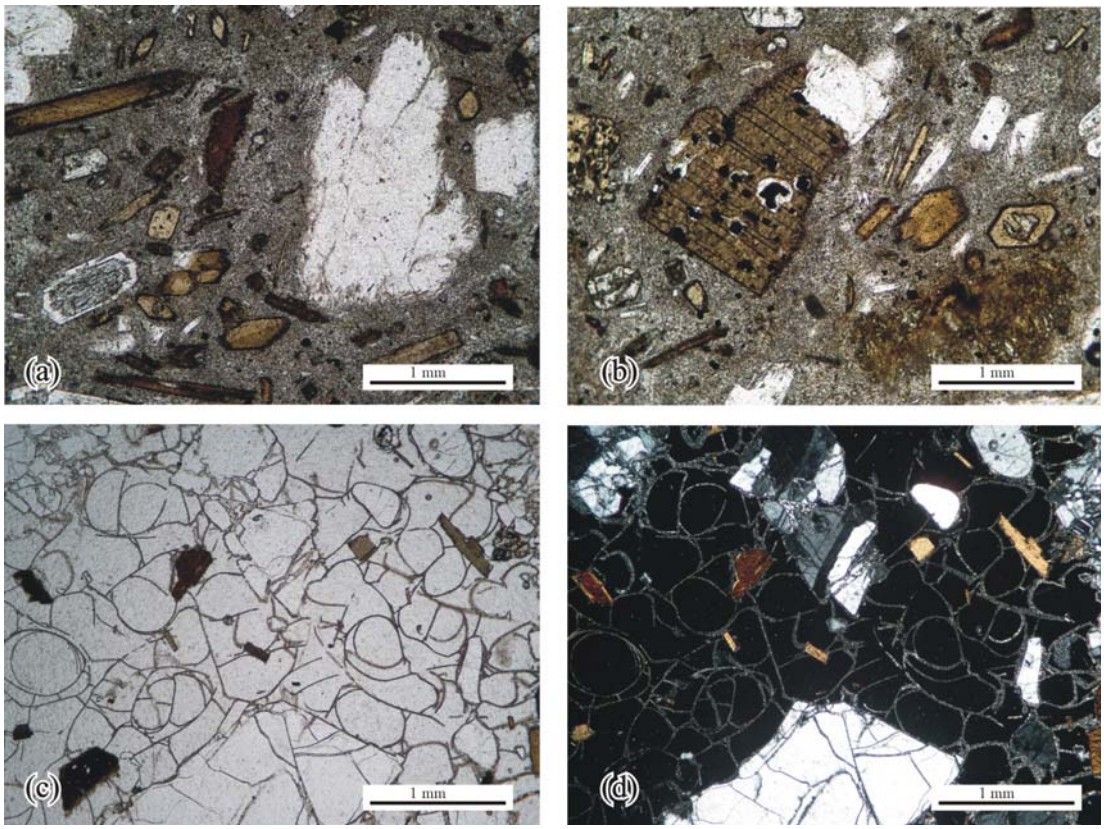


Figure 3.2. Photomicrographs from Eğretidağ rhyolitic-dacitic volcanic rocks: **(a)** resorbed plagioclase phenocrysts (//N); **(b)** biotite resorbed where opaque minerals formed (//N); **(c-d)** perlitic texture (//N and +N respectively).

3.1.3. Kuzayır basalt

Kuzayır basalt exhibits an alkaline mineralogic composition with phlogopite phenocrysts. Matrix of the lava flows also includes radiating feldspar crystals. The lavas also exhibit olivine crystals which are entirely altered to iddingsite. The mineralogy of the Kuzayır basalt resembles lamproites (see also geochemical

description of the Kuzayır basalt) but on the basis of their plagioclase contents they can not be considered as lamproites in the normal sense because of the presence of plagioclase (Foley *et al.* 1987; Mitchell & Bergman 1991; Prelević *et al.* 2005).

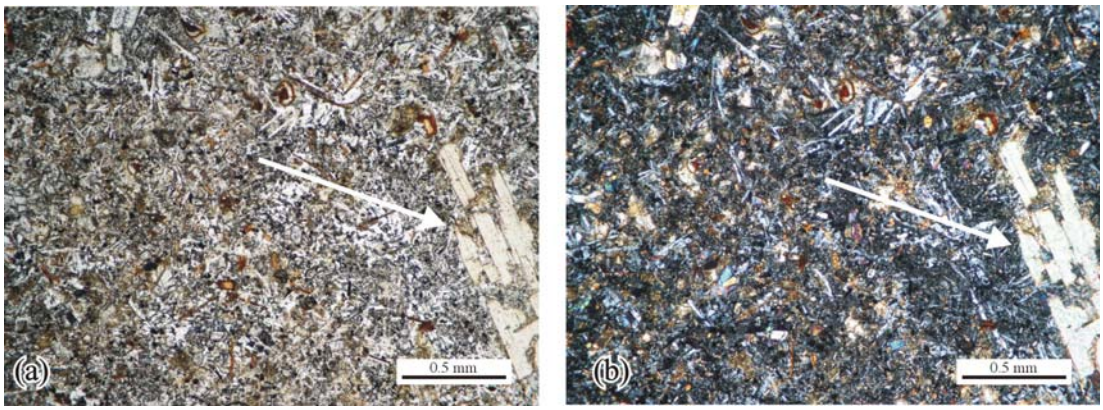


Figure 3.3. Photomicrographs from Kuzayır basalt. The matrix of the lava flow is composed of radiating feldspar crystals. See also phlogopite phenocryst (arrowed) at the right hand of the photos.

3.1.4 Yağcıdağ volcanic unit

The felsic lava samples from the Yağcıdağ have quartz (4-12%) plagioclase (Ab_{38-60} 35-70%), biotite (5-7%), amphibole (5-10%), and clynopyroxene (2-5%) phenocrysts with minor amounts of opaque minerals. Volcanic rocks characterized by porphyritic texture. The unhedral quartz phenocrysts are embayed (Figure 3.4a-b) and some are surrounded by clynopyroxene microphenocrysts (Figure 3.4c-d). Plagioclases generally subhedral and show sieve texture with clear core and surrounding inclusion-bearing phase (Figure 3.4a-b). Some plagioclases were rounded due to reaction with the liquid phase (Figure 3.4c-d).

Mafic phases of the felsic rocks of the Yağcıdağ volcanic unit are biotite, amphibole and clynopyroxene. Many clynopyroxene crystals are embayed and they were generally overprinted by amphibole. The outer rim of these amphibole overgrowths was replaced by opaque minerals (Figure 3.6a).

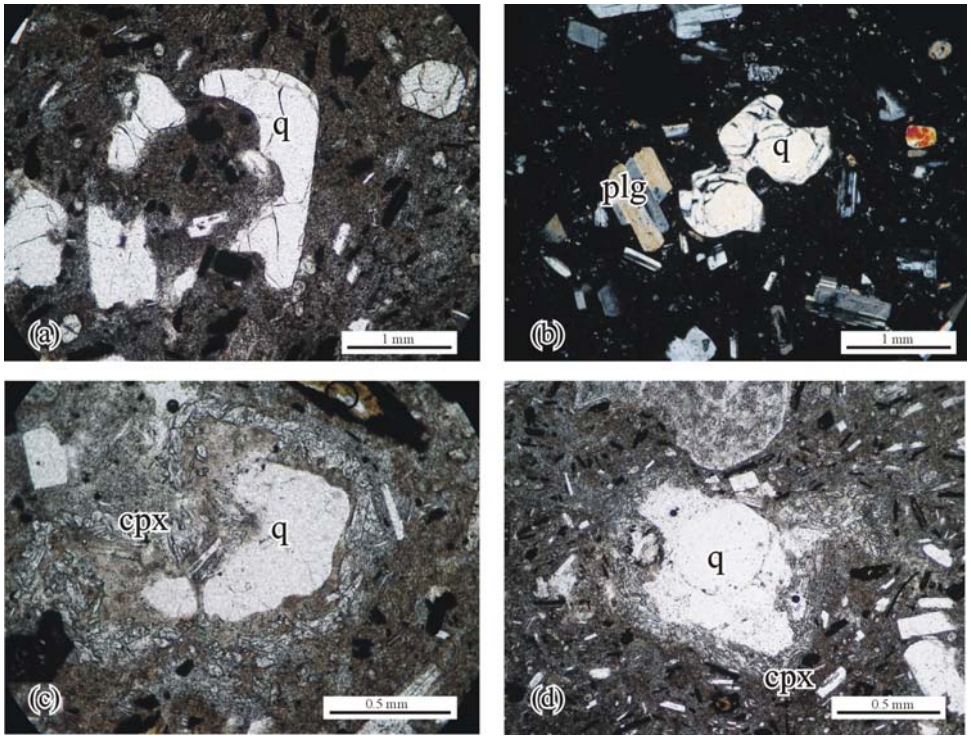


Figure 3.4. Photomicrographs from Yağcıdağ dacites: **(a-b)** embayed quartz (q) phenocrysts (//N and +N respectively); **(c-d)** embayed quartz phenocrysts were surrounded by clynopyroxenes (cpx) (//N).

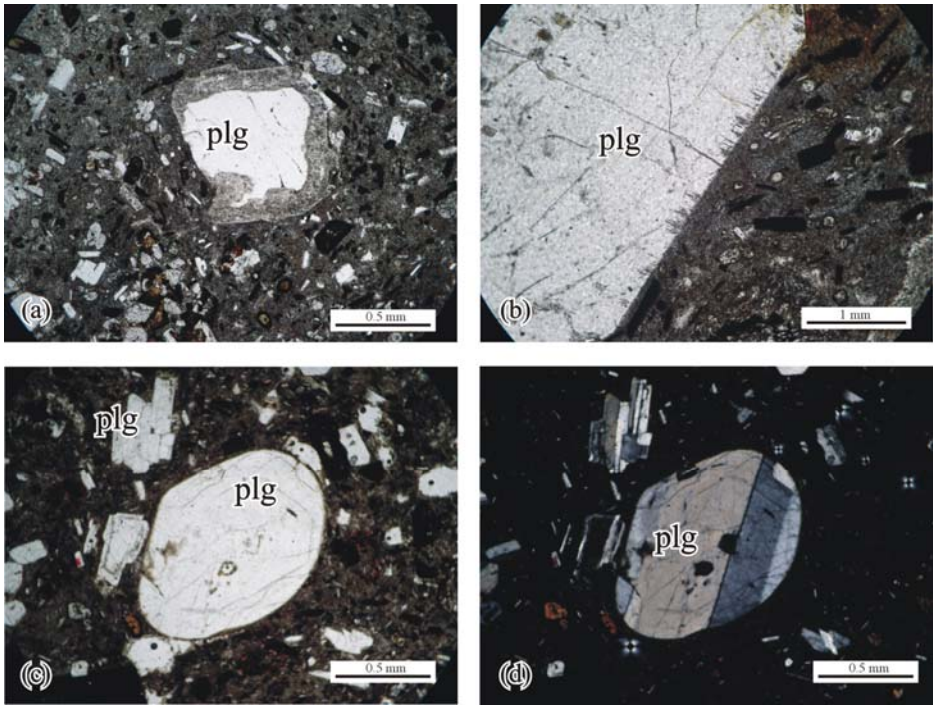


Figure 3.5. Photomicrographs from dacites of the Yağcıdağ volcanic unit: **(a-b)** euhedral plagioclase phenocrysts (plg) were resorbed through its cleavage planes (//N and +N respectively) **(c-d)** resorbed unhedral plagioclase (//N).

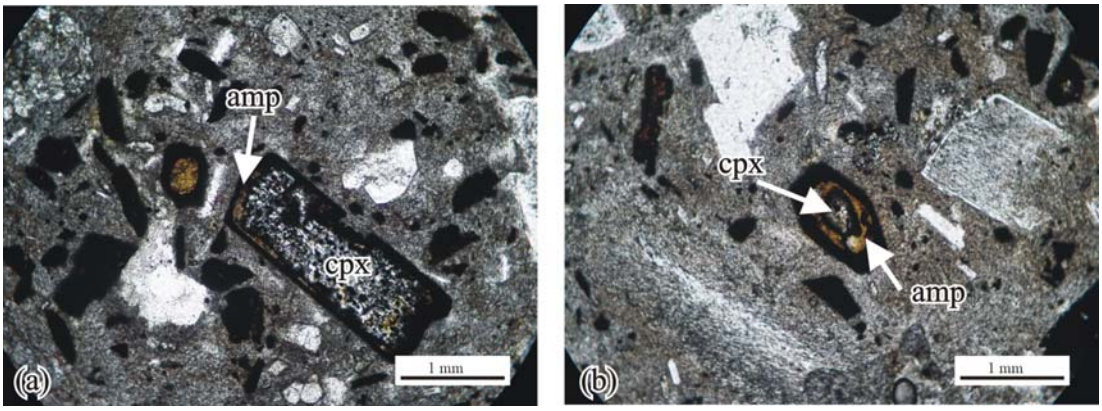


Figure 3.6. (a-b) Photomicrographs from Yağcıdağ dacites: euhedral amphibole (amp) overgrowth on earlier formed and resorbed clynopyroxene (cpx) (+N).

3.1.5. Kabaklar basalt

Kabaklar basalt is represented by olivine-phyric lava flows (Figure 3.7 and 3.8). Mineralogical composition of the lavas is represented by olivine (12%), clynopyroxene (8%) and plagioclase (5%). Xenoliths that are dunitic in composition observed in the lava flows (Figure 3.7). Olivine crystals, forming the xenoliths, are replaced by iddingsite at the outer rims of the olivine (Figure 3.7).

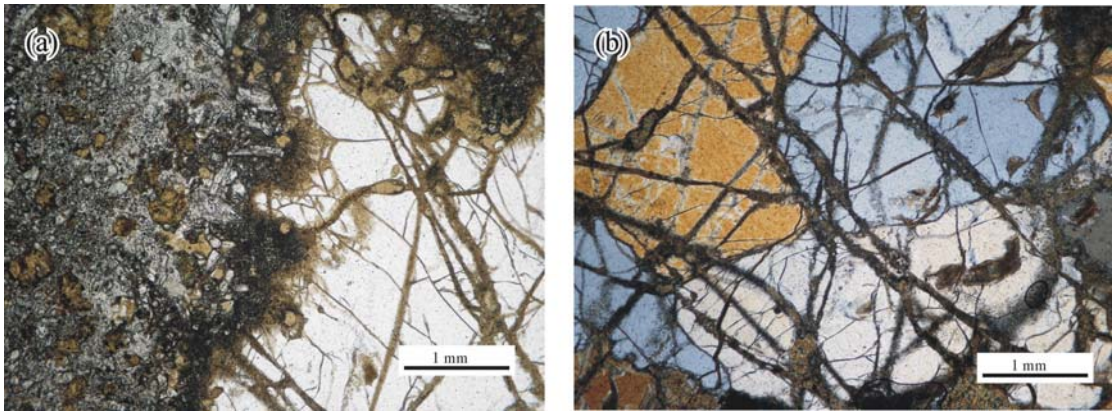


Figure 3.7. Photomicrographs from Kabaklar basalt: the margin (a) of the dunitic xenolith consisting of unhedral olivine minerals (b) in the Kabaklar basalt.

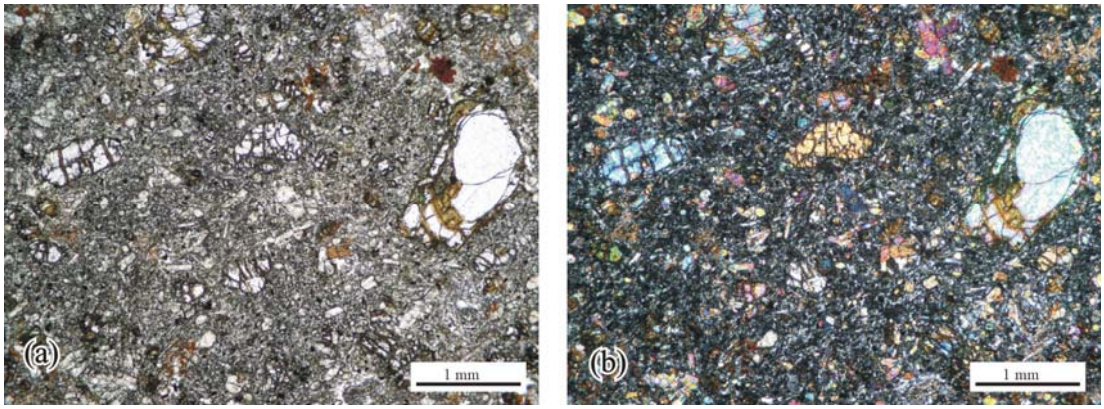


Figure 3.8. Photomicrographs from Kabaklar basalt: **(a-b)** olivine and clynopyroxene minerals occur in the matrix.

3.2 Classification and trace element characteristics

In order to classify the magmatic rocks from the Selendi Basin, and to reveal their petrologic features and magmatic evolution of the basin, representative 30 samples were collected from Menderes metamorphics (augen gneisses, 1) Rahmanlar granite (4), Kuzayır basalt (2), Eğreltidağ volcanic unit (4), Yağcıdağ volcanic unit (15) and Kabaklar basalt (4) and they were analyzed at ACME geochemical laboratories. The Turkish UTM coordinates of the samples are given in Table 3.1. The results are shown in Table 3.3.

Table 3.1. Turkish UTM coordinates of the samples which collected for geochemical analyssis

Sample number	*Rock unit*	*Field description*	*UTM coordinates*
Y19	Menderes metamorphics	gneises	0673572/4300943
H2/1	Rahmanlar granite	granite	0674406/4302063
H2/2	Rahmanlar granite	granite	0674406/4302063
Y23	Rahmanlar granite	granite	0673354/4300478
Y23/2	Rahmanlar granite	granite	0673354/4300478
0513	Eğreltidağ volcanic unit	dacite	0662096/4310771
0505	Eğreltidağ volcanic unit	rhyolite	0673366/4313057
0506	Eğreltidağ volcanic unit	dacite	0673366/4313057
0507	Eğreltidağ volcanic unit	dacite	0664988/4309140
0509/1	Kuzayır basalt	basalt	0660891/4311654
0509/2	Kuzayır basalt	basalt	0660891/4311654
031025	Yağcıdağ volcanic unit	andesite	0664200/4297125
031028	Yağcıdağ volcanic unit	dacite	0662549/4299530
031043	Yağcıdağ volcanic unit	andesite	0659815/4298642
031207	Yağcıdağ volcanic unit	dacite	0657426/4303165
031212	Yağcıdağ volcanic unit	pumice	0656915/4301840
031301	Yağcıdağ volcanic unit	dacite	0657031/4302790
YF1	Yağcıdağ volcanic unit	dacite	0662770/4296977
YF2	Yağcıdağ volcanic unit	dacite	0659496/4302789

Table 3.2 continued

0510	Yağcıdağ volcanic unit	dacite	0657381/4302983
031307	Yağcıdağ volcanic unit	dacite	0659972/4303393
0511/1	Yağcıdağ volcanic unit	dacite	0663207/4300786
0511/3	Yağcıdağ volcanic unit	dacite	0663207/4300786
KD-1	Yağcıdağ volcanic unit	dacite	0657381/4302983
KD-2	Yağcıdağ volcanic unit	dacite	0657381/4302983
KD-3	Yağcıdağ volcanic unit	dacite	0657381/4302983
0512/1	Kabaklar basalt	olivine-basalt	0668500/4299500
0512/2	Kabaklar basalt	olivine-basalt	0668500/4299500
0512/3	Kabaklar basalt	olivine-basalt	0668500/4299500
0512/4	Kabaklar basalt	olivine-basalt	0668500/4299500

3.2.1. Rahmanlar Granite

The SiO_2 contents of the Rahmanlar granite ranges from 66.08 to 73.11 *wt.%* (Table 3.2). Based on Shand's index, these rocks are peraluminous (Table 3.2). Their Na_2O contents vary from 2.85% to 3.06%, slightly lower than 3.2% which is the characteristic feature of the S-type granites (Chappel & White 1974). They also contain 1.96-2.57% normative corundum (Table 3.4). Normative corundum contents of the S-type granites are generally grater than 1% (Chappel & White 1974). Garnet-bearing Rahmanlar granite shows typical characteristics of the S-type granitoides owing to its mineralogical composition and geochemical features. Normative mineralogy of the Rahmanlar granite also includes hyperstene (Table 3.4).

Table 3.2. Shand's indexes of the Rahmanlar granite

Sample	H2/1	H2/2	Y23	Y23/2	*Shand's index*
$Al_2O_3/(CaO+Na_2O+K_2O)$	1.57	1.56	1.62	1.56	peraluminous
$(Na_2O+K_2O)/ Al_2O_3$	0.58	0.58	0.54	0.56	

The Rahmanlar granite fall in sub-alkali field in *K_2O wt% vs SiO_2 wt%* alkali-sub-alkaline diagram of Irvine & Baragar (1971) (Figure 3.9a) and fall in calc-alkaline field in *(K_2O+Na_2O) wt% - FeOt wt% - MgO wt%* (AFM) diagram (Figure 3.9b) of Irvine & Baragar (1971).

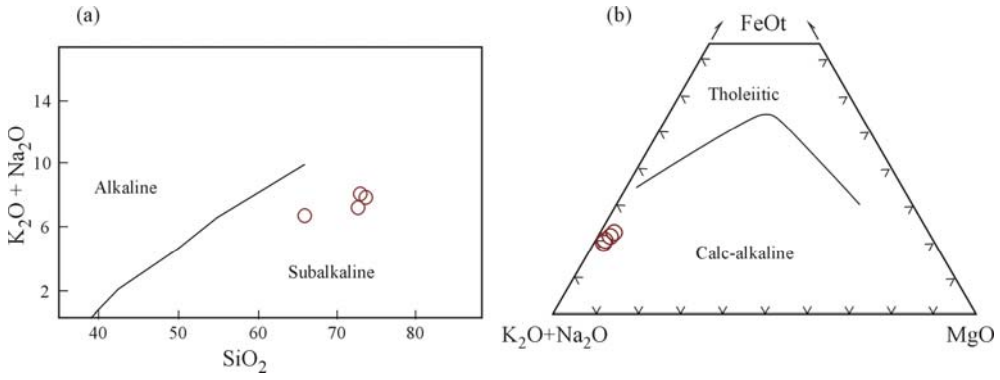


Figure 3.9. (a) Alkali – subalkaline and **(b)** tholeiitic-calc-alkaline discrimination diagrams of Irvine & Baragar (1971).

Chondrite-normalized REE diagram of these rocks are shown in Figure 3.10a. Rahmanlar granite shows LREE (light rare earth element) enrichment with respect to HREE (heavy rare earth elements) and negative Eu anomalies (Figure 3.10a). In the primitive mantle-normalized spider diagram they also show Ta, Nb, K, Sr and Ti depletion. The representative sample from augen gneisses from the Menderes Massif is also shown in these diagrams (Figure 3.10). The REE patterns of the gneisses are considerably similar to the Rahmanlar granite, excepting slightly enrichment in whole REE. Multi-element spider diagrams of these rocks are also very similar. The single difference between the patterns of the Rahmanlar granite and the hosting augen gneisses in these diagrams is that the all elements are slightly enriched whereas Sr and Eu are slightly depleted with respect to the values of the gneisses.

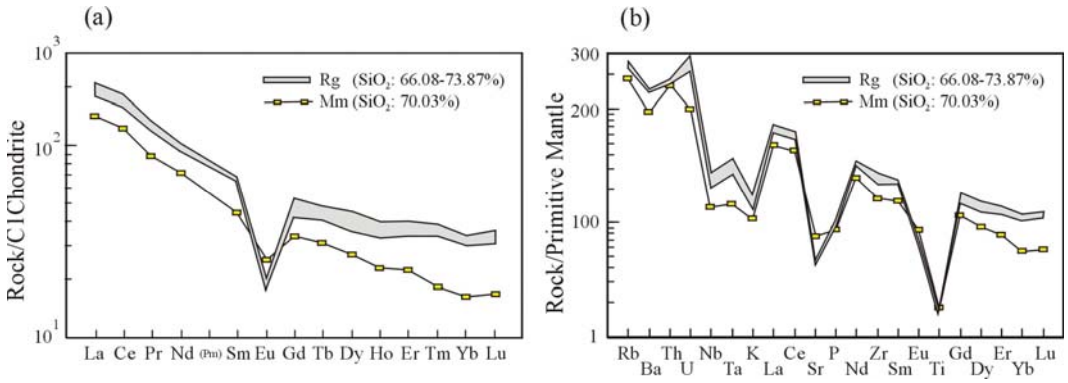


Figure 3.10. (a) C1chondrite-normalized REE and **(b)** primitive mantle-normalized multi-element spider-diagram of the Rahmanlar Granite (Rg). The augen gneisses representing the hosting Menderes Massif (Mm) is also showed in the diagram. Normalizing values are from Sun & McDonough (1989).

Table 3.3. Geochemistry of the magmatic and metamorphic rocks from the Selendi Basin.

	Gneises	Rahmanlar granite				Eğreltidağ volcanic unit				Kuzayır basalt	
	Y19	**H2/1**	**H2/2**	**Y23**	**Y23/2**	**0513**	**0505**	**0506**	**0507**	**0509/1**	**0509/2**
Major Elments (wt.%)											
SiO_2	70.03	73.11	73.87	72.79	66.08	66.59	71.46	71.94	65.99	51.21	51.47
TiO_2	0.40	0.36	0.35	0.38	0.36	0.50	0.25	0.25	0.49	1.62	1.62
Al_2O_3	15.23	14.15	13.73	13.58	12.29	15.41	12.92	13.13	15.17	12.50	12.64
Fe_2O_3	2.47	2.07	2.06	2.71	2.80	3.11	1.58	1.44	3.20	6.24	6.22
FeO^T	2.47	2.07	2.06	2.71	2.80	3.11	1.58	1.44	3.20	6.24	6.22
MnO	0.02	0.03	0.03	0.05	0.04	0.05	0.05	0.05	0.05	0.09	0.09
MgO	0.90	0.21	0.21	0.26	0.28	1.08	0.46	0.44	1.15	5.60	5.63
CaO	1.95	0.84	0.84	1.08	1.06	3.02	1.51	1.54	3.14	5.83	5.83
Na_2O	2.59	3.06	2.97	2.89	2.85	3.07	2.33	2.67	2.97	1.56	1.58
K_2O	3.32	5.13	5.01	4.40	3.98	3.97	5.13	4.84	4.14	6.78	6.76
P_2O_5	0.19	0.20	0.19	0.23	0.21	0.16	0.08	0.09	0.18	0.96	0.96
LOI	2.10	0.70	0.60	0.80	9.90	2.90	4.00	3.50	3.10	7.10	6.70
Total	99.20	99.86	99.86	99.17	99.85	99.85	99.77	99.89	99.58	99.54	99.55
LILE (ppm)											
Cs	3.80	5.10	4.90	7.90	7.20	11.70	14.30	10.90	7.20	9.70	10.30
Rb	115.50	157.90	156.50	164.80	153.10	139.60	277.40	182.20	139.40	219.90	234.30
*K**	27560.32	42585.67	41589.51	36525.72	33039.17	32956.16	42585.67	40178.29	34367.38	56282.81	56116.79
Ba	649.50	1040.40	975.30	980.50	1028.00	112.50	963.90	1004.80	2078.30	1491.80	1536.60
Pb	27.70	2.70	2.60	2.90	2.20	3.50	3.00	2.00	2.10	2.00	2.20
Sr	158.80	90.10	89.50	96.70	91.10	382.80	168.40	181.80	353.10	727.60	781.10
Ga	19.90	19.30	19.20	21.80	7.80	17.60	14.40	15.50	17.40	18.30	19.80
HFSE (ppm)											
Th	13.90	13.90	13.80	15.70	14.80	19.80	26.80	26.50	20.60	15.00	14.90
U	2.10	5.70	6.00	5.60	4.50	6.50	8.90	9.40	6.30	5.50	5.80
Zr	184.70	247.60	254.60	308.20	300.40	187.00	124.60	133.10	181.90	662.70	694.30
Hf	4.90	8.00	8.40	9.50	9.60	5.70	4.50	4.80	5.50	20.20	21.60
*Ti***	2398.00	2158.20	2098.25	2278.10	2158.20	2997.50	1498.75	1498.75	2937.55	9711.90	9711.90
Ta	0.60	1.10	1.40	1.50	1.40	1.40	1.70	1.70	1.30	2.20	2.50
Y	36.90	55.30	56.20	67.20	59.30	22.80	27.40	27.50	24.50	23.70	25.80
Nb	9.80	15.40	15.00	19.00	17.40	13.40	15.20	14.70	13.10	34.30	36.40
Others (ppm)											
Ni	7.60	5.00	5.00	3.70	5.00	5.00	5.00	10.00	5.00	79.00	81.00
V	35.00	16.00	17.00	18.00	21.00	61.00	39.00	33.00	68.00	164.00	173.00
Sc	5.00	12.00	12.00	14.00	12.00	8.00	3.00	3.00	8.00	16.00	16.00
Co	37.60	128.90	129.70	58.20	129.10	41.50	48.20	45.40	44.10	31.10	34.70
Be	3.00	3.00	3.00	3.00	3.00	2.00	4.00	3.00	2.00	5.00	7.00
W	386.50	1427.10	1396.70	671.40	1342.50	363.40	423.10	508.30	564.20	97.20	104.50

Table 3.3. continued.

	Gneises	Rahmanlar granite				Eğreltidağ volcanic unit				Kuzayır basalt	
	Y19	**H2/1**	**H2/2**	**Y23**	**Y23/2**	**0513**	**0505**	**0506**	**0507**	**0509/1**	**0509/2**
REE (ppm)											
La	33.60	44.80	44.40	42.80	49.70	40.00	33.70	32.50	49.10	74.00	78.80
Ce	75.70	100.50	96.30	98.30	113.00	80.70	66.40	63.50	92.70	159.60	173.10
Pr	8.41	11.35	11.42	11.27	12.82	8.32	7.05	6.66	9.34	18.81	19.75
Nd	33.80	44.20	44.40	47.90	47.80	30.30	25.80	22.90	32.70	70.90	73.70
Sm	6.90	9.80	9.90	10.30	10.50	5.20	4.70	5.00	5.60	11.50	12.50
Eu	1.47	1.02	1.02	1.13	1.04	1.08	0.63	0.70	1.09	2.45	2.73
Gd	6.99	8.99	8.67	10.86	9.64	3.93	3.98	3.70	4.44	7.12	7.78
Tb	1.16	1.56	1.52	1.80	1.72	0.70	0.69	0.70	0.72	1.00	1.03
Dy	6.83	9.60	9.06	11.50	10.34	3.78	4.16	4.30	4.10	4.58	5.04
Ho	1.30	1.90	1.88	2.24	1.98	0.76	0.86	0.87	0.81	0.83	0.84
Er	3.71	5.59	5.68	6.65	6.02	2.33	2.73	2.78	2.36	2.10	2.26
Tm	0.47	0.86	0.84	0.99	0.97	0.36	0.47	0.45	0.37	0.32	0.32
Yb	2.77	5.14	5.13	5.75	5.54	2.24	3.30	3.03	2.54	1.82	2.03
Lu	0.43	0.79	0.81	0.92	0.81	0.36	0.48	0.44	0.36	0.26	0.25

	Yağcıdağ volcanic unit											
	031025	**031028**	**031043**	**031207**	**031212**	**031301**	**YF1**	**YF2**	**0510**	**031307**	**0511/1**	**0511/3**
Major Elments (wt.%)												
SiO_2	60.76	63.64	60.95	63.21	71.12	59.56	64.93	63.06	62.68	60.27	60.25	60.33
TiO_2	1.00	0.59	0.99	0.81	0.06	0.85	0.56	0.84	0.83	1.02	0.90	0.88
Al_2O_3	14.63	15.46	15.48	16.04	12.65	15.16	15.54	16.04	16.32	15.33	15.72	15.61
Fe_2O_3	4.59	4.60	4.76	4.41	1.39	5.22	3.49	4.51	4.57	5.22	4.80	4.75
FeO^T	4.59	4.60	4.76	4.41	1.39	5.22	3.49	4.51	4.57	5.22	4.80	4.75
MnO	0.07	0.07	0.06	0.06	0.04	0.07	0.05	0.05	0.05	0.06	0.07	0.07
MgO	2.89	2.32	2.36	1.59	0.06	3.36	1.53	1.45	1.63	2.69	3.01	3.01
CaO	4.96	4.58	4.40	4.22	0.72	5.81	3.92	3.98	4.02	5.41	5.29	5.24
Na_2O	2.35	2.67	2.63	2.92	1.03	2.31	2.75	2.78	3.04	2.69	2.85	2.89
K_2O	5.15	3.00	4.49	3.93	5.54	3.69	3.83	3.97	4.09	4.41	4.21	4.06
P_2O_5	0.62	0.19	0.44	0.31	0.02	0.39	0.17	0.33	0.32	0.52	0.42	0.40
LOI	2.30	2.10	2.60	1.80	6.70	2.9	2.50	2.30	2.30	1.70	2.30	2.60
Total	99.34	99.25	99.17	99.31	99.34	99.36	99.28	99.32	99.85	99.34	99.83	99.85

Table 3.3. continued.

	Yağcıdağ volcanic unit											
	031025	**031028**	**031043**	**031207**	**031212**	**031301**	**YF1**	**YF2**	**0510**	**031307**	**0511/1**	**0511/3**
LILE (ppm)												
Cs	10.60	5.50	6.90	8.40	29.00	10.05	13.40	8.60	9.10	7.10	5.20	5.00
Rb	201.30	91.70	185.30	163.90	271.30	158.50	173.30	162.50	156.40	172.10	158.60	152.40
*K**	42751.70	24903.90	37272.84	32624.11	45989.20	30631.80	31793.98	32956.16	33952.32	36608.73	34948.47	33703.28
Ba	932.90	938.20	2141.60	717.90	582.10	841.70	616.90	762.80	772.80	1020.10	884.20	867.20
Pb	3.50	4.80	3.20	3.20	2.00	2.30	2.80	4.00	2.60	2.50	4.80	4.50
Sr	602.20	674.60	546.80	491.00	44.00	532.30	406.80	483.80	471.60	611.70	540.30	518.30
Ga	22.10	18.30	21.70	21.60	16.90	20.20	22.90	22.60	20.60	22.20	20.90	19.80
HFSE (ppm)												
Th	16.60	29.30	21.70	17.40	27.40	15.80	16.00	18.40	19.40	19.80	18.00	15.40
U	6.30	6.60	5.00	5.90	8.20	5.40	5.50	5.80	5.40	5.70	6.00	5.80
Zr	466.90	174.60	363.90	275.70	144.20	284.40	192.70	273.70	258.00	402.00	340.60	337.10
Hf	13.70	5.00	9.90	8.30	5.50	8.60	5.50	8.20	8.30	11.40	10.60	9.90
*Ti***	5995.00	3537.05	5935.05	4855.95	359.70	5095.75	3357.20	5035.80	4975.85	6114.90	5395.50	5275.60
Ta	1.60	1.10	1.60	1.40	1.60	1.20	1.10	1.30	1.40	1.60	1.60	1.60
Y	24.80	25.60	49.80	26.40	35.60	29.60	21.30	27.60	25.70	31.20	25.40	24.40
Nb	21.50	14.90	21.10	17.10	18.20	16.40	13.10	17.30	16.70	25.40	21.40	20.60
Others (ppm)												
Ni	18.70	13.90	21.00	9.80	0.50	41.10	8.90	8.30	10.00	13.40	10.00	19.00
V	114.00	66.00	97.00	77.00	0.50	121.00	63.00	78.00	72.00	116.00	105.00	103.00
Sc	14.00	15.00	14.00	12.00	7.00	17.00	10.00	13.00	12.00	15.00	13.00	12.00
Co	40.50	27.80	40.40	31.70	21.30	37.90	65.20	34.90	39.40	32.50	27.40	19.60
Be	6.00	3.00	5.00	4.00	4.00	5.00	4.00	6.00	5.00	6.00	5.00	6.00
W	201.90	167.70	182.00	225.90	170.00	264.10	506.30	240.20	194.70	185.70	143.80	108.40
REE (ppm)												
La	43.80	59.50	67.40	47.40	44.20	42.00	36.00	50.70	48.70	64.50	51.80	50.10
Ce	93.10	111.80	128.10	95.30	92.10	87.40	75.20	101.50	94.90	120.30	107.60	107.20
Pr	10.30	11.94	14.48	10.35	9.59	9.73	7.82	10.72	10.95	14.82	11.79	11.96
Nd	42.00	42.90	56.60	36.50	35.60	37.60	31.30	43.10	41.50	57.40	47.10	44.50
Sm	7.30	7.60	10.30	6.60	7.40	6.90	6.20	7.80	7.30	10.30	8.40	7.90
Eu	1.76	1.52	2.17	1.62	0.55	1.64	1.26	1.76	1.62	2.36	1.87	1.78
Gd	6.00	5.47	8.72	5.33	6.14	5.56	4.56	5.71	5.44	7.50	6.54	5.91
Tb	0.82	0.79	1.23	0.76	0.99	0.87	0.70	0.80	0.81	1.10	0.92	0.89
Dy	4.55	4.67	7.30	4.42	6.07	4.81	3.67	4.56	4.33	5.06	4.76	4.57
Ho	0.81	0.84	1.39	0.76	1.16	0.86	0.71	0.90	0.81	0.98	0.78	0.83
Er	2.23	2.30	3.77	2.21	3.43	2.48	2.02	2.41	2.45	2.73	2.33	2.31
Tm	0.31	0.30	0.58	0.36	0.52	0.42	0.27	0.37	0.37	0.37	0.35	0.33
Yb	1.99	2.45	3.44	2.34	2.83	2.35	1.93	2.09	2.34	2.37	2.08	2.18
Lu	0.30	0.33	0.53	0.36	0.50	0.36	0.30	0.34	0.31	0.38	0.30	0.29

Table 3.3. continued.

	Yağcıdağ volcanic unit			Kabaklar basalt			
	KD-1	**KD-2**	**KD-3**	**0512/1**	**0512/2**	**0512/3**	**0512/4**
Major Elments (wt.%)							
SiO_2	60.09	59.71	59.23	48.41	47.94	48.30	47.75
TiO_2	0.52	0.53	0.65	1.11	1.09	1.08	1.10
Al_2O_3	15.22	15.07	14.68	13.40	13.30	13.24	13.64
Fe_2O_3	4.53	4.97	5.15	7.87	7.94	8.08	7.77
FeO^T	4.53	4.97	5.15	7.87	7.94	8.08	7.77
MnO	0.07	0.14	0.13	0.12	0.13	0.13	0.12
MgO	2.80	2.08	2.74	11.70	11.76	11.57	11.90
CaO	3.96	5.23	5.58	9.09	9.25	9.15	8.96
Na_2O	2.40	2.78	2.87	3.27	3.19	3.23	3.39
K_2O	3.35	3.32	3.54	1.49	1.55	1.53	1.54
P_2O_5	0.14	0.15	0.34	0.68	0.71	0.73	0.68
LOI	6.80	5.90	4.90	2.40	2.70	2.80	2.70
Total	99.89	99.89	99.83	99.67	99.68	99.70	99.68
LILE (ppm)							
Cs	23.40	34.20	3.00	7.30	8.50	8.50	8.60
Rb	129.90	134.20	124.20	46.40	55.50	55.00	53.90
*K**	27809.36	27560.32	29386.60	12368.94	12867.02	12700.99	12784.00
Ba	751.70	865.10	1111.30	1496.80	1831.20	1774.20	1769.80
Pb	20.00	17.70	11.00	2.40	2.20	2.40	2.50
Sr	284.80	371.00	472.10	733.50	873.10	880.00	869.70
Ga	16.80	15.80	17.30	12.60	15.00	14.80	15.00
HFSE (ppm)							
Th	13.50	13.80	18.60	16.90	20.70	20.90	19.80
U	4.90	4.10	5.20	5.30	7.00	6.30	6.90
Zr	125.10	117.60	170.90	269.40	315.90	322.10	323.20
Hf	4.20	3.80	5.00	7.50	9.20	9.20	9.40
*Ti***	3117.40	3177.35	3896.75	6654.45	6534.55	6474.60	6594.50
Ta	0.90	0.80	0.90	1.20	1.30	1.30	1.30
Y	21.20	21.60	25.80	25.80	30.60	1.30	30.40
Nb	8.80	8.80	11.60	18.90	22.30	1.30	21.70
Others (ppm)							
Ni	14.00	17.00	59.00	292.00	278.00	295.00	292.00
V	88.00	100.00	120.00	178.00	210.00	200.00	208.00
Sc	11.00	11.00	12.00	27.00	27.00	27.00	27.00
Co	26.60	29.20	45.30	45.40	55.20	49.60	48.60
Be	2.00	2.00	2.00	3.00	4.00	4.00	4.00
W	218.20	272.00	362.90	179.30	204.30	101.10	100.40

Table 3.3. continued.

	Yağcıdağ volcanic unit			Kabaklar basalt			
	KD-1	**KD-2**	**KD-3**	**0512/1**	**0512/2**	**0512/3**	**0512/4**
REE (ppm)							
La	32.40	30.60	35.60	60.90	74.80	72.10	74.30
Ce	66.10	62.90	74.10	129.90	161.20	154.10	156.60
Pr	6.94	6.84	8.21	14.68	17.70	17.66	17.62
Nd	26.10	24.80	32.90	56.90	66.30	65.60	68.00
Sm	4.80	4.70	6.00	10.80	12.60	13.10	13.00
Eu	0.93	1.09	1.34	2.48	2.84	3.01	2.96
Gd	3.24	3.59	4.54	7.80	9.23	9.53	8.83
Tb	0.58	0.56	0.70	1.01	1.25	1.24	1.20
Dy	3.42	3.76	4.33	4.97	6.03	5.83	6.15
Ho	0.74	0.75	0.90	0.86	1.02	1.01	1.02
Er	2.12	2.21	2.53	2.26	2.60	2.64	2.65
Tm	0.35	0.35	0.39	0.31	0.41	0.38	0.39
Yb	2.16	2.09	2.59	2.13	2.29	2.22	2.23
Lu	0.33	0.37	0.40	0.25	0.32	0.30	0.33

* $K = \%K_2Ox0.83013x10^6$

** $Ti = \%TiO_2x0.59950x10^6$

Table 3.4. Normative mineralogy of the magmatic rocks of the Selendi Basin.

	Q	Or	Ab	An	Ne	C	Di	Hy	Fo	Fa	Mt	Il	Ap	Total
Rahmanlar Granite														
H2/1	33.06	30.00	25.57	2.96	0.00	2.42	0.00	1.92	0.00	0.00	2.97	0.68	0.43	100.00
H2/2	34.71	29.26	24.79	3.02	0.00	2.26	0.00	1.95	0.00	0.00	2.95	0.66	0.41	100.00
Y23	36.49	25.93	24.34	4.00	0.00	2.57	0.00	1.50	0.00	0.00	3.92	0.72	0.50	100.00
Y23/2	34.53	25.60	26.20	4.38	0.00	1.96	0.00	1.67	0.00	0.00	4.42	0.74	0.50	100.00
Eğreltidağ volcanic unit														
505	35.62	31.36	20.35	7.26	0.00	0.97	0.00	1.41	0.00	0.00	2.37	0.49	0.18	100.00
506	34.93	29.40	23.17	7.31	0.00	0.90	0.00	1.44	0.00	0.00	2.14	0.49	0.20	100.00
507	24.04	24.62	25.23	14.61	0.00	0.46	0.00	5.05	0.00	0.00	4.66	0.94	0.40	100.00
513	24.88	23.49	25.96	14.06	0.00	0.90	0.00	4.90	0.00	0.00	4.51	0.95	0.35	100.00
Kuzayır basalt														
0509/1	0.00	40.76	13.40	7.14	0.00	0.00	13.14	10.39	0.56	0.15	9.20	3.13	2.13	100.00
0509/2	0.00	40.47	13.52	7.46	0.00	0.00	12.81	10.90	0.38	0.10	9.13	3.12	2.12	100.00
Yağcıdağ volcanic unit														
510	17.80	23.82	25.30	17.80	0.00	0.24	0.00	6.26	0.00	0.00	6.53	1.55	0.69	100.00
31025	14.42	30.15	19.66	13.96	0.00	0.00	5.43	6.57	0.00	0.00	6.59	1.88	1.34	100.00
31028	22.43	17.55	22.32	21.06	0.00	0.00	0.27	8.27	0.00	0.00	6.60	1.11	0.41	100.00
31043	16.15	26.41	22.10	17.02	0.00	0.00	1.72	6.93	0.00	0.00	6.86	1.87	0.96	100.00
31207	19.18	22.90	24.31	18.72	0.00	0.00	0.10	6.30	0.00	0.00	6.30	1.52	0.67	100.00
31212	44.90	35.00	9.30	3.69	0.00	3.93	0.00	0.87	0.00	0.00	2.15	0.12	0.05	100.00
31301	15.07	21.52	19.25	19.77	0.00	0.00	5.16	9.35	0.00	0.00	7.46	1.59	0.84	100.00
YF1	23.27	22.71	23.30	18.50	0.00	0.09	0.00	6.52	0.00	0.00	5.07	1.07	0.37	100.00
YF2	20.58	23.25	23.26	17.64	0.00	0.61	0.00	5.89	0.00	0.00	6.47	1.58	0.71	100.00
KD-1	20.28	20.41	20.89	19.40	0.00	0.75	0.00	10.16	0.00	0.00	6.77	1.02	0.31	100.00
KD-2	17.43	20.04	23.98	19.18	0.00	0.00	5.19	5.46	0.00	0.00	7.36	1.03	0.33	100.00
KD-3	13.91	20.96	24.28	16.69	0.00	0.00	7.35	7.37	0.00	0.00	7.47	1.24	0.74	100.00
31307	13.15	25.42	22.15	16.25	0.00	0.00	5.61	10.04	0.00	0.00	7.38	1.89	1.11	100.00
0511/1	13.01	24.53	23.73	17.35	0.00	0.00	4.85	7.09	0.00	0.00	6.86	1.68	0.90	100.00
0511/3	13.47	23.72	24.13	17.36	0.00	0.00	4.80	7.23	0.00	0.00	6.80	1.65	0.86	100.00
Kabaklar basalt														
0512/1	0.00	8.46	23.74	16.76	1.52	0.00	17.96	0.00	14.56	2.60	10.96	2.03	1.43	100.00
0512/2	0.00	8.83	22.17	16.72	2.05	0.00	18.54	0.00	14.54	2.58	11.09	1.99	1.49	100.00
0512/3	0.00	8.62	22.62	16.26	1.83	0.00	18.18	0.00	14.34	3.54	11.15	1.95	1.52	100.00
0512/4	0.00	8.77	21.61	16.78	3.24	0.00	17.54	0.00	15.07	2.70	10.85	2.01	1.43	100.00

Q: Quartz; Or: Orthoclase; Ab: Albite; An: Anorthite; Ne: Nepheline; C: Corundum; Di: Diopside; Hy: Hyperstene; Fo: Forsterite; Fa: Fayalite; Mt: Magnetite; Il: Ilmenite; Ap: Apatite.

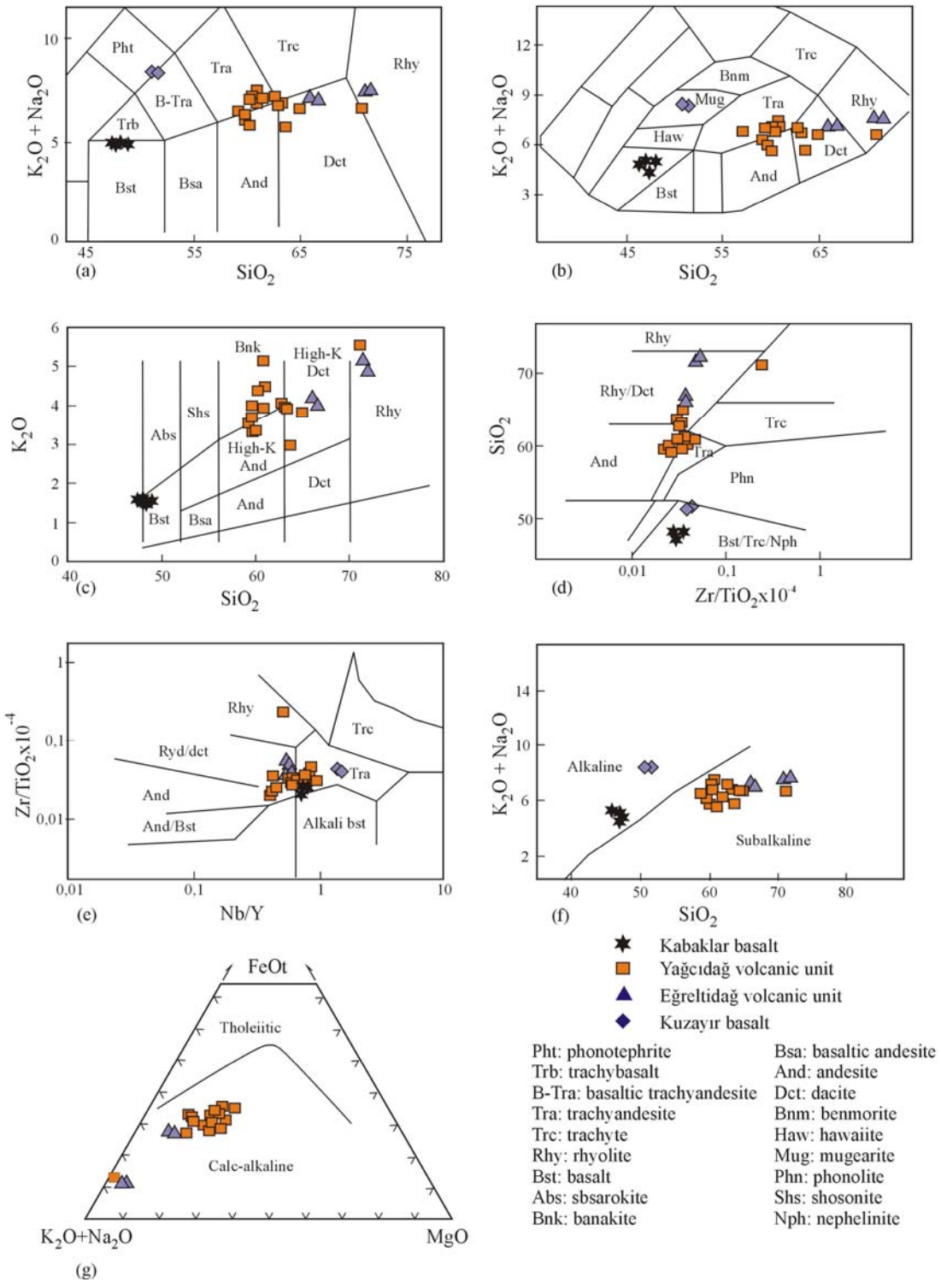


Figure 3.11. Total alkalis (K_2O+Na_2O) wt.% vs SiO_2 wt.% classification diagram of **(a)** LeBas *et al.* (1986) and **(b)** Cox *et al.* (1979); **(c)** K_2O wt.% vs SiO_2 wt.% classification diagram of Pecerillo & Taylor (1976); **(d)** SiO_2 wt.% vs Zr/TiO_2x10^{-4} and **(e)** Zr/TiO_2x10^{-4} vs Nb/Y diagrams of Winchester & Floyd (1977); **(f)** alkali-subalkaline classification and **(g)** tholeiitic-calc-alkaline classification diagrams of Irvine & Baragar (1971).

3.2.2. Kuzayır basalt

In the classification diagrams (Figure 3.11), the rocks of the Kuzayır basalt fall in the phonotephrite, basaltic trachyandesite, mugearite, basalt/trachyte/nephelinite fields and exhibit an alkaline character in the *K_2O wt % vs SiO_2 wt %* alkali-subalkali diagram of Irvine & Baragar (1971). Normative mineralogy of the Kuzayır basalt includes diopside, hyperstene and olivine and do not contain any normative quartz (Table 3.4). The normative K-feldspar contents of the Kuzayır basalt are considerably high (47.47-40.76 %; Table 3.4).

The Kuzayır basalt is named in this study as ultrapotassic, for the first time, on the basis of their high K_2O contents (>3 wt. %) and high K_2O/Na_2O (>3%) ratios (cf. Foley *et al.* 1987). Another criteria, providing from geochemistry of these lavas, is their high Mg# (100 Mg/Mg + Fe)) and MgO contents (>3 wt %; Foley *et al.* 1987; Wilson 1995). According to the Bergman (1987), ultrapotassic magnesian igneous rocks with K_2O/Na_2O >5 (wt %) and SiO_2 in the range 45 – 55 (wt %) are called as lamproites. These values of the Kuzayır basalt are 4.28 – 4.35 and 51.21 – 51.47 (wt %), respectively, thus they can also be accepted as lamproitic rocks.

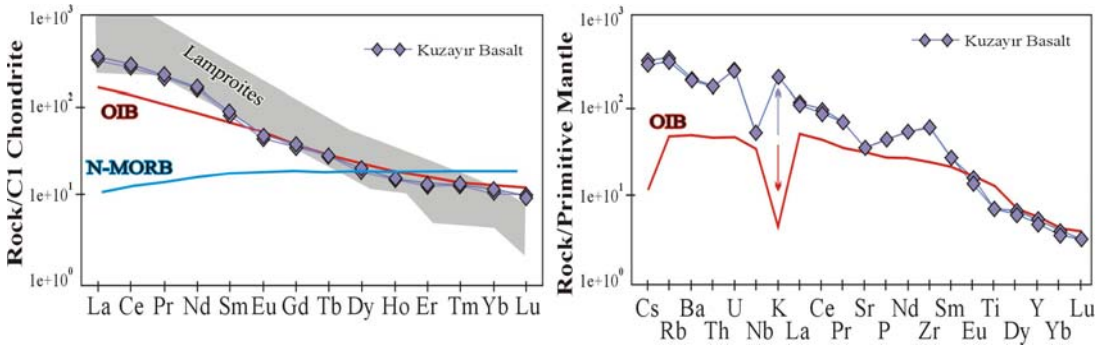


Figure 3.12. (a) C1 Chondrite-normalized REE diagram and **(b)** primitive mantle-normalized multi element spider-diagram of the Kuzayır basalt. The data for lamproites from Mitchell & Bergman (1991). OIB, N-MORB data and coefficients for normalization are after Sun & McDonough (1989).

The Kuzayır basalt shows a slight enrichment in LREE (light rare earth elements) and a slight depletion in HREE (heavy rare earth elements) with respect to the OIB (ocean island basalt) magmas and shows a similar REE pattern with the lamproites (Mitchel & Bergman 1991) in the chondrite-normalized REE diagram (Figure 3.12a).

The Kuzayır basalt exhibits an enrichment in LILE (large ion litophile elements such as Cs, Rb, Ba, K, Th and U) in the range of 300-500 times primitive mantle (especially in K; Figure 3.12b). They are depleted in HFSE (high field strength elements), with Ta (not shown), Nb and Ti troughs and high LILE/HFSE ratios (Figure 3.12).

3.2.3. Eğreltidağ volcanic unit

The felsic rocks of the Eğreltidağ volcanic unit show a compositional trend from dacite to rhyolite in the classification diagrams (Figure 3.11a-e). These rocks fall into sub-alkali field in *K_2O wt % vs SiO_2 wt %* alkali-subalkali diagram of Irvine & Baragar (1971) (Figure 3.11f) and have also calc-alkali character in *(K_2O+Na_2O) wt % - FeOt wt % - MgO wt %* (AFM) diagram (Figure 3.11g) of Irvine & Baragar (1971). The felsic rocks of the unit are hyperstene-normative and also include 24 - 35% normative quartz (Table 3.3). In fact, the felsic members of the unit contain normative corundum of about 1%, being less than those of the Rahmanlar granite and greater than those of the Yağcıdağ volcanic unit. These rocks also have similar Shand's index features with the Rahmanlar granite (Table 3.5).

Table 3.5. Shand's indexes of the Eğreltidağ volcanic unit (Ev).

Sample	0513	0505	0506	0507	*Shand's index*
$Al_2O_3/(CaO+Na_2O+K_2O)$	1.53	1.44	1.45	1.48	peraluminous
$(Na_2O+K_2O)/ Al_2O_3$	0.46	0.58	0.57	0.47	peraluminous

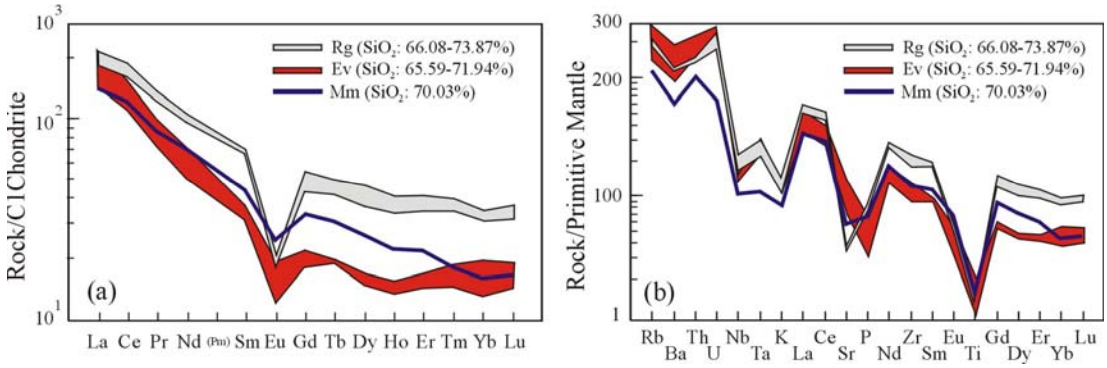


Figure 3.13. (a) C1 Chondrite-normalized REE diagram and **(b)** Primitive mantle-normalized multi element spider-diagram of the Eğreltidağ volcanic rocks (Ev). The Rahmanlar granite (Rg) and representative sample from the Menderes metamorphics (Mm) is also shown in the diagram. Normalizing values are from Sun & McDonough (1989).

The Eğreltidağ volcanic unit shows enrichment in LREE, similarly to the Rahmanlar granite, in the chondrite-normalized REE diagram, but they were depleted in HREE (Figure 3.13a). Similarly to the Rahmanlar granite, but stronger Eu negative anomalies are seen in the Eğreltidağ volcanic unit. Eğreltidağ volcanic unit are enriched in LILE at a similar rate with the Rahmanlar granite in the primitive mantle-normalized spider-diagram (Figure 3.13b). The multi-element patterns of the unit in this diagram differ from the Rahmanlar granite with respect to HFSE (high field strength elements such as Nd, Zr). They are characterized also by stronger Sr and Ti negative anomalies (Figure 3.13b).

3.2.4. Yağcıdağ Volcanic unit

The Yağcıdağ volcanic unit shows a more scattered compositional range varying from andesite, to trachyandesite, trachyte and dacite (Figure 3.11a-e). One samples from the Yağcıdağ volcanic unit (pumice from pumice-fall deposits) falls in rhyolite field. All samples of the Yağcıdağ volcanic unit show a sub-alkaline character (Figure 3.11f) and fall in calc-alkali field in the AFM diagram (Figure 3.11g). The Yağcıdağ volcanic unit is hyperstene-normative and contains 14-44% normative quartz (Table 3.3).

Intra-element variation diagrams (Harker variation diagrams) for the Yağcıdağ volcanic unit are given in Figure 3.14. All volcanic rocks of the unit show good correlation with the CaO, Fe_2O_3, P_2O_5, K_2O, MgO and TiO_2 (Figure 3.14a). Excep for K_2O, major element oxides show a positive correlation with increasing SiO_2 contents. Similarly, trace elements, except for Rb, show a good negative correlation with increasing SiO_2 (Figure 3.14b).

Yağcıdağ volcanic unit shows enrichment in LREE in the range of 300-500 times chondritic values (Figure 3.15a). They also show a strong negative Eu anomaly and a slight enrichment in HREE in this diagram. The primitive mantle-normalized spider diagram for the Yağcıdağ volcanic rocks (Figure 3.15b) shows that these rocks are enriched in LILE in the range of 100-500 times primitive mantle values. They are characterized by strong HFSE anomalies (such as Nb, Ta and Ti). The enriched

samples from the Yağcıdağ volcanic unit (i.e. rhyolitic pumice) show strong negative anomalies at Sr and P. These rocks also depleted in K (Figure 3.15b). This diagram also shows that the Yağcıdağ volcanic unit is variably enriched in many elements, probably indicating variable degree of AFC (Assimilation and Fractional Crystallization) processes.

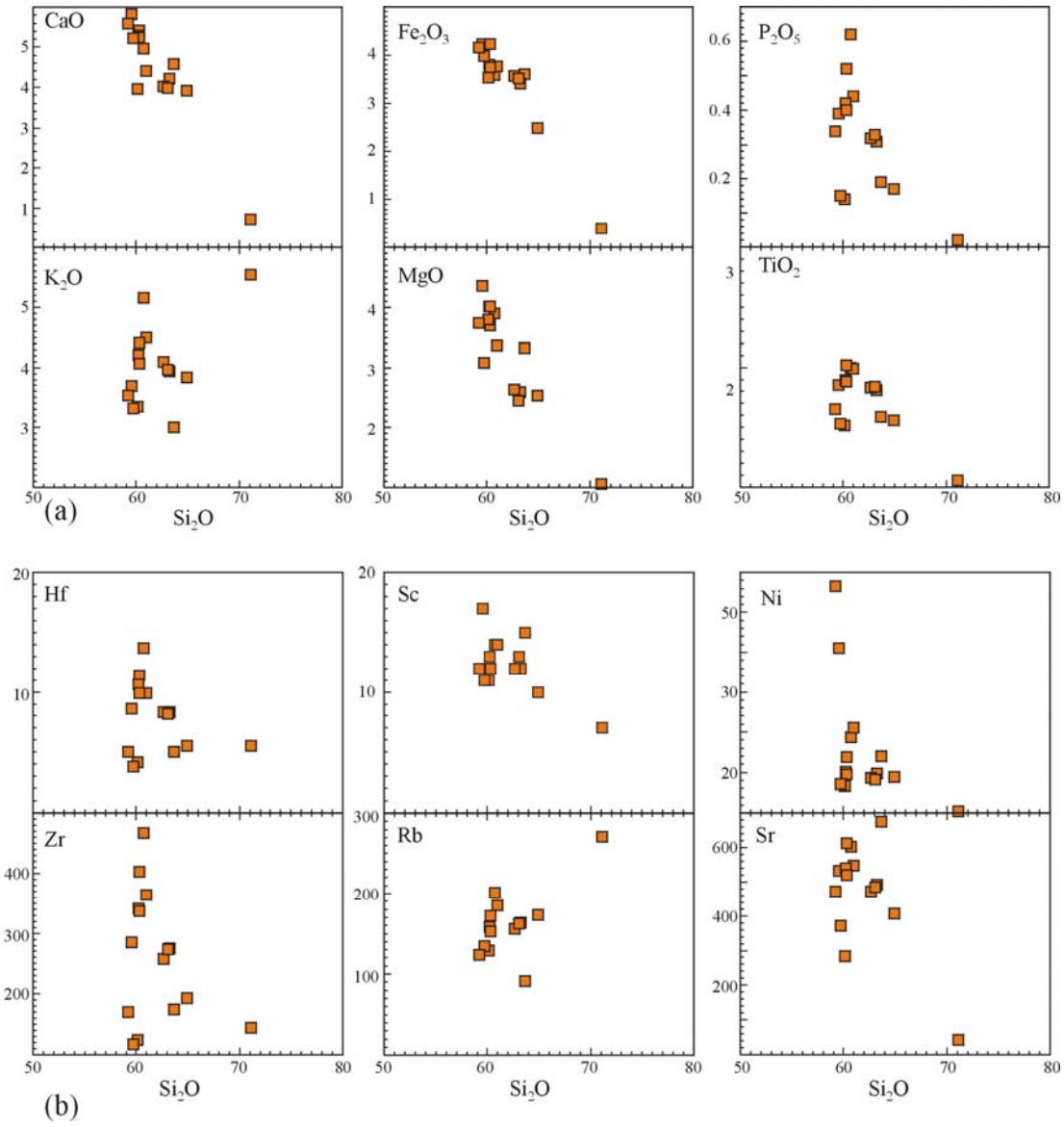


Figure 3.14. Harker variation diagrams of the Yağcıdağ volcanic unit: **(a)** major oxides (in wt %) and **(b)** trace elements (in ppm).

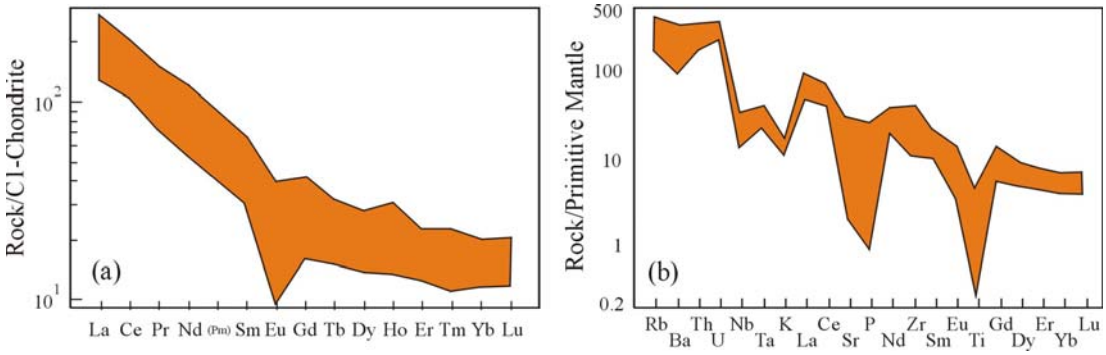


Figure 3.15. (a) C1-chondrite-normalized REE diagram and **(b)** Primitive mantle-normalized multi element spider-diagram of the Yağcıdağ volcanic rocks. Normalizing values are from Sun & McDonough (1989).

3.2.5. Kabaklar Basalt

According to the previous studies (Ercan & Öztunalı, 1983; Ercan *et al.*, 1983; Ercan *et al.*, 1992) these rocks were named as Kula volcanic unit. However, this study shows that these rocks differ from the Kula volcanic unit based on their geochemical features.

Olivine-bearing Kabaklar volcanic unit plot in trachybasalt, basalt and basalt/trachyte/nephelinite fields (Figure 3.11a-e). The Kabaklar basalt shows alkali character in AFM diagram (Figure 3.11f). These rocks are nepheline-normative and do not contain any normative hyperstene and quartz (Table 3.4).

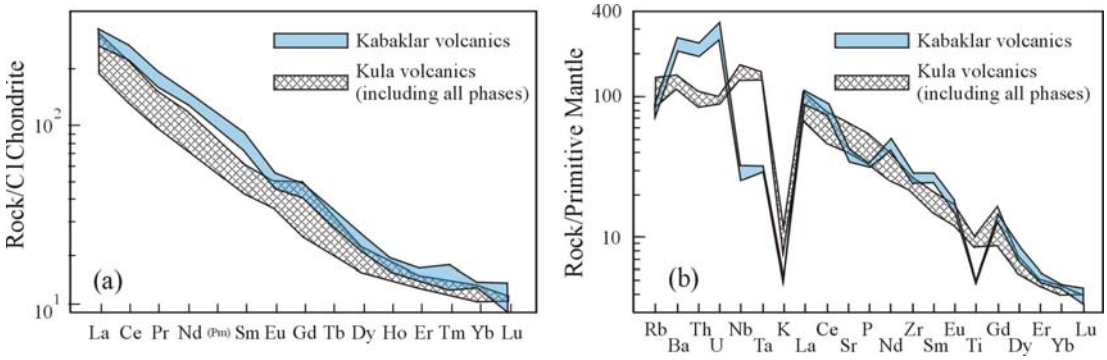


Figure 3.16. (a) C1-chondrite-normalized REE diagram and (b) Primitive mantle-normalized multi element spider-diagram of the Kabaklar basalt. Normalizing values are from Sun & McDonough (1989). The data for the Kula volcanic unit are from Alıcı *et al.* (2002). In these diagrams, Kula volcanic unit include all phases (namely Burgaz, Elekçitepe and Divlittepe volcanic unit) of the Kula basaltic volcanism.

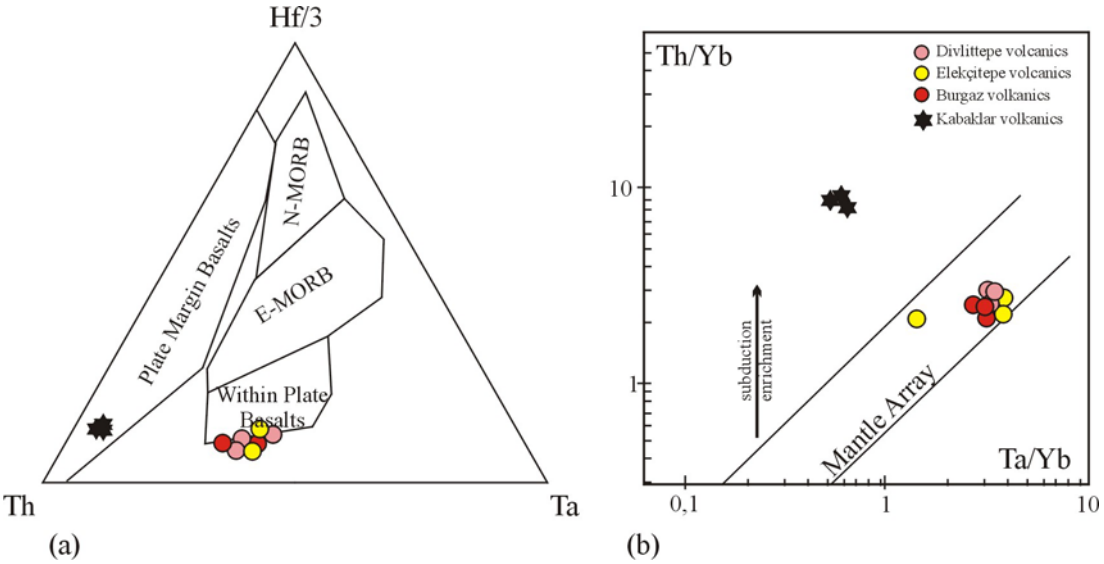


Figure 3.17. (a) Hf/3 – Th – Ta diagram (after Wood 1980) and **(b)** Ta/Yb vs Th/Yb diagram (after Pearce 1983) for the Kabaklar volcanic unit. Kula volcanic unit (Burgaz, Elekçitepe and Burgaz volcanic unit) are also shown in the diagrams. The data for the Kula volcanic unit from Alıcı *et al.* (2002).

Kabaklar volcanic unit is slightly enriched in all REE with respect to the Kula volcanic unit in the chondrite-normalized REE diagram (Figure 3.16a). They are enriched in LREE in the range of 200-300 times chondritic values. The degree of enrichment is less in HREE being 10 times chondritic values. In this diagram, one can easily see a slight Eu negative anomaly, probably resulting from the affects of plagioclase, which absent for the Kula volcanic unit (Figure 3.16a). Primitive mantle-normalized spider-diagram for these rocks is shown in Figure 3.16b. In this diagram analyses from the Kula volcanic unit is also plotted. It is apparent that the Kabaklar volcanic unit differs from the Kula volcanic unit, particularly when HFSE and LILE contents are considered. Ba, Th and U contents of the Kabaklar volcanic unit 200-300 times enriched with respect to the Kula volcanic unit (Figure 3.16a). Ti is highly depleted in the Kula volcanic unit. Another important feature in the diagram is the Ta and Nb anomalies; this is absent in the Kula volcanic unit. This geochemical feature is called as subduction zone component (e.g., Pearce 1983). Similar differences also appear in the *Hf/3–Th–Ta* (Figure 3.17a) and *Ta/Yb–Ta/Yb* diagrams (Figure 3.17b). In the *Hf/3–Th–Ta* diagram, Kabaklar basalt fall into plate margin basalt field, whereas Kula basalts, within plate basalt field (Figure 3.17a). Subduction zone magmas-like geochemical feature (subduction zone component) of the Kabaklar basalt can also be inferred in *Ta/Yb–Ta/Yb* diagram (Figure 3.17b).

Thus, the higher *Th/Yb* and lower *Ta/Yb* ratios of the Kabaklar volcanic unit differentiate these rocks significantly from the Kula volcanic unit.

CHAPTER FOUR

PETROGENESIS OF THE MAGMATIC ROCKS

4.1. Eğreltidağ volcanic unit and Rahmanlar granite: an anatexitic origin?

As identified by geological (field) data, the Rahmanlar granite and the Eğreltidağ volcanic unit have a genetic relationship with the basement rocks (i.e., Menderes metamorphics). One can easily see in Figure 3.13a that the Rahmanlar granite shows enrichment in elements from LREE (light rare earth elements) to HREE (heavy rare earth elements) with respect to those of the Menderes metamorphics with an increasing enrichment degree harmoniously with the increasing atomic numbers. In the same way, the REE pattern of the Eğreltidağ volcanic unit apparently shows that the decreasing enrichment degree with respect to the Rahmanlar granite is harmoniously goes up through the MREE (medium rare earth elements) and HREE (heavy rare earth elements). Also note that the different degree of Eu negative anomalies among the rocks units increase from Menderes Massif to the Rahmanlar granite and finally to the Eğreltidağ volcanic unit. This geochemical trace reflects either (i) the presence of the plagioclase in the source or (ii) plagioclase as a fractionating phase from the melt, since Eu is a compatible element in the plagioclase. Similar aspects can be seen in the primitive mantle-normalized spider-diagram (Figure 3.13b). These geochemical similarites among three units reflect close genetic relations, and suggest that the melting and fractional crystallization which is probably combined with the assimilation (AFC).

To test these relations, melting modeling diagrams have been plotted using certain elements (Figure 4.1). Figures 4.1a and b show *Rb vs Ba* and *Zr vs Y* partial melting modeling diagrams. The modal mineralogy of the source metamorphics has been accepted as K-feldspar (60%), plagioclase (20%), biotite (10%) and garnet (10%). Melting calculations, with partition coefficients are given in Table 4.1.

Table. 4.1. Melting calculations for the Menderes metamorphics to produce the Rahmanlar granite. Results are plotted in Figure 4.1.

	Kd_{garnet}	$Kd_{biotite}$	$Kd_{K\text{-}feldspar}$	$Kd_{plagioclase}$	ΣK_d
Rb	0.0010	2.2400	0.1000	0.0500	0.1926
Ba	0.0010	4.5000	0.0400	0.2300	0.3256
Sr	0.0020	0.0800	0.3000	1.2000	0.5742
Zr	0.3000	0.0010	0.1000	0.0100	0.0836
Y	2.0000	0.2000	0.0010	0.0300	0.2210

Batch Melting ($C_L/C_0=1/[D_0+F(1-D_0)]$

	0.1%	10 %	20%	30%	40%	50%	60%	70%	80%
Rb	597.19	422.55	326.20	265.63	224.03	193.69	170.60	152.42	137.74
Ba	1990.66	1652.50	1410.48	1230.30	1090.94	979.93	889.43	814.24	750.76
Sr	276.35	257.47	240.84	226.23	213.29	201.75	191.40	182.06	173.58
Zr	2187.96	1054.52	692.28	515.27	410.35	340.93	291.60	254.74	226.15
Y	166.76	123.64	98.03	81.21	69.32	60.47	53.62	48.16	43.72
Rb/Sr	2.16	1.64	1.35	1.17	1.05	0.96	0.89	0.84	0.79
Fractional Melting ($C_L/C_0=1/D_0[(1-F)^{[(1/Do)-1]}$									
Rb	597.18	385.57	235.33	134.45	70.45	32.81	12.87	3.85	0.70
Ba	1990.65	1603.69	1256.52	952.91	692.45	474.66	298.99	164.77	71.15
Sr	276.35	255.77	234.38	212.28	189.35	165.41	140.18	113.25	83.84
Zr	2187.82	695.90	191.03	44.11	8.12	1.10	0.09	0.00	0.00
Y	166.76	115.31	76.04	47.43	27.50	14.44	6.56	2.37	0.57
Rb/Sr	2.16	1.51	1.00	0.63	0.37	0.20	0.09	0.03	0.01

The *Ba-Rb* diagram (Figure 4.1a) suggests that the Rahmanlar granite was produced by 25-30% fractional melting (or 50-65% batch melting) of the gneisses. In this diagram Rb have been used because of the Rb shows a good-positive correlation with SiO_2 as differentiation index, and Ba is an incompatible element in the phases of the gneisses. The results have also been obtained from *Zr vs Y* diagram (Figure 4.1b); it suggests a fractional melting, approximately 35-40% of melting degree which is slightly higher than those of the Ba vs. Rb diagram. In the *Ba vs Rb/Sr* diagram (Figure 4.1c), granite field has higher *Rb/Sr* ratios from those of the theoretically yielding granite melts by 35-45% fractional melting. This result may be rise from fractional crystallization of plagioclase (or any mineral in the granite). The partition coefficients of the Rb and Sr in the plagioclase are 0.05 and 1.2, respectively, thus fractionation of this phase from the melt would increase the Rb/Sr ratio in the residual melts. On the other hand, Ba is slightly incompatible element in the plagioclase, and hence fractional crystallization of this phase from the melt would slightly increase the Ba in the residual melt. In the *Sr vs Y* diagram (Figure 4.1d); granite field has lower Sr values from the hypothetically expecting field. Here, again, this result may rise from the plagioclase fractionation. The melting curves in Figure 4.1a and b are the reverse of the fractionation trends, and thus, these diagrams reveal that the melting degree is at least 30-45%.

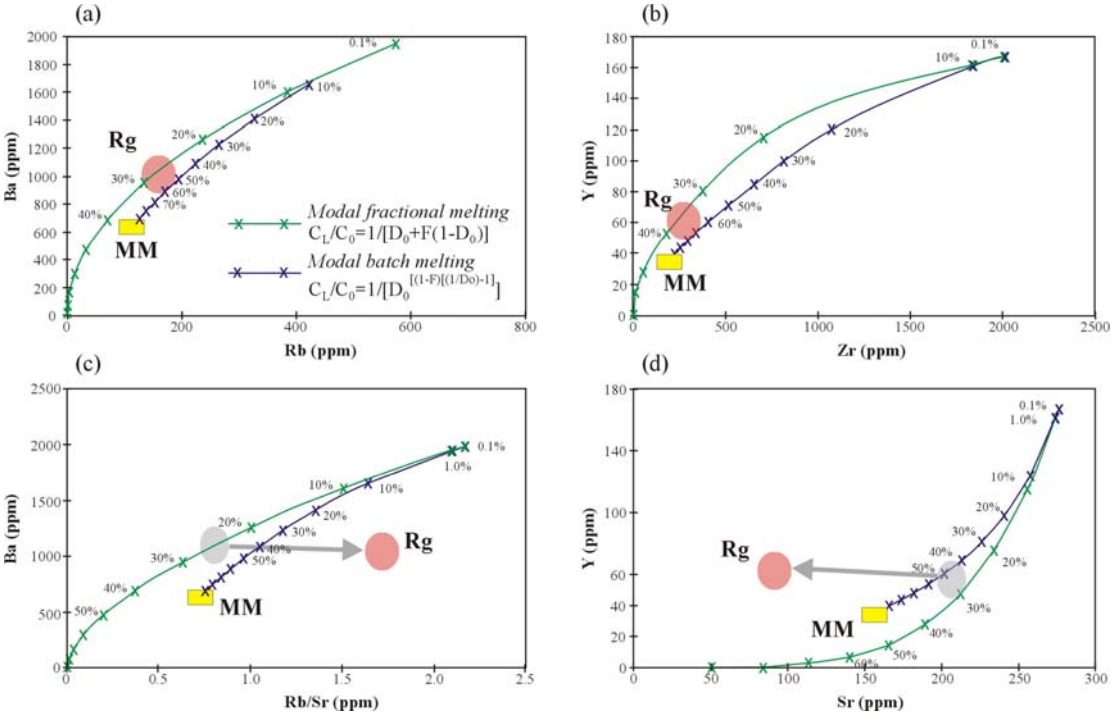


Figure 4.1. (a) Rb-Ba, **(b)** Zr-Y, (c) Rb/Sr-Ba and **(d)** Sr-Y diagrams for the Rahmanlar granite (Rg) and representative sample of the Menderes metamorphics (Mm). The curves represent the batch and fractional melting trends. The grey field in **(c)** and **(d)** represents the hypothetical granite field, producing by 25-30% fractional melting of the Mm.

The results of the melting modeling are consistent with the REE- and spider-diagrams which indicate the plagioclase effect in the generation of the Rahmanlar granite. The modal mineralogy of the Rahmanlar granite and the many rock units of the Menderes Massif include garnets. The presence of the garnet in the source rocks appears in the HREE contents of the resulting melts because HREE are compatible in garnet, hence would be retained in the source. The HREE-enriched nature of the Rahmanlar granite with respect to the Menderes massif may have given rise from the lower garnet contents of the gneisses of the Menderes metamorphics. All these evidence authorizes us to speculate that the Rahmanlar granite was produced by partial fractional melting (at least 25-40 % melting degree) of the Menderes metamorphics.

The stratigraphic and tectonic relations also indicate that the Eğreltidağ volcanic unit was produced from the same source of Rahmanlar granite (see also Chapter II and V for further discussion). We can accept that the Rahmanlar granite represents

the plutonic equivalent and/or residue of the Eğreltidağ volcanic unit. Figure 3.13a shows that the Eğreltidağ volcanic unit has lover HREE contents and presents stronger Eu anomalies. These indicate that the source rocks of the Eğreltidağ volcanic unit include garnet (because of the HREE depletion) and plagioclase (because of the Eu depletion). This mineralogy is consistent with those of the Rahmanlar granite.

The Th/Yb and Ta/Yb ratios, and thus the diagram based on these, is independent of fractional crystallization and/or partial melting (Figure 4.2; Pearce 1983). The metasomatism and enrichment of the source region by subduction, or crustal contamination of the magmas results in an enrichment of Th with respect to the Ta. This enrichment is reflected by higher Th/Yb ratio. In the *Th/Yb vs Ta/Yb* diagram, the Eğreltidağ volcanic unit (and also Rahmanlar granite) show a higher Th/Yb ratio from the mantle array (Figure 4.2) indicating that (1) this melt is generated from a metasomatised mantle lithosphere or (2) they are experienced to crustal contamination, (3) or more likely as it supported by other geochemical data, they were produced by melting of a basement rocks which has similar geochemical characteristics with the subduction-modified melts, i.e. Menderes metamorphics; or (4) they were generated from a melt carrying subduction-modified geochemical features, i.e. Rahmanlar granite (Figure 4.2). This interpretation must be taken into consideration with the silica contents of the lavas. SiO_2 contents of all these rock units are high.

It can be also discussed that the higher Th/Yb ratios of the Eğreltidağ volcanic unit with respect to the Rahmanlar granite (i.e. these lavas caries higher subduction zone components), probably raised from magma mixing between crustal- and subduction zone-related magmatism. The hydrous phase in the Eğreltidağ volcanic unit is hornblende. This may indicates that these melts are not a unified crustal melts. In fact, it is possible that these rocks might have been mixed by more mafic melts, such as Kuzayır basalt.

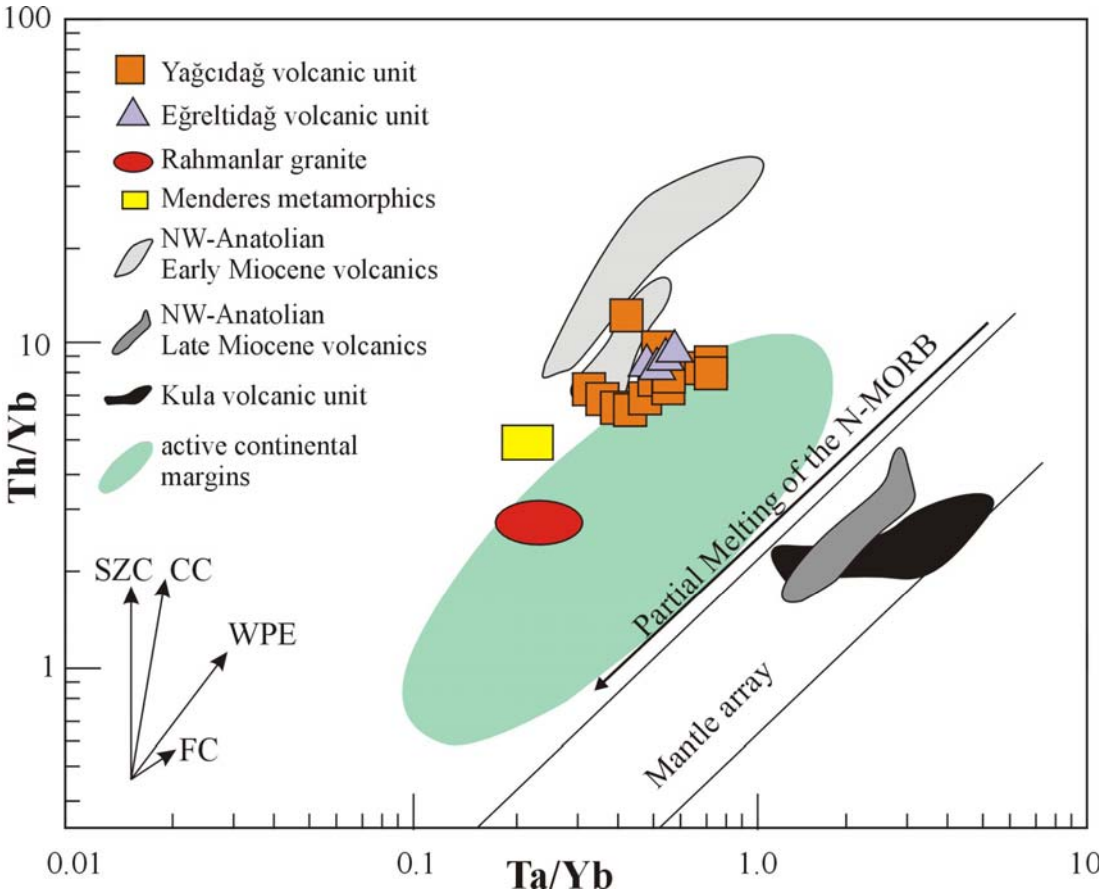


Figure 4.2. Th/Yb vs. Ta/Yb diagram for the Eğreltidağ and Yağcıdağ volcanic unit (after Pearce 1983). The data for NW Anatolian Miocene volcanic rocks from Aldanmaz *et al.* (2000), Kula volcanic unit from Alıcı *et al.* (2002). SZC: subduction zone component; CC: crustal contamination, WPE: within plate enrichment; FC: fractional crystallization.

To test the fractionating phases in the Eğreltidağ volcanic unit, the Rb-Sm diagram have also been plotted (Figure 4.3). In this diagram Rb represents the differentiation index because it's positive correlation with the increasing SiO_2 (i.e. highly incompatible). Sm is used because it is has higher partition coefficient compared with the pyroxenes, and thus using of this elements can separates the hydrous (amphibole-bearing) and anhydrous (amphibole-free) crystallization.

In the *Rb-Sm* diagram Rahmanlar granite is also shown as the source region or starting melt of the Eğreltidağ volcanic unit (Figure 4.3). The lower Sm contents of the Eğreltidağ volcanic unit (especially with respect to the Rahmanlar granite) can explain by garnet fractionation or residual garnet (in the source region, i.e. Rahmanlar granite). The trend of the Eğreltidağ volcanic unit suggests a hydrous crystallization assemblage with dominantly amphibole fractionation. It should be

noted that the effect of the garnet is less than the amphibole in this diagram (Figure 4.3). The petrographic evidence from the Rahmanlar granite and Eğreltidağ volcanic unit is also consistent with this interpretation.

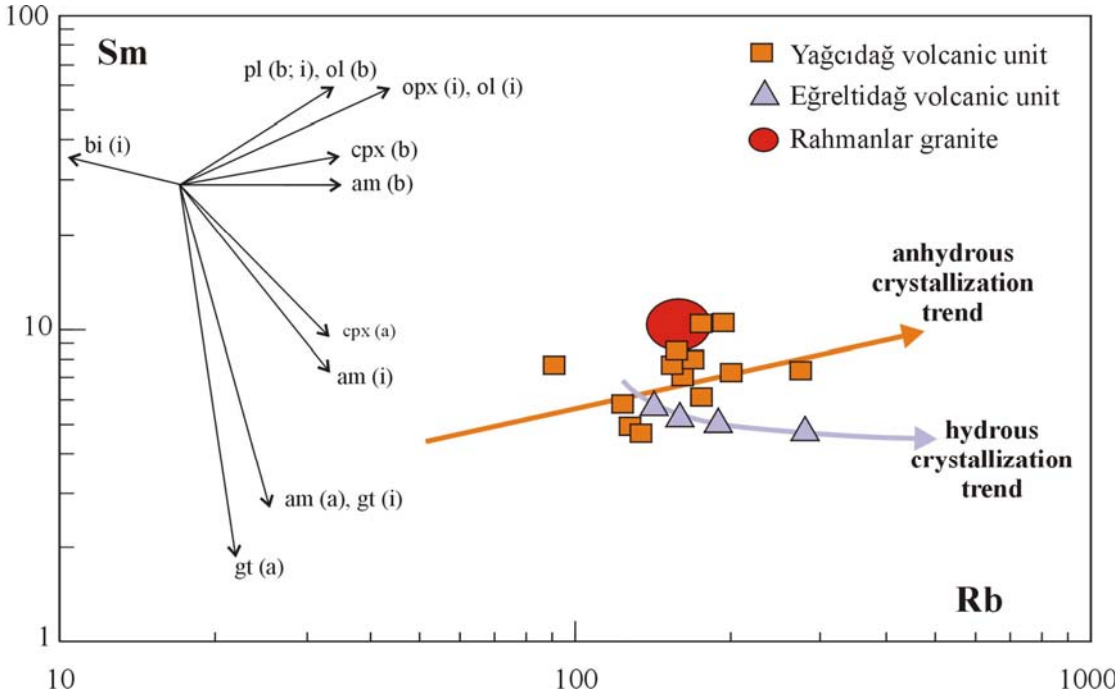


Figure 4.3. Rb-Sm diagram for the Eğreltidağ and Yağcıdağ volcanic unit showing theoretical fractional crystallization trends (fractionation trends from Aldanmaz *et al.* 2000). Ol: olivine, pl: plagioclase, cpx: clynopyroxene, am: amphibole, opx: orthopyroxene, gt: garnet, bi: biotite fractionation in (a) acidic, (b) basic and (i) intermediate melts. Rg: Rahmanlar granite as source region of the Eğreltidağ volcanic unit.

4.2. Kuzayır basalt: mantle-derived lamproitic melts

In this study it is concluded that the Kuzayır basalt is lamproitic rock. Lamproites are common but volumetrically minor igneous rocks relative to the other mantle-derived alkaline rocks (Mitchell & Bergman 1991). In addition to the continental rift zones and aulacogens, in generally lamproites are postorogenic magmatic products (Mitchell & Bergman 1991). They may represent examples of partial melting of enriched and depleted mantle source rocks (Prelević *et al.* 2005). It has been concluded by many works that many Mediterranean primitive ultrapotassic rocks originated from a mantle source that were enriched by metasomatic agents, probably raised from an ancient subducting slab (see Mitchell & Bergman 1991 and Prelević *et al.* 2005 for detailed description and discussions).

The Kuzayır basalt has been plotted in Group I ultrapotassic rocks field in *CaO vs* Al_2O_3 and in *CaO vs* SiO_2 (wt.%) (Figure 4.4a, b; after Foley *et al.* 1987). Group I rocks for these diagrams include lamproites. They also plotted in the lamproite field in the K_2O-*MgO*-Al_2O_3 ternary diagram (Bergman 1987). Figure 4.4d shows the variation of K_2O wt % vs SiO_2 wt % for K-series and high-K series volcanic rocks from the Roman Province of Italy (Wilson 1995) and the Kuzayır basalt. In this diagram, the Kuzayır basalt is plotted in the high-K series rocks and show fractional crystallization or crustal contamination trend. Their fractionated nature also appear in the K_2O *vs* K_2O/Al_2O_3 and K_2O *vs* K_2O/*CaO* (wt %) diagrams (Figure 4.4, Murphy *et al.* 2002) showing clinopyroxene fractionation trend is obvius. In the *Th/Yb vs Ta/Yb* diagram of Pearce (1983) they plott in active continental margin field because of their high Th/Yb ratios with respect to the magmas derived from partial melting of the mantle (Figure 4.4c). Their subduction-like geochemistry also appears in the Nb-Zr diagram of Thompson & Fowler (1986). In this diagram the rocks are plotted in the subduction/post-collision field (Figure 4.4e) because of their low Nb contents. In other words they are depleted in HFSE, i.e. Ta and Nb elements.

The Kuzayır basalt presents similar geochemical features with the Leucite Hills lamproites (Mitchell & Bergmann 1991, Figure 4.5a, b). In this diagrams fractionation from the Gaussberg lamproites (Muess-Schumacher *et al.* 1995) trends are also shown (after Murphy *et al.* 2002). On the basis of these diagrams, Kuzayır basalts were experienced to clinopyroxene fractionation (Figure 4.5b).

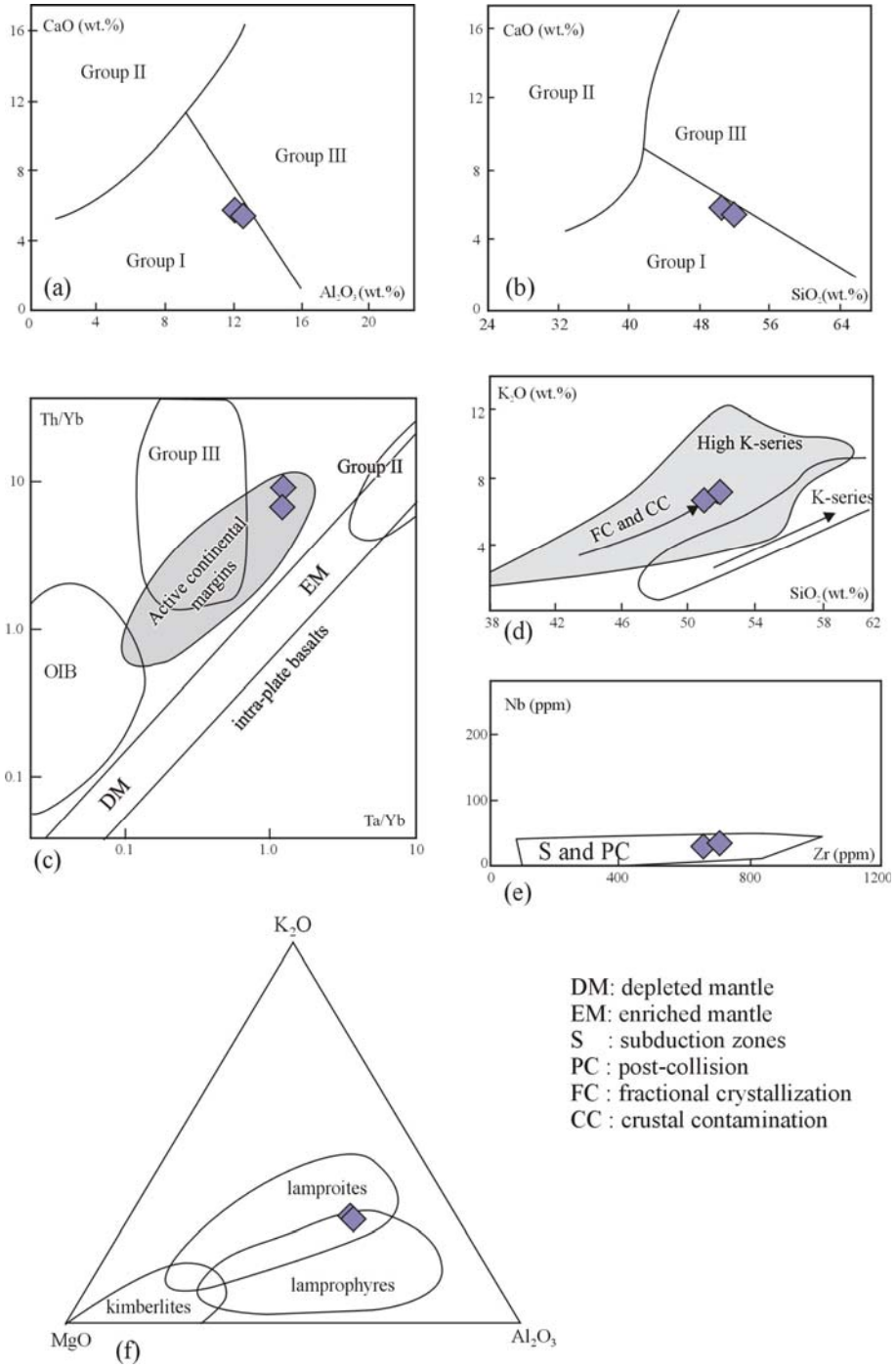


Figure 4.4. Classifications of the ultrapotassic rocks on the basis of wt % CaO vs Al_2O_3 **(a)** and of wt % CaO vs SiO_2 **(b)** (after Foley *et al.* 1987). **(c)** Variation of Th/Yb vs Ta/Yb (after Pearce 1983). Group III ultrapotassic rocks from the Roman Province (Rogers *et al.* 1985) and Group II ultrapotassic lavas from the western branch of the East African Rift (Mitchell & Bell 1976). Diagram is from Wilson (1995). **(d)** Variation of wt % K_2O vs SiO_2 for K-series and high-K series volcanic rocks from the Roman Province of Italy (after Wilson 1995; data from Peccerillo & Manetti 1985). **(e)** Variation of Nb vs Zr for potassic and ultrapotassic volcanic rocks (after Thompson & Fowler 1986 in Wilson 1995). **(f)** K_2O-MgO-Al_2O_3 diagram for the kimberlites, lamproites and lamprophyres (after Bergman 1987 in Wilson 1995).

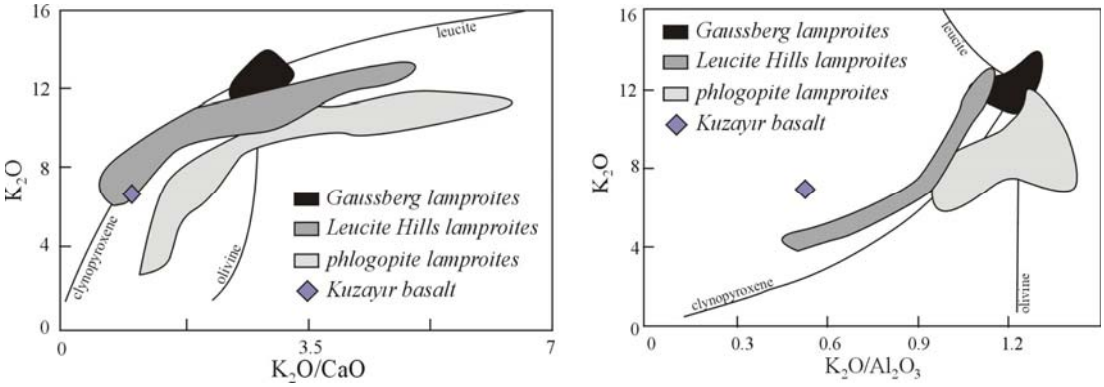


Figure 4.5. (a) K_2O vs K_2O/Al_2O_3 (wt %) and **(b)** K_2O vs K_2O/CaO (wt %) systematics of the Kuzayır basalt, comprising with Gaussberg lamproites (Muess-Schumacher *et al.* 1995), phlogopite lamproites and Leucite Hill lamproites (Mitchell & Bergmann 1991). Diagram also shows the fractionation trends of clynopyroxene, leucite and olivine from the Gaussberg lamproites (Murphy *et al.* 2002).

4.3. Yağcıdağ volcanic unit: subduction zone melts?

The Yağcıdağ volcanic unit is evolved magmas with respect to the partial melts from primitive or enriched mantle on the basis of their low Ni contents (mainly > 40 ppm). In the *Th/Yb-Ta/Yb* diagram, the calc-alkaline rocks of the Yağcıdağ volcanic unit lie in a trend under the trends of NW Anatolian Early Miocene volcanic unit and AFC or FC (i.e. they have lower Th/Yb ratios; Figure 4.2) indicating that this melt might be generated from a subduction-modified mantle-lithosphere or directly from a subduction zone. The HFSE (Ta, Nb and Ti) negative anomalies with respect to the neighboring LILE or REE in the primitive-mantle – normalized diagram (Figure 3.15b) have generally been explained as subduction zone geochemical signature (e.g., Pearce 1983).

To evaluate the fractional crystallization, *Sm-Rb* (ppm) diagram has been used (Figure 3.20). The Yağcıdağ volcanic unit plotted on a trend which can be explained by plagioclase, orthopyroxene, clinopyroxene and olivine fractionation (anhydrous assemblages) according to the theoretical fractionation trends (Figure 4.3).

It is difficult to distinguish that the subduction-related magmatism from the post-orogenic one by using single geochemical data. Generally, regional geologic evolution is used to separate these different tectonic settings (see: Chapters I and V for detailed discussion on the case of western Anatolia).

4.4. Kabaklar basalt: melting of the subduction-modified sub-continental lithosphere

The geochemical features of the Kabaklar basalt revealed that they can not be correlated simply with the Kula volcanic unit. It has been concluded in literature that the Kula volcanic unit have two distinct mantle sources: (1) OIB-like asthenospheric and (2) lithospheric mantle. The melts from these sources were mixed to form Kula volcanic unit (McKenzie & O'Nions 1995; Alıcı *et al.* 2002).

The Kabaklar basalt differs from the Kula volcanic unit on the basis of their Th-enriched and Ta-Nb- depleted nature and Eu anomalies in chondrite-normalized REE diagram. This indicates that they were derived from a different source or they were contaminated by crust at higher ratios with respect to the Kula volcanic unit (Figures 3.16 and 3.17b).

Figure 4.6 shows the *La/Sm-La*, *Sm/Yb-Sm*, *La/Yb-Zr/Nb* and *Sm/Yb-La/Sm* binary plots to constrain the source characteristics of the Kabaklar alkaline basaltic rocks and to compare with the Kula volcanic unit. Theoretical melting curves were taken from Aldanmaz *et al.* (2000 and 2005), therefore the details will not be repeated in here. In Figure 4.6a, La and Sm have been used, because La is highly incompatible and Sm is not. These phases are also independent from garnet and spinel; hence this diagram can provide information on the bulk composition of the source (Aldanmaz *et al.* 2000, 2005). Figure 4.6a show that the alkaline magmas of the Kabaklar basalt can not be produced by partial melting of the DMM (depleted MORB mantle, from McKenzie & O'Nions 1991 and 1995) even with very small melting degrees (0.1%). La is a highly incompatible element in the mantle mineralogy (garnet- or spinel-facies lherzolite). The La contents of the Kabaklar basalt are greater than PM (primitive mantle, from Sun & McKenzie 1989) and hence, the Kabaklar basalt must have been produced by enriched (not depleted) mantle source. This diagram reveals that these magmas were produced by 2-9% partial melting of an enriched mantle source; here is WAM (Western Anatolian Mantle, from Aldanmaz 2000).

In Figure Figure 4.6b, Sm and Yb are used to constrain the source mineralogy. Yb is incompatible with clinopyroxene. The Sm/Yb ratios of the Kabaklar basalt are higher than the mantle array. According to this diagram, Kabaklar basalt was produced by partial melting of the WAM, in garnet + spinel facies lherzolite (but garnet > spinel).

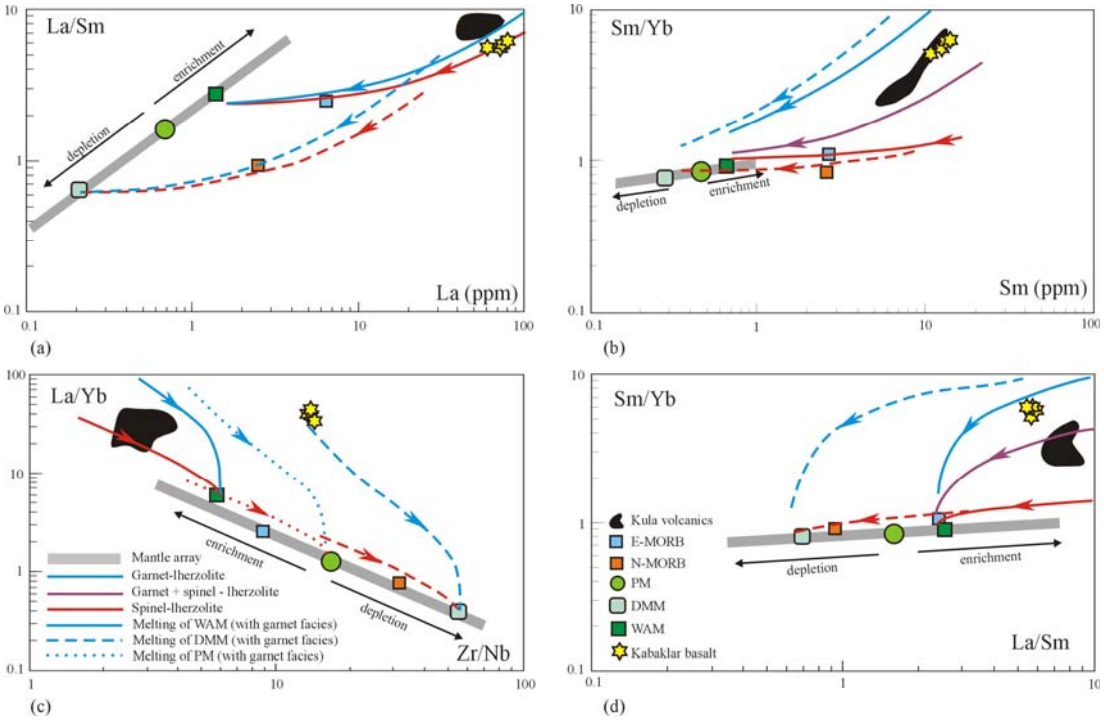


Figure 4.6. (a) *La/Sm-La*, **(b)** *Sm/Yb-Sm*, **(c)** *La/Yb-Zr/Nb* and **(d)** *Sm/Yb-La/Sm* binary plots showing melt trends using the non-modal-batch melting equations of Shaw (1970) (melting curves from Aldanmaz *et al.* 2000 and 2005). Arrows indicate the increasing melting degree. The data for Kula volcanic unit are from Alıcı *et al.* (2002). E-MORB and N-MORB: enriched- and normal- mid-oceanic ridge basalts, PM: primitive mantle; DMM: depleted MORB mantle, WAM: Western Anatolian Mantle; E-MORB, N-MORB and PM compositions are from Sun & McDonough (1989); WAM composition is from Aldanmaz *et al.* (2000), DMM composition is from McKenzie & O'Nions (1991 and 1995).

The *La/Yb vs Zr/Nb* diagram (Figure 4.6c) is useful to constrain the source mineralogy, because of these ratios independent from fractional crystallization of mantle phases. In this diagram, on the contrary to other plots, Kabaklar basalt was plotted close to the garnet-lherzolite melting curve, which has a starting composition in DM (depleted mantle) composition. This is because of the Nb-depleted nature of the Kabaklar basalt (which causes higher Zr/Nb ratios). This probably reflects that the source mantle rocks of the Kabaklar basalt carry subduction component. This is also, again, separates the Kabaklar basalt from the Kula volcanic unit.

In the *Sm/Yb vs La/Sm* diagram (Figure 4.6d), it is clear that the Kabaklar basalt is produced by low-degree partial melting (2-7%) of the garnet-dominant garnet+spinel facies lherzolite (in harmony with the geochemical composition of WAM).

CHAPTER FIVE

DISCUSSION AND CONCLUSION

5.1. Introduction

The main targets of this chapter are: (1) to revise stratigraphy of the Selendi Basin and to show the differences from the Uşak-Güre basin, (2) to discuss origin of granitic intrusion and its relation to Miocene volcanic activity, (3) to establish the origin and mechanism of volcanic activity, and (4) to interpret the tectono-magmatic evolution of the Selendi Basin on the basis of field, petrographic and geochemical data presented in the previous chapters.

5.2. Revised stratigraphy of the Selendi Basin

The stratigraphy of the Selendi Basin is not simple as it was thought and can not be considered to comprise two distinct sequences separated by unconformity; the correlation of its stratigraphy with that of other basins, as suggested by previous studies (e.g., Ercan *et al.* 1983; Seyitoğlu 1997; Purvis & Robertson 2004) is not possible as well. New field based and geochemical data of this study show that the tectonostratigraphic and tectonomagmatic evolution of the basin is more complex than previously considered.

The tectonic contact between ophiolitic and metamorphic basement rocks was previously was mapped as a thrust fault (Ercan *et al.* 1983; Seyitoğlu 1997). Recently Purvis & Robertson (1997, 2004, 2005a, b) proposed that this contact represents a ductile-to brittle top-to-the-NE shear zone (i.e. detachment fault), but no structural data about the kinematic nature of the tectonic contact is presented. This study provides evidence, on the basis of geological mapping and kinematic analysis, that the ophiolitic rocks overlie the Menderes metamorphics along a low-angle normal fault; this structure is herein named as Kula detachment (Ersoy *et al.* 2004, 2005) and it represents a transition from ductile to brittle deformation.

Seyitoğlu (1997) proposed that the Hacıbekir Group was deposited along N-S-trending normal faults in both Uşak-Güre and Selendi Basins. On the other hand, Purvis & Robertson (2004, 2005a, b) suggested that the sedimentary rocks in the basin (including Hacıbekir and İnay groups) were deposited in a depocenter formed by corrugations of a main breakaway fault (detachment fault).

Firstly, the field-based data show that the Hacıbekir Group in the Selendi Basin displays lithological, sedimentological and structural characteristics different than that of the Uşak-Güre Basin. In the Uşak-Güre Basin the main characteristics of the unit are:

(1) post-sedimentary deformational structures; they may indicate that the unit was transported to the northeast following its deposition;
(2) unconformably overlie the ophiolites;
(3) do not contain any metamorphic rocks such as augen gneisses from the Menderes Massif;
(4) do not include any blocks of limestone or ophiolite.

On the other hand, in the Selendi Basin the Hacıbekir group displays the following characteristics:

(1) the lower contact of the Hacıbekir Group with the Menderes Massif is a low-angle detachment fault;
(2) include blocks of limestone and ophiolitic rocks
(3) accompanied by bimodal volcanism
(4) composed mainly of metamorphic clasts derived from the Menderes Massif, mainly augen gneisses.

As the Hacıbekir Group has a key role in better understanding of basin's tectono-magmatic evolution in western Turkey, the group must be evaluated separately for the Selendi & Uşak-Güre basins.

In-line with Purvis & Robertson (1997), the following field data suggest that the Hacıbekir Group is a typical supra-detachment sedimentary sequence in Selendi

Basin: (a) it overlies the Menderes metamorphics along a tectonic contact, (b) ophiolites overlie the massif along a top-to-the-NE low-angle normal fault (c) the ophiolites also occur as olistoliths in the Hacıbekir Group. These relationships indicate that the deposition of the Hacıbekir Group was coeval with the tectonic transportation of the ophiolitic rocks of the İzmir-Ankara zone above the Menderes Massif during probably latest Oligocene - Early Miocene time (Figure 5.1). The overall southwestward tilted geometry of the Hacıbekir Group may support this interpretation. This is in contrast with Purvis & Robertson model (2004, 2005a, b) where both the Hacıbekir and İnay groups are considered as the basin fill. On the other hand, the İnay Group can not be included to supra-detachment sedimentary rocks in the basin, because it unconformably overlie the detachment fault in the Kula region (see Figure 2.11), indicating that the activity of the detachment fault ceased prior to the deposition of the İnay Group (Figure 5.1).

5.3. Magmatic activity within the Selendi Basin

It is apparent from the field and geochemical data that the first magmatic activity in the basin was started at the time of detachment faulting, coeval with the deposition of the Hacıbekir Group. This magmatic activity was resulted in two-contrasting, bimodal character: (1) mantle-derived, mafic, alkaline and ultrapotassic (Kuzayır basalt) and (2) crustal-derived, felsic calc-alkaline in character (Rahmanlar granite and Eğreltidağ volcanic unit). This implies that the first magmatic activity in the region might related to the probably first exhumation of the Menderes Massif, opposite to the previous studies which concluded that the late Cenozoic magmatic activity in western Turkey was started with intermediate and calc-alkaline in composition (e.g., Yılmaz *et al.* 2001; Aldanmaz 2000).

The geochemical data revealed that the Rahmanlar granite was produced by partial fractional melting (in the range of 25-35% melting degree) of the augen gneisses, but unfortunately, it is not possible by using only geochemical data, to decide on the tectonic regime that caused anatexis to produce Rahmanlar granite. The Rahmanlar granite shows the same kinematic features (D_2 mylonitic foliation; see Chapter II) with the surrounding mylonitic gneisses. But they are not affected by D_1.

D_2 deformation is the manifestation of an extensional event responsible for the exhumation of Menderes Massif in the footwall of detachment fault. The granite occur in the immediate footwall of detachment fault mapped in this study. Therefore, it is concluded that Rahmanlar granite is a typical syn-extensional granite emplaced during D_2 deformation and slightly deformed during the latest increments of the same D_2 deformation.

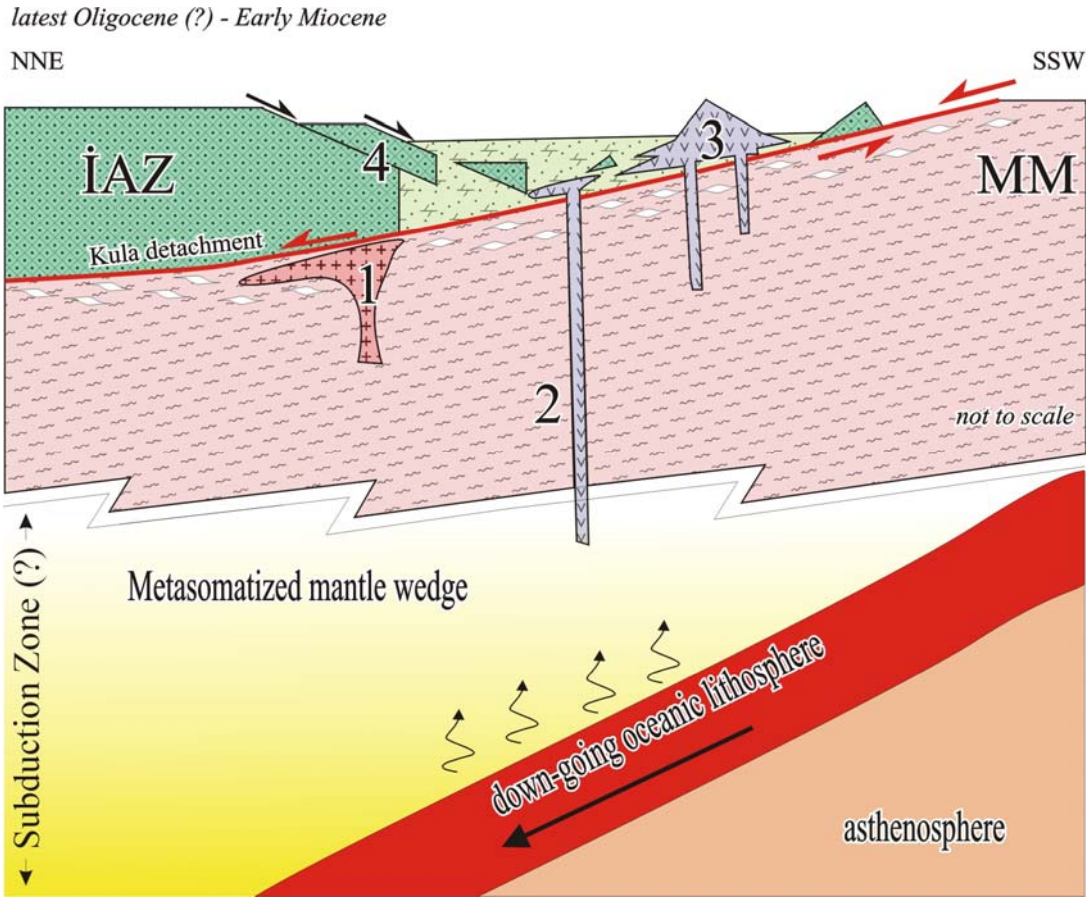


Figure 5.1. Schematic cross section showing the tectono-magmatic evolution of the Selendi Basin. 1: syn-extensional granite formation (Rahmanlar granite); 2: mantle-derived "lamproitic" magmatism (Kuzayır basalt); 3: crust-derived felsic volcanism (Eğreltidağ volcanic unit); 4: movement of the ophiolite blocks from the İzmir Ankara Zone (İAZ) to supra-detachment basin in which Hacıbekir Group was deposited, MM: Menderes Massif.

Recent studies, carried out in western Anatolia have showed that the extensional regime started at least in earliest Miocene (Seytioğlu & Scott 1991, 1992b, 1994, 1996a-b; Hetzel *et al.* 1995b; Collins & Robertson 1998; Koçyiğit *et al.* 1999a, b; Ring *et al*. 2003; Bozkurt and Sözbilir 2004; Catlos & Çemen 2005; Ring & Collins 2005). For instance, Işık & Tekeli (2001), Işık *et al.* (2003, 2004), have described the

Simav core complex, situated to the north of the study area, and documented isotopic ages from the complex (Figure 2.2). On the one hand, recently, Catlos & Çemen (2005) have shown that the Cenozoic extension in the Gördes submassif (the part of the Menderes Massif remains in the north of the Gediz Graben) and probably the entire Menderes Massif have begun in Late Oligocene, on the basis of monazite ages from the massif. The deformation age of the metamorphic rocks is 22.8 Ma (Figure 2.2) and the cooling age of the Eğrigöz granodiorite is 23-20 Ma (Işık *et al.* 2004). The deformational features of the Simav core complex (Işık & Tekeli, 2001; Işık *et al.*, 2003, 2004; Ring & Collins 2005), confirm with the Kula detachment (Ersoy *et al.* 2004). These data imply that, again, Hacıbekir Group was deposited during latest Oligocene (?) – earliest Miocene, and was accompanied with core complex formation in an extensional regime. The core-complex formation was accompanied by the intrusion of the Rahmanlar granite in Selendi Basin.

Another interesting characteristic of the Hacıbekir Group in the Selendi Basin is the occurrence of volcanic rocks suggesting syn-depositional bimodal volcanism, which produced first felsic calc-alkaline dacitic-rhyolitic (Eğreltidağ volcanic unit) and then mafic alkaline "lamproitic" volcanic suites (Kuzayır basalt). The geochemical data revealed that the Eğreltidağ volcanic unit is closely associated with the Rahmanlar granite, and probably they were produced by the melting of the Menderes Massif with minor mantle component. On the one hand, Kuzayır basalt formed from subduction-related or subduction-modified mantle-derived melts. This implies that deposition of the Hacıbekir Group was also accompanied with crust- and mantle-derived volcanism. Okay & Satır (2000) proposed that the latest Oligocene extensional regime was primarily related to the roll-back of the subduction zone rather than gravitational collapse. It is possible that a subduction zone (probably Aegean subduction zone) was exist during latest Oligocene-earliest Miocene and migrated to the south, because of: (a) alignment of the volcanic rocks becomes progressively younger from north to south (Figure 1.6); thus confirming the migration of the subduction; (b) occurrence of fine-grained and/or evaporate-bearing Lower Miocene sediments (Helvacı & Alanso 2000); this requires a flat topography rather than an elevated over-thickened crust which is required in order to give rise to

gravitational collapse, and (c) widespread occurrences of mainly Oligocene plutons in western Anatolia; they might have provided the neccessary thermal anomalies in the crust in a subduction system (see Okay & Satır 2000 for detail discussion) and finally, (d) almost the whole volcanic rocks of the Neogene age carry a subduction-related geochemical features. Many studies defending that the Early-Middle Miocene calc-alkaline volcanic rocks in the western Anatolia were formed in a post-orogenic tectonic setting rather than a subduction system (e.g Yılmaz 1989; Savaşçın & Güleç 1990; Güleç 1991; Aldanmaz *et al.* 2000; Yılmaz *et al.* 2001) and accepted that the extensional tectonics in western Anatolia commenced in Middle Miocene; and they also proposed that volcanism older than middle Miocene was related to thickened crust. On the other hand, Seyitoğlu & Scott (1991) suggested that the extensional tectonics commenced earlier, in latest Oligocene as a consequence of the orogenic collapse of the over-thickened crust. Later, Seyitoğlu & Scott (1992b) and Seyitoğlu *et al.* (1997) suggested that the volcanic evolution of the region as a whole, was related to thinning of the crust and hence increasing asthenospheric contribution following orogenic collaps. The authors used chemical characteristics of these volcanics as they change from calc-alkaline to alkaline in time. In fact, as seen in Palaeotectonic map of Şengör & Yılmaz (1981; Figure 1.3) the southern branch of the oceanic crust of the Neo-Tethys, of course, was already subducting to northward from Early-Middle Eocene closure of the northern branch of the Neo-Tethys to recent. The main objections to the roll-back processes of the Aegean subduction zone are (a) the starting age of the extension (see chapter I), and (b) the distance between the trench and the arc which is thought to be so big. On the basis of these studies mentioned above, it can be accepted that the presence of a subduction zone beneath the Anatolides were present during earliest Miocene.

Another data which can support the presence of a subduction zone during the deposition of the Hacıbekir Group is the presence of interfingering lamproitic mafic volcanic rocks. Geochemical features of these lavas indicate that they may have been generated from subduction-related or subduction-modified mantle lithosphere in an extensional setting. If there is no subduction event in western Anatolia during earliest Miocene, these melts would be generated from a mantle lithosphere that was

metasomatized and enriched by previous subduction event. But according to the geological construction of the western Anatolia and the previous studies which presumed that there is no subduction event during this time interval, there can not be any Benioff zone in the south of the İzmir – Ankara ocean. In other words, the geochemical features of these lavas require an active Benioff zone or previously subducted Benioff zone. This interpretation also confirms that the deposition of the Hacıbekir group and interfingering volcanic rocks occurred in a supra-detachment basin accompanying by core complex formation above a subduction zone.

The Yağcıdağ volcanic unit also has subduction-related geochemical feature with their calc-alkaline intermediate composition indicating that the subduction event has continued until Middle Miocene in western Anatolia.

The age of the İnay Group is highly controversial in the literature. Ercan *et al.* (1983) suggested a Late Miocene – Early Pliocene age. On the other hand, Seyitoğlu (1997) proposed, on the basis of radiometric and palinologic data, that the group was deposited during Early Middle Miocene. Radiometric age of the Yağcıdağ volcanic unit vary from 14.9 Ma (K-Ar; Seyitoğlu 1997) to 18.0 Ma (K-Ar; Ercan *et al.* 1997) and 18.8 Ma (Ar/Ar; Purvis & Robertson 2004). The field data show that the explosive products of the Yağcıdağ volcanic unit (ash fall deposits) intercalated with the İnay Group, where the Ahmetler formation grading to Ulubey formation (Figure 2.35). The geological maps and the cross sections (Figures 2.23, 30-33, 35, 37) of the region also show that the products of the Yağcıdağ volcanic unit are underlain by the Ahmetler formation, but also, are overlain by the Ulubey formation. This implies that the fine-grained sediments of the İnay Group changed to carbonate rocks simultaneously with emplacement of the Yağcıdağ volcanic unit (Figure 5.2).

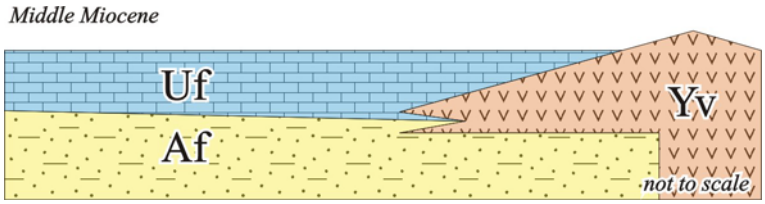


Figure 5.2. Shematic cross section showing the stratigraphic relationship of Yağcıdağ volcanic unit (Yv), Ahmetler formation (Af) and Ulubey formation (Uf).

The conclusions of this study can be summarized as follows:

1. This study, for the first time, describes the contact relationship between ophiolitic rocks and the Menderes metamorphics, on the basis of field-based studies, kinematic analyses and petrographic descriptions. The tectonic contact represents a northeast-facing low-angle ductile to brittle normal fault (Kula detachment).
2. The deformation along the Kula detachment was accompanied with the emplacement of syn-extensional granite (Rahmanlar granite) in the footwall.
3. Hacıbekir Group has different lithological, stratigraphical and tectonic features in the Uşak-Güre and Selendi Basins. It was deposited on the Kula detachment, synchronously with ophiolite transportation in the hangingwall of the detachment fault.
4. The deposition of the Hacıbekir Group was also accompanied by bimodal volcanism: first is related to crustal melts (Eğreltidağ volcanics), and the other is related to the mantle-derived "lamproitic" melts (Kuzayır basalt).
5. Entire data summarized above, confirm that the extensional tectonics in the region was begun during latest Oligocene (?) – earliest Miocene.
6. The deposition of the İnay Group, during middle Miocene (?), postdates the activity of the Kula detachment.
7. İnay Group interfingers with Yağcıdağ volcanic unit. On the basis of previous studies and geochemical data, Yağcıdağ volcanic unit was related a subduction system.
8. NE-trending faults forming the actual basin shape cut the İnay Group and older units, and hence they could not be responsible to deposition of the İnay Group.
9. The Kabaklar basalt, previously mapped as Kula volcanics, differs from the Kula volcanics on the basis of their geochemical features. These rocks might be related to NE-trending fault systems.

REFERENCES

Abbott, M.M. & Van Ness, H.C. (1972). Thermodynamics, Schaum's Outline Series in Engineering, 346 pp., McGraw-Hill. *International Journal of Earth Sciences*, 10.1007/s00531-005-0470-7.

Akkök, R. (1983). Structural and metamorphic evolution of the northern part of the Menderes Massif: new data from the Derbent area and their implication for the tectonics of the massif. *Journal of Geology*, 91, 342-350.

Aldanmaz, E., Gourgaud, A. & Kaymakçı, N. (2005). Constraint on the composition and thermal structure of the upper mantle beneath NW Turkey: Evidence from mantle xenoliths and alkali primary melts. *Journal of Geodynamics*, 39, 277-316.

Aldanmaz, E., Pearce, J.A., Thirwall, M.F. & Mitchell, J.G. (2000). Petrogenetic evolution of late Cenozoic, post-collision volcanism in western Anatolia, Turkey. *Journal of Volcanology and Geothermal Research*, 102, 67-95.

Alıcı, P., Temel, A. & Gourgaud, A. (2002). Pb-Nd-Sr isotope and trace element geochemistry of Quaternary extension-related alkaline volcanism: a case study of Kula region (western Anatolia, Turkey), *Journal of Volcanology and Geothermal Research*, 115, 487-510.

Atherton, M.P. & Ghani, A.A. (2002). Slab breakoff: a model for Caledonian, Late Granite syn-collisional magmatism in the orthotectonic (metamorphic) zone of Scotland and Donegal, *Ireland. Lithos*, 62, 65-85.

Aubouin, J. (1959). Contribution àl'étude de la Grèce septentrionale; les confins de l'Epire et de la Thessalie. – *Annales Geologiques Des Pays Helleniques*, 10, 1-483.

Avigad D. & Garfunkel Z. (1991). Uplift and exhumation of high-pressure metamorphic rocks: the example of the Cycladic blueschist belt (Aegean Sea). *Tectonophysics*, 188: 357-372.

Avigad D., Ziv A. & Garfunkel Z. (2001). Ductile and brittle shortening, extension-parallel folds and maintenance of crustal thickness in the central Aegean (Cyclades, Greece). *Tectonics*, 20, 277-287.

Avigad, D., Garfunkel, Z., Jolivet, L. & Azańŏn, J. M. (1997). Back arc extension and denudation of Mediterranean eclogites. *Tectonics*, 16, 924-41.

Barka, A.A. & Kadinsky-Cade, K. (1988). Strike-slip fault geometry in Turkey and its influence on earthquake activity. *Tectonics*, 7, 663-84.

Benda, L. & Meulenkamp, J.E. (1979). Biostratigraphic correlation in the Eastern Mediterranean Neogene: 5. Calibration of sporomorph associations, marine microfossils and mammal zones, marine and continental stages and the radiometric scale. *Annales Geologiques Des Pays Helleniques*, 1, 61–70.

Bergman, S.C. (1987). Lamproites and other Potassium-rich igneous rocks: a review of their occurrence, mineralogy and geochemistry. In: J. G. Fitton and B. J. G. Upton (Eds.), Alkaline Igneous Rocks. *Geological Society of London Special Publication*, 30, 103-190.

Bingöl, E., Delaloye, M. & Ataman, G. (1982). Granitic intrusions in western Anatolia: a contribution to the geodynamic study of this area. *Eclogae geol. Helv.*, 75, 437-446.

Bird, P. (1979). Continental delamination and the Colorado Plateau. *Journal of Geophysical Research*, 84, 7561-7571.

Borsi, J., Ferrara, G., Innocenti, F. & Mazzuoli, R. (1972). Geochronology and petrology of recent volcanics in the easthern Aegean Sea (West Anatolia and Lesvos Iceland). *Bullettin of Volcanology*, 36, 473-496.

Bozkurt, E. (2000). Timing of extension on the Büyük Menderes Graben, western Turkey, and its tectonic implications, in: E. Bozkurt, J.A. Winchester, J.D.A. Piper (Eds.), Tectonics and Magmatism in Turkey and the Surrounding Area, vol. 173, *Geological Society of London Special Publication*, 73, 385–403.

Bozkurt, E. (2001a). Neotectonics of Turkey, a synthesis. *Geodinamica Acta*, 14, 3-30.

Bozkurt, E. (2001b). Late Alpine evolution of the central Menderes Massif, western Anatolia, Turkey. *International Journal of Earth Sciences*, 89, 728-44.

Bozkurt, E. (2003). Origin of NE-trending basins in western Turkey. *Geodinamica Acta*, 16, 61-81.

Bozkurt, E. & Oberhänsli, R. (2001). Menderes Massif (western Turkey): Structural, Metamorphic and Magmatic Evolution. *International Journal of Earth Sciences, Special Issue*, 89, 679-882.

Bozkurt, E. & Park, R.G. (1994). Southern Menderes Massif: an incipient metamorphic core complex in western Anatolia. *Journal of Geological Society London*, 151, 213–216.

Bozkurt, E. & Park, R.G. (1997a). Evolution of a mid-tertiary extensional shear zone in the southern Menderes Massif, Western Turkey. *Bulletin de la Société Géologique de France*, 168, 3–14.

Bozkurt, E. & Park, R.G. (1997b). Microstructures of deformed grains in the augen gneisses of southern Menderes Massif and their tectonic significance. *Geologische Rundschau,* 86, 103-119.

Bozkurt, E. & Satır, M. (2000). New Rb-Sr geochronology from the southern Menderes Massif (southwestern Turkey) and its tectonic significance. *Geological Journal*, 35, 285–96.

Bozkurt, E. & Sözbilir, H. (2004). Geology of the Gediz Graben: new field evidence and tectonic significance. *Geological Magazine*, 141, 63-79.

Bozkurt, E. (1995). Deformation during main Menderes metamorphism (MMM) and its tectonic signifcance: evidence from southern Menderes Massif, western Turkey. EUG VIII, Strasbourg, 9-13 April, *Terra Abstracts*, 7, 7-176.

Bucher, W.H. (1956). Role of gravity in orogenesis. *Geological Society of America Bulletin*, 67, 1295-1318.

Candan, O., Dora, O.Ö., Çetinkaplan, M., Oberhänsli, R., Partzsch, J.H., Warkus, F.C. & Dürr, S. (2001). Pan-African high-pressure metamorphism in the Precambrian basement of the Menderes Massif, western Anatolia, Turkey. *International Journal of Earth Sciences*, 89, 679-882.

Candan, O., Dora, O.Ö., Oberhänsli, R., Çetinkaplan, M., Oelsener, F.C. & Dürr, S. (1998). Two different high-pressure metamorphisms in the Menderes Massif: Pan-African and Tertiary events. *Geological Congress Turkey*, Abstracts, 52-54

Candan., O. (1995). Menderes Masifinde kalntı granulit fasiyesi metamorfizması (in Turkish with English Abstract). *Turkish Jornal of Earth Science*, 4, 35-55.

Candan., O. (1996). Çine asmasifindeki (Menderes Masifi) gabroların metamorfizması ve diğer asmasiflerle karşılatırılması [in Turkish with English Abstract]. *Turkish Jornal of Earth Science*, 4, 123-139.

Carey, S.W. (1958). A tectonic approach to continental drift. in: S.W. Carey (Editor), Continental Drift: A Symposium.Geology Department, *University of Tasmania, Hobart*, pp. 177-355.

Carminati, E., Wortel, M.J.R., Meijer, P.Th. & Sabadini, R. (1998a). The two-stage opening of the western-central Mediterranean basins: A forward modeling test to a new evolutionary model. *Earth and Planetary Science Letters*, 160, 667-679,

Carminati, E., Wortel, M.J.R., Spakman, W. & Sabadini, R. (1998b). The role of slab detachment processes in the opening of the western-central Mediterranean basins: Some geological and geophysical evidence. *Earth and Planetary Science Letters*, 160, 651-665.

Catlos, E.J. & Çemen, İ. (2005). Monazite ages and the evolution of the Menderes Massif, western Turkey. *International Journal of Earth Sciences*, 94, 204-217.

Çemen, İ., Göncüoğlu, M.C. & Dirik, K. (1999). Structural evolution of the Tuzgolu Basin in Central Anatolia, Turkey. *Journal of Geology*, 107:693-706

Chappell, B.J. & White, A.J.R. (1974). Two Contrasting Granite Types. *Pacific Geology*, 8, 173-174.

Collins, A.S. & Robertson, A.H.F. (1998). Processes of Late Cretaceous to Late Miocene episodic thrust-sheet translation in the Lycian Taurides, SW Turkey. *Journal of the Geological Society, London*, 155, 759-772.

Coney, P.J. & Harms, T.A. (1984). Cordilleran metamorphic core complexes: Cenozoic extensional relics of Mesozoic compression. *Geology*, 12, 550-554.

Coulon, C., Megartsi, M'hamed, Fourcade, S., Maury, R.C., Bellon, H., Louni-Hacini, A., Cotton, J., Coutelle, A. & Hermitte, D. (2002). Post-collisional transition from calc-alkaline to alkaline volcanism during the Neogene in Oranie (Algeria): magmatic expression of a slab breakoff. *Lithos*, 62, 87-110.

Cox, K.G., Bell, J.D. & Pankhurst, R.J. (1979). The Interpretation of Igneous Rocks, *George Allen and Unwin*, London.

Davies, J.H. & von Blanckenburg, F. (1999). Slab breakoff: a model of lithosphere detachment and its test in the magmatism and deformation of collisional orogens. *Earth and Planetary Science Letters*, 129, 85-102.

De Boorder, H., Spakman, W., White, S.H. & Wortel., M.J.R. (1998). Late Cenozoic mineralization, orogenic collapse and slab detachment in the European Alpine Belt. *Earth and Planetary Science Letters*, 164, 569-575.

Dewey, J.F. & Şengör, A.M.C. (1979). Aegean and surrounding regions: complex multiplate and continuum tectonics in a convergent zone. *Geological Society of America Bulletin*, 90, 89-92.

Dewey, J.F. (1980). Episodicity, sequence, and style at convergent plate boundaries. *Geological Association of Canada Special Paper*, 20, 553-573.

Dewey, J.F. (1988). Extensional collapse of orogens. *Tectonics*, 7, 1123-1139.

Dewey, J.F., Hempton, M.R., Kidd, W.S.F., Şaroğlu, F. & Şengör, A.M.C. (1986). Shortening of continental lithosphere: the neotectonics of EasternAnatolia - a young collision zone. In: Coward, M.P. & Ries, A.C. (eds) Collision Tectonics. *Geological Society Special Publications*, 19, 3-36.

Dora, O.Ö., Candan, O., Dürr, S. & Oberhänsli R. (1995). New evidence on the geotectonic evolution of the Menderes Massif: in: Pişkin, Ö., Ergün. M., Savaşcın, M.Y. & Tarcan, G. (eds.): Proc. *International Earth Science Colloqium on the Aegean Region*, 9-14 October 1995, İzmir-Güllük, Turkey, 1, 53-72.

Doust, H. & Arıkan, Y. (1974). The Geology of the Thrace Basin: *Türkiye II. Petrol Kongresi*, 119-136.

Dürr, S. (1975). Über Alter und geotektonische Stellung des Menderes Kristallins / SW – Anatolien und seine Äquivalente in der Mittleren Aegean. Habilitation Thesis, *University of Marburg.*

Elkins-Tanton L.T. (2005). Continental magmatism caused by lithospheric delamination, inPlates, Plumes & Paradigms (ed. Foulger, G. R., J.H. Natland, D.C. Presnall and D.L.Anderson), *Geological Society of America*.

Elsasser, W.M. (1971). Sea-floor spreading as thermal convection. *Journal of Geophysical Research*, 76, 1101-1112.

Emre, T. & Sözbilir, H. (1997). Field evidence for metamorphic core complex, detachment faulting and accommodation faults in the Gediz and Büyük Menderes Grabens (Western Turkey), in: Ö. Pişkin, M. Ergün, M.Y. Savaşçın, G. Tarcan (Eds.), *IESCA Proceedings*, 73-94.

Emre, T. (1996). Gediz Grabeninin jeolojisi ve Tektoniği, *Turkish Jurnal of Earth Science*, 5, 171-185.

England, P.C. & Houseman, G.A. (1989). Extension during continental convergence, with application to the Tibetan Plateau. *Journal of Geophysical Research*, 94, 17561-17579.

England, P.C. (1982). Some numerical investigations of large scale continental deformation. In: Hsü , K.J. (Ed.), Mountain Building Processes. *Academic Press*, New York, 129-139.

Ercan, E., Dinçel, A., Metin, S., Türkecan, A. & Günay, A. (1978). Uşak yöresindeki Neojen havzalarının jeolojisi (Geology of the Neogene basins in Uşak region). *Bulletin of the Geological Society of Turkey*, 21, 97-106.

Ercan, E., Türkecan, A., Dinçel, A. & Günay, E. (1983). Kula – Selendi (Manisa) dolaylarının jeolojisi (Geology of Kula – Selendi (Manisa) area). *Jeoloji Mühendisliği,* 17, 3-28.

Ercan, T. & Öztunalı Ö. (1982). Characteristic features and "base surges" bed forms of Kula volcanics. *Bullettin of Geological Society of Turkey*, 25, 117-125.

Ercan, T. & Öztunalı, Ö. (1983). Demirci-Selendi çevresinde Senozoyik yaşlı volkanitlerin petrolojisi ve kökensel yorumu. *Yerbilimleri*, 10, 1-15.

Ercan, T., Dinçel, A., Türkecan, A. & Erdoğdu, G. (1992). Petrochemical characteristics and genetic interpretation of the basaltic volcanism of Kula (Manisa), Turkey. *Geologica Balcanica*, 22, 51-73.

Ercan, T., Satır, M., Kreuzer, H., Türkecan, A., Günay, E., Çevikbaş, A., Ateş, M. & Can, B. (1985). Batı Anadolu Senozoyik volkanitlerine ait yeni kimyasal, izotopik ve radyometrik verilerin yorumu (Interpretation of new chemical, isotopic and radiometric data on Cenozoic volcanics of western Anatolia). *Bullettin of Geological Society of Turkey*, 28, 121-136.

Ercan, T., Satır, M., Sevin D. & Türkecan, A. (1997). Batı Anadolu'daki Tersiyer ve Kuvaterner yaşlı volkanik kayaçlarda yeni yapılan radyometrik yaş ölçümlerinin yorumu (Some new radiometric ages from Tertiary and Quaternary volcanic

rocks from West Anatolia). *Bulletin of the Mineral Research and Exploration,* Ankara, 119, 103-112.

Ercan, T., Satır, M., Steinitz, G., Dora, A., Sarifakioğlu, E., Adis, C., Walter, H-J. & Yıldırım,T. (1996). Features of the Tertiary volcanism in the Biga Peninsula and in the islands of Gökçeada, Bozcaada and Tavan adasi (in Turkish). *Bulletin of the Mineral Research and Exploration,* Ankara, 117, 55–86.

Erdoğan, B. (1990). İzmir-Ankara Zonu'nun, İzmir ile Seferihisar Arasındaki Bölgede Stratigrafik Özellikleri ve Tektonik Evrimi. *TPJD Bülteni*, 2, 1-20.

Erdogan, B., Altiner, D., Gungör, T. & Özer, S. (1990). Stratigraphy of Karaburun Peninsula. *Bulletin of the Mineral Research and Exploration,* Ankara, 111, 1-20.

Ersoy Y., Helvacı C., Sözbilir, H. & Erkül, F. (2004). Evidence for top to northeast movement of the Neo-Tethyan ophiolites on the Menderes metamorphic massif, Kula detachment fault, western Anatolia, Turkey, 32nd. *International Geological Congress*, 2004, Abstracts, 1, 695.

Ersoy, Y., Helvacı, C., Bozkurt, E., Erkül, F. & Sözbilir, H. (2005). Oligocene-Lower Miocene olistostromal sedimentary sequence structurally above the Menderes Metamorphic Core Complex, Selendi Basin, western Anatolia and its tectonic implications. *International Symposium on the Geodynamics of Eastern Mediterranean*, 15-18 June 2005, İstanbul, Abstracts, 75.

Ferrari L. (2004). Slab detachment control on mafic pulse and mantle heterogeneity in central Mexico. *Geology*, 32, 77-80.

Foley, S.F., Venturelli, G., Green, D.H. & Toscani, L. (1987). The ultrapotassic rocks: characteristics, classification, and constraints for petrogenetic models. *Earth-Science Reviews*, 24, 81–134.

Fytikas M., Innocenti F., Manetti P., Mazzuoli R., Peccerillo A. & Villari L. (1985). Tertiary to Quaternary evolution of volcanism in the Aegean region. *Geological Society London Special Publications*, 17, 687-699.

Fytikas, M., Giuliani, O., Innocenti, F., Marinelli, G. & Mazzuoli, R. (1976). Geochronological data on recent magmatism of the Aegean Sea. *Tectonophysics*, 31, 29–34.

Fytikas, M., Giulianni, O., Innocenti, F., Manetti; P., Mazzuoli, R., Peccerillo, A. & Villari, L. (1980). Neogene volcanism of the Northern and Central Aegean region. *Annales Geologiques Des Pays Helleniques,* 30, 106.

Fytikas, M., Innocenti, F., Manetti, P., Mazzuoli, R., Peccerillo, A. & Villari, L. (1984). Tertiary to Quaternary evolution of volcanism in the Aegean region. In: J.E. Dixon, and A. H. F. Robertson, (eds). The Geological evolution of the Eastern Mediterranean. *Geological Society Special Publication*, 17, 687-699.

Gessner, K., Piazolo, S., Güngör, T., Ring, U., Kröner, A. & Passchier, C.W. (2001a). Tectonic significance of deformation patterns in granitoid rocks of the Menderes nappes, Anatolide belt, southwest Turkey, *International Journal of Earth Science*, 89, 766–780.

Gessner, K., Ring, U., Chrıstopher, J., Hetzel, R., Passchıer, C. W. & Güngör, T. (2001b). An active bivergent rolling-hinge detachment system: central Menderes metamorphic core complex in western Turkey. *Geology*, 29, 611-14.

Godfriaux, Y. (1965). Etude géologique de la région de l'Olympe. – Thèse d'Etat, *Université de Lille*, 280p.

Göncüoğlu, M.C., Özcan., A., Turhan., N. & Işık, A. (1992). Stratigraphy of the Kütahya region. *In Field Guide Book for the Symposium on the Geology of the Black See Region*, Ankara, 3-11.

Görür, N. & Okay, A.I. (1996). A fore-arc origin for the Thrace Basin, NW Turkey. *Geologische Rundschau,* 85, 662– 668.

Görür, N., Oktay, F.Y., Seymen, I. & Şengör, A.M.C. (1984). Palaeotectonic evolution of the Tuzgölü basin complex, Central Turkey: sedimentary record of a Neo-Tethyan closure. In: The Geological Evolution of the Eastern Mediterranean

(J.E. Dixon & A.H.F. Robertson, eds), pp. 467–482. *Geological Society Special Publication*, 17, Blackwell Scientific, Oxford.

Görür, N., Şengör, A. M. C., Sakınç, M., Tüysüz, O., Akkök, R., Yiğitbaş, E., Oktay, F. Y., Barka, A. A., Sarıca, N., Ecevitopğlu, B., Demirbağ, E., Ersoy, Ş., Algan, O., Güuneysu, C. & Akyol, A. (1995). Rift formation in the Gökova region, southwest Anatolia: implications for the opening of the Aegean Sea. *Geological Magazine*, 132, 637.50.

Görür, N., Şengör, A.M.C., Akkök, R. & Yılmaz, Y. (1983). Sedimentological data regarding the opening of the northern branch of Neo-Tethys in the Pontides. *Geological Society of Turkey Bulletin*, 26, 11-20.

Güleç, N. (1991). Crust-mantle interaction in western Turkey: implications from Sr and Nd isotope geochemistry of Tertiary and Quaternary volcanics. *Geological Magazine*, 23, 417-435.

Gvirtzman, Z. & Nur, A. (1999). The formation of Mount Etna as the consequence of slab rollback. *Nature*, 401, 782-785.

Helvacı, C. & Alonso, R.N. (2000). Borate deposits of Turkey and Argentina; a summary and geological comparison. *Turkish Journal of Earth Sciences*, 24, 1-27.

Herzer, R., Sutherland, R. & Henrys, S. (2003). Subduction initiation, roll-back and evolution to a stable geometry: Recent and future surveys of the early Tonga-Kermadec subduction system. European Geophysical Society, *Geophysical Research abstracts*, 5, 13812.

Hetzel, R., Passchier, C.W., Ring, U. & Dora, O.Ö. (1995a). Bivergent extension in orogenic belts: The Menderes Massif (southwestern Turkey). *Geology*, 23, 455-458.

Hetzel, R., Ring, U., Akal, C. & Troesch, M. (1995b). Miocene NNE-directed extensional unroofing in the Menderes Massif, southwestern Turkey. *Journal of Geological Society*, London, 152, 639-654.

Hetzel, R., Romer, R.L., Candan, O. & Passchier, C.W. (1998). Geology of the Bozdağ area, central Menderes Massif, SW Turkey: Pan-African basement and Alpine deformation. *Geologische Rundschau*, 87, 394-406.

Hirschmannn, M.M., Asimow, P.D., Ghiorso, M.S. & Stolper, E.M. (1999). Calculation of peridotite partial melting from thermodynamic models of minerals and melts. III. Controls on isobaric melt production and the effect of water on melt production, *Journal of Petrology*, 40, 831-851.

Irvine, N. & Baragar, W.R.A. (1971). A guide to chemical classification of the common volcanic rocks. *Canadian Journal of Earth Science*, 8, 523-548.

Işık, V. & Tekeli, O. (2001). Late orogenic crustal extension in the northern Menderes Massif (western Turkey): evidence for metamorphic core complex formation. *International Journal of Earth Sciences*, 89, 757-65.

Işık, V., Seyitoğlu, G. & Çemen, İ. (2003). Ductile-brittle transition along the Alasehir shear zone and its structural relationship with the Simav detachment, Menderes massif, western Turkey. *Tectonophysics*, 374, 1-18.

Işık, V., Tekeli, O. & Seyitoğlu G. (2004). The $^{40}Ar/^{39}Ar$ age of extensional ductile deformation and granitoid intrusions in the northern Menderes core complex: Implications for the initiation of extensional tectonics in western Turkey. *Journal of Asian Earth Science*, 23, 555-566.

Iwamori, H., McKenzie, D. & Takahashi, E. (1995). Melt generation by isentropic upwelling. *Earth and Planetary Science Letters*, 134, 253-256.

Jackson, J. & McKenzie, D. (1984). Active tectonics of the Alpine-Himalayan Belt between western Turkey and Pakistan. *Geophysical Journal of the Royal Astronomical Society*, 77, 185-264

Jackson, J. & Mckenzie, D. (1988). The relationship between plate motions and seismic moment tensors and rates of active deformation in the Mediterranean and Middle East. *Geophysical Journa*l, 93, 45-73.

John, M.J. & Parkinson, C.D. (2002). Petrologic case for Eocene slab breakoff during the Indo-Asian collision. *Geology*, 30, 591-594.

Jolivet L., Faccenna C., Goffé B., Mattei M., Rossetti F., Brunet C., Storti F., Funiciello R., Cadet J.P., D'Agostino N. & Parra T. (1998). Midcrustal shear zones in postorogenic extension: example from the northern Tyrrhenian Sea. *Journal of Geophysical Research*, 103, 123-160.

Jolivet, L. & Patriat, M. (1999). Ductile extension and the formation of the Aegean Sea. In The Mediterranean basins: Tertiary Extension within the Alpine Orogen (eds B. Durand, L. Jolivet, F. Horvath and M. Seranne), *Geological Society of London*, 156, 427–56.

Jolivet, L., Daniel, J.M., Truffert, C. & Goffé, B. (1994). Exhumation of deep crustal methamorphic rocks and crustal extension in arc and back-arc regions. *Lithos*, 33, 3-30.

Jolivet, L., Rimmelé, G., Oberhänsli, R., Goffé, B. & Candan, O. (2004). Correlation of synorogenic tectonic and metamorphic events in the Cyclades, the Lycian Nappes and the Menderes Massif. Geodynamic implications: *Bulletin de la Société Géologique de France*, 175, 217–238.

Kanamori, H. (1977). Seismic and aseismic slip along subduction zones and their tectonic implications. In: Talwani, M., Pitman III, W.C. (Eds.), Island Arcs, Deep Sea Trenches and Back-Arc Basins. Maurice Ewing Ser. *American Geophysical Union*, 1, 1-14.

Karig, D.E. (1974). Evolution of arc systems in the Western Pacific. *Annual Reviews of Earth and Planetary Sciences,* 2, 51-78.

Kastens, K. (1991). Rate of outward growth of the Mediterranean Ridge accretionary complex. *Tectonophysics*, 199, 25-50.

Kay, R.W. & Kay, S.M. (1991). Creation and destruction of lower continental crust: *Geologische Rundschau*, 80, 259-278.

Kay, R.W. & Kay, S.M. (1993). Delamination and delamination magmatism, *Tectonophysics*, 219, 177-189.

Keskin, M. (2003). Magma generation by slab steepening and breakoff beneath a subduction-accretion complex: an alternative model for collision-related volcanism in eastern Anatolia, Turkey. *Geophysical Research Letters*, 30, 8045

Kissel, C. & Laj, C. (1988). Tertiary geodynamical evolution of the Aegean arc: a paleomagnetic reconstruction. *Tectonophysics*, 146, 183-201.

Koçyiğit, A., Yusufoğlu, H. & Bozkurt, E. (1999a). Evidence from the Gediz Graben for episodic two-stage extension in western Turkey. *Journal of the Geological Society*, London, 156, 605-616.

Koçyiğit, A.,Yusufoğlu, H. & Bozkurt, E. (1999b). Reply to 'Discussion on evidence from the Gediz Graben for episodic two-stage extension in western Turkey. *Journal of the Geological Society*, London, 156, 1240-1242.

Konak, N., Akdeniz, N. & Öztürk, E.N. (1987). Geology of the South ofMenderes Massif. IGCP Proj. 5: Guide Book field excursionWestern Anatolia, Turkey. *Mineral Research and Exploration Institute of Turkey Publication,* 42–53.

Le Bas, M.J., Le Maitre, R.W., Streckeisen, A. & Zanettin, B. (1986). Chemical classification of volcanic rocks based on the total alkali-silica diagram. *Journal of Petrology*, 27, 745-750.

Le Pichon, X. & Angelier, J. (1979). The Hellenic arc and trench system: a key to the neotectonic evolution of the eastern Mediterranean area. *Tectonophysics*, 60, 1-42.

Le Pichon, X. & Angelier, J. (1981). The Aegean Sea. *Philosophical Transactions of Royal Society*, London, 300, 357-372.

Le Pichon, X., Chamot-Rooke, C., Lallemant, S., Noomen, R. & Veis, G. (1995). Geodetic determination of the kinematics of Central Greece with respect to

Europe: implications for Eastern Mediterranean tectonics. *Journal of Geophysical Research*, 100, 12675-12690.

Lewis, G.N. & Randall, M. (1961). *Thermodynamics*, McGraw-Hill.

Lips, A.L.W. (1998). Temporal constraints on the kinematics of the destabilization of an orogen; syn- to post-orogenic collapse of the Northern Aegean region, PhD. Thesis, *Geol. Ultraiect.,* 166, 223.

Lips, A.L.W., Cassard, D., Sözbilir, H., Yılmaz, H. & Wijbrans, J. (2001). Multistage exhumation of the Menderes Massif, western Anatolia (Turkey), *International Journal of Earth Science,* 89, 781-92.

Lister, C.R.B. (1975). Gravitational drive on oceanic plates caused by thermal contraction. *Nature*, 257, 663-665.

Lister, G.S., Banga, G. & Feenstra, A. (1984). Metamorphic core complexes of Cordilleran type in the Cyclades, Aegean Sea, Greece. *Geology*, 12, 221-225.

Lonergan, L. & White, N. (1997). Origin of the Betic-Rif mountain belt. *Tectonics*, 16, 504-522.

Loos, S. & Reischmann, T. (1999). The evolution of the southern Menderes Massif in SW Turkey as revealed by zircon dating. *Journal of the Geological Society*, London 156, 1021-1030.

Mahéo, G., Guillot, S., Blichert-Toft, J., Rolland, Y. & Pécher, A. (2002). A slab breakoff model for the Neogene thermal evolution of South Karakorum and South Tibet. *Earth and Planettary Science Letters*, 195, 45-58.

Maury, R.C., Fourcade, S., Coulon, C., El Azzouzi, M., Bellon, H., Coutelle, A., Ouabadi, A., Semroud, B., Megartsi, M., Cotten, J., Belanteur, O., Louni-Hacini, A., Pique, A., Capdevila, R., Hernandez, J. & Rehault, J.P. (2000). Post-collisional Neogene magmatism of the Mediterranean Maghreb margin; a consequence of slab breakoff. *Comptes Rendus de l'Academie des Sciences*, 331, 159-173.

McClay, K.R., Norton, M.G., Coney, P. & Davis, G.H. (1986). Collapse of the Caledonian orogen and the old red sandstone. *Nature* 323, 147-149.

McKenzie, D.P & O'Nions, R.K. (1995). The source regions of ocean island basalts. *Journal of Petrology*, 36, 133-159.

McKenzie, D.P. & Bickle, M.J. (1988). The volume and composition of melt generated by extension of lithosphere, *Journal of Petrology*, 29, 625-679.

McKenzie, D.P. & O'Nions, R.K. (1991). Partial melting distributions from inversion of rare earth elementconcentrations. *Journal of Petrology*, 32, 1021-1091.

McKenzie, D.P. & O'Nions, R.K. (1995). The source regions of ocean island basalts. *Journal of Petrology*, 36, 133-159.

McKenzie, D.P. (1969). Speculations on the consequences and causes of plate motions, *Geophysical Journal of the Royal Astronomical Society*, 18, 1-32.

Mckenzie, D.P. (1978a). Some remarks on the development of sedimentary basins. *Earth and Planetary Science Letters*, 40, 25-32.

Mckenzie, D.P. (1978b). Active tectonics of the Alpine- Himalayan belt: the Aegean Sea and surrounding regions. *Geophysical Journal of Royal Astronomical Society*, 55, 217-54.

Meijer, P.T. & Wortel, M.J.R. (1997). Present-day dynamics of the Aegean region: a model analysis of the horizontal pattern of stress and deformation. *Tectonics*, 16, 879-895.

Meijer, P.T. (1995). Dynamics of active continental margins: the Andes and the Aegean region. *Ph.D. thesis*, Utrecht University, The Netherlands, 218.

Ménard, G. & Molnar, P. (1988). Collapse of a Hercynian Tibetan Plateau into a late Paleozoic European Basin and range province. *Nature*, 334, 235-237.

Mercier, J.L. (1981). Extensional-compressional tectonics associated with the Aegean Arc: comparison with the Andean Cordillera of south Peru-north Bolivia. *Philosophical Transactions of the Royal Society*, London, 300, 337-355.

Meulenkamp, J. E., Wortel, M. J. R., Van Wamel, W. A., Spakman, W. & Hoogerduyn Strating, E. (1988). On the Hellenic subduction zone and the geodynamic evolution of Crete since the late middle Miocene. *Tectonophysics*, 146, 203-215.

Mitchell R.H. & Bergman S.C. (1991). Petrology of lamproites. Plenum, New York, 447 pp.

Mitchell, R.H. & Bell, K. (1976). Rare earth element geochemistry of potassic lavas from the Birunga and Toro – Ankole regions of Uganda, Africa. *Contribution to Mineralogy and Petrology*, 58, 293-303.

Molnar, P. & Atwater, T. (1978). Interarc spreading and Cordilleran tectonics as alternates related to the age of subducted oceanic lithosphere. *Earth and Planetary Science Letters*, 41, 330-340.

Molnar, P. & Chen, W.P. (1982). Seismicity and mountain building. in Hsu, K, J, ed., Mountain building processes. *Academic Press*, New York, 41-57.

Molnar, P. & Chen, W.P. (1983). Focal depths and fault plane solutions earthquakes under the Tibetan plateau. *Journal of Geophysical Research*, 88, 1180-1196.

Molnar, P. & Lyon-Caen, H. (1988). Some simple physical aspects of the support, structure and evolution of mountain belts. *Geological Society of America*, Special Paper, 218, 179– 207.

Muess-Schumacher, U., Keller, J., Konova, V. & Suddaby, P. (1995). Petrology and age determinations of the ultramafic (lamproitic) rocks from the Yakokut Complex, Aldan Shield, Eastern Siberia. *Mineralogical Magazine*, 59, 409-428.

Murphy, D.T., Collerson, K.D. & Kamber, B.S. (2002). Lamproites from Gaussberg, Antartica: Possible transition zone melts of Archaean subducted sediments. *Journal of Petrology*, 43, 981-1001.

Nemcok, M., Pospisil, L., Lexa, J. & Donelick, R. A. (1998). Tertiary subduction and slab break-off model of the Carpathian--Pannonian region, *Tectonophysics*, 295, 307-340.

Oberhänsli, R., Candan, O., Dora O.Ö. & Dürr, H. (1997). Eclogites within the Menderes Massif, western Turkey. *Lithos*, 41, 135-150.

Oberhänsli, R., Monie, P., Candan, O., Warkus, F.C., Partzsch, J.H. & Dora, O.Ö. (1998). The age of blueschist metamorphism in the Mesozoic cover series of the Menderes Massif. *Swiss Bulletin of Mineralogy and Petrology*, 8, 309-316.

Okay, A.İ. & Kelley, S.P. (1994). Tectonic setting, petrology and geochronology of jadeite glaucophane and chloritoid glaucophane schists from north-west Turkey. *Journal of Metamorphic Geology*, 12, 455-466.

Okay, A.İ. & Satır, M. (2000). Coeval plutonism and metamorphism in a latest Oligocene metamorphic core complex in northwest Turkey. *Geological Magazine*, 5, 495-516.

Okay, A.İ. & Siyako, M. (1993). The New Position of the İzmir-Ankara Neo-Tethyan Suture Between İzmir and Balıkesir (in Turkish). In Tectonic and Hydrocarbon Potential of Anatolia and Surraunding Regions, *Preceedings of the Ozan Sungurlu Symposium*, Ankara, ed., S. Turgut, 333-55.

Okay, A.İ. & Tüysüz, O. (1999). Tethyan sutures of northern Turkey. In The Mediterranean Basins: Tertiary extension within the Alpine orogen (eds B. Durand, L. Jolivet, F. Horváth and M. Séranne), pp. 475–515. *Geological Society of London*, Special Publication no. 156.

Okay, A.İ. (1986). High pressure - low temperature metamorphic rocks of Turkey. *Geological Society of America Memoir*, 164, 333-47.

Okay, A.İ. (1996). Granulite facies gneisses from the Pulur region, eastern Pontides. *Turkish Journal of Earth Sciences*, 5, 55–61.

Okay, A.İ. (2000). Was the Late Triassic orogeny in Turkey caused by the collision of an oceanic plateau? In: Bozkurt, E., Winchester, J.A. & Piper, J.D.A. (eds), Tectonics and Magmatism in Turkey and Surrounding Area. *Geological Society*, London, Special Publications, 173, 25-41.

Okay, A.İ. (2001). Stratigraphic and metamorphic inversions in the central Menderes Massif: a new structural model. *International Journal of Earth Sciences*, 89, 709–727.

Okay, A.İ., Harris, N.B.W. & Kelley, S.P. (1998). Exhumation ofblueschists along a Tethyan suture in northwest Turkey. *Tectonophysics*, 285, 275-299.

Okay, A.İ., Satır, M., Maluski, H., Siyako, M., Monie, P., Metzger, R. & Akyüz, S. (1996). Paleo- and Neo-Tethyan events in northwestern Turkey: Geologic and geochronologic contraints. *The Tectonic Evolution of Asia*, 420-441.

Okay, A.İ., Satır, M., Tüysüz, O., Akyüz, S. & Chen, F. (2001). The tectonics of the Strandja Massif: late Variscan and mid-Mesozoicdeformation and metamorphism in the northern Aegean. *International Journal of Earth Sciences*, 90, 217-233.

Okay, A.İ., Şengör, A.M.C. & Görür, N. (1994). Kinematic history of the opening of the Black Sea and its effect on the surrounding regions. *Geology*, 22, 267–70.

Oxburgh, E.R. & Parmentier, E.M. (1978). Thermal processes in the formation of continental lithosphere, *Philosophical Transactions for the Royal Society of London*, 288, 415-429.

Özer, S. & Sözbilir, H. (2003). Presence and tectonic significance of Cretaceous rudist species in the so-called Permo-Carboniferous Göktepe Formation, central Menderes Massif, western Turkey. *International Journal of Earth Sciences*, 92, 397-404.

Özer, S. (1998). Rudist bearing Upper Cretaceous metamorphic sequences of the Menderes Massif (western Turkey). *Geobios*, 22, 235-249.

Parra, T., Vidal, O. & Jolivet, L. (2002). Relation between the intensity of deformation and retrogression in blueschist metapelites of Tinos Island (Greece) evidenced by chlorite-mica local equilibria. *Lithos*, 63, 41-66.

Passchier, C.W. & Simpson, C. (1986). Porphyroclast systems as kinematic indicators. *Journal of Structural Geology*, 8, 831-843.

Pearce, J.A. & Parkinson, I.J. (1993). Trace element models for mantle melting: application to volcanic arc petrogenesis, in: H.M. Prichard, T. Alabaster, N.B. Harris, C.R. Neary (Eds.), Magmatic Processes and Plate Tectonics, *Geological Society Specical Publications*, 76, 373-403.

Pearce, J.A. & Peate, D.W. (1995). Tectonic implications of the composition of volcanic arc magmas. *Annual Review of Earth and Planetary Sciences*, 23, 251–285.

Pearce, J.A. (1982). Trace element characteristics of lava from destructive plate boundaries. Andesites, 525-548. Ed: R.S. Thorpe, *Wiley*, New York.

Pearce, J.A. (1983). Role of the sub-continental lithosphere in magma genesis at active continental margins. In: Hawkesworth, C.J., Norry, M.J. (Eds.), Continental basalts and mantle xenoliths. *Shiva Publishing*, Nantwich, pp. 230–249.

Pearce, J.A., Baker, P.E., Harvey, P.K. & Luff, I.W. (1995). Geochemical evidence for subduction fluxes, mantle melting and fractional crystallization beneath the South Sandwich island arc. *Journal of Petrology*, 36, 1073– 1109.

Pecerillo, A. & Manetti, P. (1985). The potassium alkaline volcanicsm of central-southern Italy: a review of the data relevant to petrogenesis and geodynamic significance. *South African Journal of Geology*, 88, 379-394.

Pecerillo, A. & Taylor, S.R. (1976). Geochemistry of Eocene calc-alkaline volcanic rocks from the Kastamonu area, northern Turkey. *Contribution to Mineralogy and Petrology*, 58, 63-81.

Pe-Piper, G. & Piper, D.J.W. (1989). Spatial and temporal variation in Late Cenozoic back-arc volcanic rocks, Aegean Sea Region. *Tectonophysics*, 169, 113-134.

Platt, J.P. & Vissers, R.L.M. (1989). Extensional collapse of thickened continental lithosphere: A working hypothesis for the Alboran Sea and Gibraltar arc. *Geology*, 17, 540-543.

Platt, J.P., Soto, J.I., Whitehouse, M.J., Hurford, A.J. & Kelley, S.P. (1998). Thermal evolution, rate of exhumation, and tectonic significance of metamorphic rocks from the floor of the Alboran extensional basin, western Mediterranean. *Tectonics*, 17, 671–689.

Prelević, D., Foley, S.F., Romer, R.,L., Cvetković, V. & Downes, H. (2005). Tertiary Ultrapotassic Volcanism in Serbia: Constraints on Petrogenesis and Mantle Source Characteristics. *Journal of Petrology*, 46, 1443-1487.

Presnall, D.C., G.H. Gudfinnson, M.J. & Walter (2002). Generation of mid-ocean ridge basalts at pressures from 1 to 7 Gpa. *Geochemica Cosmochimica Acta*, 66, 2073-2090.

Purvis, M. & Robertson, A.H.F. (1997). Multistage rifting in rapidly extending continental crust (west Turkey). *Terra*, Abstracts, 9, 398.

Purvis, M. & Robertson, A.H.F. (2004). A pulsed extension model for the Neogene–Recent E–W-trending Alaşehir Graben and the NE–SW-trending Selendi and Gördes Basins, western Turkey, *Tectonophysics*, 391, 171-201.

Purvis, M. & Robertson, A.H.F. (2005a). Sedimentation of the Neogene–Recent Alaşehir (Gediz) continental graben system used to test alternative tectonic models for western (Aegean) Turkey, *Sedimentary Geology*, 173, 373-408.

Purvis, M. & Robertson, A.H.F. (2005b). Miocene sedimentary evolution of the NE-SW-trending Selendi and Gördes Basins, Western Turkey: implications for extensional processes. *Sedimentary Geology*, 174, 31-62.

Ramberg, H. (1980). Diapirism and gravity-collapse in the Scandinavian Caledonides. *Journal of Geological Society*, London, 137, 262– 270.

Rey, P., Vanderhaeghe, O. & Teyssier, C. (2001). Gravitational collapse of the continental crust: definition, regimes and modes. *Tectonophysics*, 342, 435-449.

Rimmelé, G., Jolivet, L., Oberhänsli, R. & Goffé, B. (2003a). Deformationhistory of the high-pressure Lycian Nappes and implications fortectonic evolution of SW Turkey. *Tectonics*, 22, 1007-1029.

Rimmelé, G., Oberhänsli, R., Goffé, B., Jolivet, L., Candan, O. & Çetinkaplan, M. (2003b). First evidence of high-pressuremetamorphism in the 'Cover Series' of the southern MenderesMassif. Tectonic and metamorphic implications for the evolutionof the SW Turkey. *Lithos*, 71, 19-46.

Ring, U. & Collins, A.S. (2005). U-Pb SIMS dating of synkinematic granites: timing of core-complex formation in the northern Anatolide belt of western Turkey. *Journal of Geological Society*, London, 162, 289-298.

Ring, U., Gessner, Güngör, T. & Passchier, C. (1999). The Menderes Massif of Turkey and the Cycladic Massif in Aegean- do they really corralte? *Journal of Geological Society*, London, 156, 3-6.

Ring, U., Johnson, C., Hetzel, R. & Gessner, K. (2003). Tectonic denudation of a Late Cretaceous-Tertiary collisional belt: regionally symmetric cooling patterns and their relation to extensional faults in the Anatolide belt of western Turkey. *Geological Magazine*, 140, 421-441.

Robertson, A.H.F. & Grasso, M. (1995). Overview of the Late Tertiary–Recent tectonic and paleo-environmental development of the Mediterranean region. *Terra Nova*, 7, 114-27.

Rogers, N.W., Parker, R.J., Hawkesworth, R.J. & Marsh, J.S. (1985). The geochemistry of potassic lavas from Vulsini, Central Italy, and implications for mantle enrichment process beneath the Roman region. *Contribution to Mineralogy and Petrology*, 90, 244–257.

Rollinson, H. (1993). Using Geochemical Data: Evaluation, Presentation, Interpretation, Longman Geochemistry Series, *Prentice Hall*, London, 352 p.

Rosenbaum, G., Lister, G.S. & Duboz, C. (2002). Reconstruction of the tectonic evolution of the western Mediterranean since the Oligocene . In: Rosenbaum, G. and Lister, G. S. 2002. Reconstruction of the evolution of the Alpine-Himalayan orogeny. *Journal of the Virtual Explorer*, 8, 107-130.

Royden L.H. (1993). Evolution of retreating subduction boundaries formed during continental collision. *Tectonics*, 12, 629-638.

Savaşçın, Y. & Güleç, N. (1990). Neogene volcanism of western Anatolia-Field excursion B3. *International Earth Science Congress on Aegean Region*, İzmir, Turkey.

Savaşçın, Y. & Oyman, T. (1998). Tectono-Magmatic Evolution of Alkaline Volcanics at the Kırka-Afyon-Isparta Structural Trend, Sw Turkey. *Turkish Journal of Science*, 7, 201-214.

Schliestedt, M., Altherr, R. & Matthews, A. (1987). Evolution of the Cycladic crystalline complex: petrology, isotope geochemistry and geochronology. In: Chemical transport in metasomatic processes (ed Helgeson, H. C.) Nato Advanced Study Institutes Series, *D. Reidel Publishing Company*, Boston, pp. 389-428

Schott, B. & Schmeling, H. (1998). Delamination and detachment of a lithospheric root . *Tectonophysics*, 296, 225-247.

Şengör, A.M.C. & Yılmaz, Y. (1981). Tethyan Evolution of Turkey: A Plate Tectonic Approach. *Tectonophysics*, 75, 181-241.

Şengör, A.M.C. (1979). The North Anatolian Transform Fault: its age, offset and tectonic significance. *Journal of the Geological Society*, London, 136, 269-82.

Şengör, A.M.C. (1987). Cross-faults and differential stretching of hanging walls in regions of low-angle normal faulting: examples from western Turkey. From Coward, M.P., Dewey, J.F., Hancock, P.L. (eds.), 1987, Continental Extensional Tectonics. *Geological Society Special Publication*, 28, 575-589.

Şengör, A.M.C., Görür, N. & Şaroğlu, F. (1985). Strike-slip faulting and related basin formation in zones of tectonic escape: Turkey as a case study. In: Biddle, K. & Christie-Blick, N. (eds), Strike-Slip Deformation, Basin Formation and Sedimentation. *Society of Economic Paleontologists and Mineralogists*, Special Publications 37, 227-64.

Şengör, A.M.C., Özeren, S., Genç, T. & Zor, E. (2003). East Anatolian high plateau as a mantle-supported, north-south shortened domal structure. *Geophysical Research Letters*, 30, 8045

Şengör, A.M.C., Satır, M. & Akkök, R. (1984). The timing of tectonic events in the Menderes Massif, western Turkey: implication for tectonic evolution and evidence for Pan-African basement in Turkey. *Tectonics*, 3, 693-707.

Seyitoğlu, G. & Scott, B.C. (1991). Late Cenozoic crustal extension and basin formation in west Turkey. *Geological Magazine*, 128, 155-166.

Seyitoğlu, G. & Scott, B.C. (1992a). The age of the Büyük Menderes graben (west Turkey) and its tectonic implications. *Geological Magazine*, 129, 239-242.

Seyitoğlu, G. & Scott, B.C. (1992b). Late Cenozoic volcanic evolution of the NE Aegean region. *Journal of Volcanology and Geothermal Research*, 54, 157-176.

Seyitoğlu, G. & Scott, B.C. (1994). Late Cenozoic basin development in west Turkey. Gördes basin: tectonics and sedimentation. *Geological Magazine*, 131, 631-637.

Seyitoğlu, G. & Scott, B.C. (1996a). Age of Alasehir graben (west Turkey) and its tectonic implications. *Geological Journal*, 31, 1-11.

Seyitoğlu, G. & Scott, B.C. (1996b). The cause of N-S extensional tectonics in western Turkey: Tectonic escape vs. Back-arc spreading vs. Orogenic collapse. *Journal of Geodynamics*, 22, 145 - 153.

Seyitoğlu, G. (1997). Late Cenozoic tectono-sedimentary development of the Selendi and Uşak-Güre basins: a contribution to the discussion on the development of east-west and north trending basins in western Anatolia. *Geological Magazine*, 134, 163-175.

Seyitoğlu, G., Anderson, D., Nowell, G. & Scott, B.C. (1997). The evolution from Miocene potassic to Quaternary sodic magmatism in western Turkey: implications for enrichment processes in the lithospheric mantle. *Journal of Volcanology and Geothermal Research*, 76, 127-147.

Seyitoğlu, G., Çemen, İ. & Tekeli, O. (2000). Extensional folding in the Alasehir (Gediz) graben, western Turkey. *Journal of the Geological Society*, London, 157, 1097-1100.

Seyitoğlu, G., Işık, V. & Çemen, İ. (2004). Complete Tertiary exhumation history of the Menderes massif, western Turkey: an alternative working hypothesis. *Terra Nova*, 16, 358-364.

Seyitoğlu, G., Tekeli, O., Çemen, İ., Şen, S. & Işık, V. (2002). The role of flexural rotation/rolling hinge model in the tectonic evolution of the Alasehir graben, western Turkey. *Geological Magazine*, 139, 15-26.

Shaw, D.M. (1970). Trace element fractionation during anatexis. *Geochimica et Cosmochimica Acta*, 34, 237–243.

Smith, A.T. & Toksöz, M.N. (1972). Stress distribution beneath island arcs. *Geophys. J.R. Astron. Soc*., 29, 289-318.

Sözbilir, H. & Emre, T. (1996). Supra-detachment basin and rift basin developed during the neotectonic evolution of the Menderes Massif, *Abstracts of the Geological Congress of Turkey*, 288, 30-31.

Sözbilir, H. (2002). Geometry and origin of folding in the Neogene sediments of the Gediz Graben, western Anatolia, Turkey. *Geodinamica Acta*, 15, 277-288.

Spakman, W. Wortel, M.J.R. & Vlaar, N.J. (1988). The Hellenic subduction zone; a tomographic image and its geodynamic implications. Geophysical Research Letters, 15, 60-63.

Spence, W. (1987). Slab pull and the seismotectonics of subducting lithosphere. *Reviews of Geophysics*, 25, 55-69.

Stampfli, G.M., Vavassis, I., De Bono, A., Rosselet, F., Matti, B. & Bellini, M. (2004). Remnants of the Paleotethys oceanic suture zone in the Western Tethyan area, in Cassinis, G., and Decandia, F.A., eds., Stratigraphic and structural evolution of the Late Carboniferous to Triassic continental and marine succession in Tuscany (Italy): regional reports and general correlation, Roma.

Sun, S.S. & McDonough, W.F. (1989). Chemical and isotopic systematics of oceanic basalts: implications for mantle compositions and processes. In: Saunders, A.D., Norry, M.J. (Eds.), Magmatism in the Oceanic Basin. *Geological Society of London*, Special Publication, London, 313– 345.

Taymaz, T., Jackson, J.A. & McKenzie, D. (1991). Active tectonics of the north and central Aegean Sea. *Geophysical Journal International*, 106, 433–490.

Taymaz, T., Jackson, J.A. & Westaway, R. (1990). Earthquake mechanisms in the Hellenic Trench near Crete. *Geophysical Journal International*, 102, 695–731.

Teng,, L.S., Lee, C.T., Tsai, Y.B. & Hsiao, Li-Y. (2000). Slab breakoff, as a mechanism for flipping of subduction polarity in Taiwan. *Geology*, 28, 155-158.

Thompson, R.N. & Fowler, M.B. (1986). Subduction-related shosonitic and ultrapotassic magmatism: a study of Siluro-Ordovician syenites from the Scottish Caledoniens. *Contribution to Mineralagy and Petrology*, 94, 507-522.

Thomson, S.N., Stockhert, B. & Brix, M.R. (1998). Thermochronology of the high-pressure metamorphic rocks of Crete, Greece. Implications for the speed of tectonic processes. Geology, 26, 259-262.

Toksöz, N. & Bird, P. (1977). Formation and evolution of marginal basins and continental plateaus. In Talwanı, M. & Pitman, W.C. (eds) Island Arcs, Deep Sea Trenches and Backarc Basins. *American Geophysical Union, Maurice Ewing Series*, 1, 379-393.

Turner, S.P., Platt, J.P., George, R.M.M., Kelley, S.P., Pearson, D.G. & Nowell, G.M. (1999). Magmatism associated with orogenic collapse of the Betic-Alboran domain, SE Spain: *Journal of Petrology*, 40, 1011–1036.

Tüysüz, O. (1993). Stratigraphic and petrologic characteristics of two parallel magmatic belts in Central Anatolia and their significance in the tectonic evolution of Anatolian Neo-Tethys. EUG VII, *Terra Abstracts*, 5, 271.

Uyeda, S. & Kanamori, H. (1979). Back-arc opening and the mode of subduction. *Journal of Geophysical Research*, 84, 1049-1061.

van de Zedde, D.M.A. & Wortel, M.J.R. (2001). Shallow slab detachment as a transient source of heat at midlithospheric depth. *Tectonics*, 20, 868-882.

van der Meulen, M.J., Buiter, S.J.H., Meulenkamp, J.E. & Wortel., M.J.R. (2000). An early Pliocene uplift of the central Apenninic foredeep and its geodynamic significance. *Tectonics*, 19, 300-313.

von Bemmelen, R.W. (1954). Mountain Building. Martinus Nijhoff, *The Hague*, 177.

von Blanckenburg, F. & Davies (1995). Slab breakoff: a model for syncollisional magmatism and tectonics in the Alps. *Tectonics*, 14, 120-131.

Walcott C., R. & White S., H. (1998). Constraints on the kinematics of post-orogenic extension imposed by stretching lineations in the Aegean region. *Tectonophysics*, 298, 155-175.

Wedepohl, K.H. & Baumann, A. (1999). Central European Cenozoic plume volcanism with OIB characteristics and indications of a lower mantle source. *Contribution to Mineralogy and Petrology*, 136, 225-230.

Westaway, R. (1994). Present-day kinematics of the Middle East and Eastern Mediterranean. *Journal of Geophysical Research*, 99, 12071-90.

Westaway, R., Pringle, M., Yurtmen, S., Demir, T., Bridgland, D., Rowbotham, G. & Maddy, D. (2004). Pliocene and Quaternary regional uplift in western Turkey: the Gediz River terrace staircase and the volcanism at Kula, *Tectonophysics*, 391, 121-169.

Wilson, M. (1989). Igneous Petrogenesis, a global tectonic approach. *Unwin Hyman*, London, pp. 466.

Wilson, T.J. (1995), Cenozoic transtension along the Transantarctic Mountains-West Antarctic Rift boundary, southern Victoria Land, Antarctica. *Tectonics*, 14, 531-545.

Winchester, J.A. & Floyd, P.A. (1977). Geochemical discrimination of different magma series and their differentiation products using immobile elements. *Chemical Geology*, 20, 325-343.

Wood, D.A. (1980). The application of a Th–Hf–Ta diagram to problems of tectonomagmatic classification and to establishing the nature of crustal contamination of basaltic lavas of the British tertiary volcanic province. *Earth Planetary Science Letters*, 50, 11–30.

Yamaji, A. (2003). Slab rollback suggested by latest Miocene to Pliocene forearc stress and migration of volcanic front in southern Kyushu, northern Ryukyu Arc. *Tectonophysics*, 364, 9-24.

Yılmaz, Y. (1989). An approach to the origin of young volcanic rocks of Western Turkey. In A. M. C. Şengör (Editor), Tectonic evolution of the Tethyan Region. *Kluwer Academic Publishers*, 159-189.

Yılmaz, Y. (1990). Comparison of young volcanic associations of western and eastern Anatolia formed under a compressional regime: a review. *Journal of Volcanology and Geothermal Research,* 44, 1-19.

Yılmaz, Y., Genç, S.C., Gürer, O.F., Bozcu, M., Yılmaz, K., Karacık, Z., Altunkaynak, Ş. & Elmas, A. (2000). When did the western Anatolian grabens begin to develop? In: Bozkurt, E., Winchester, J. A. & Piper, J. D. A. (eds), Tectonics and Magmatism in Turkey and the Surrounding Area. *Geological Society*, London, Special Publications 173, 353.84.

Yılmaz, Y., Genç, Ş.C., Karacık, Z. & Altunkaynak, Ş. (2001). Two contrasting magmatic associations of NW Anatolia and their tectonic significance, *Journal of Geodynamics*, 31, 243-271.

Zeck, H.P., Monié, P., Villa, I. & Hansen, B.T. (1992). Very high rates of cooling and uplift in the Alpine belt of the Betic Cordilleras, southern Spain. *Geology*, 20, 79-82.

Zeilinga de Boer, J. (1989). The Greek enigma: is development of the Aegean Orogene dominated by forces related to subduction or obduction? *Marine Geology*, 87, 31-54.